SOVIET
ATOMIC
ENERGY

АТОМНАЯ ЭНЕРГИЯ
(ATOMNAYA ÉNERGIYA)

TRANSLATED FROM RUSSIAN

SOVIET ATOMIC ENERGY

CONSULTANTS BUREAU, NEW YORK AND LONDON

SOVIET ATOMIC ENERGY

CONTENTS

STATE-OF-THE-ART AND DEVELOPMENT PROSPECTS FOR NUCLEAR POWER STATIONS
CONTAINING PRESSURIZED-WATER REACTORS (VVÉR)

G. A. Shasharin, E. I. Ignatenko,
and V. M. Boldyrev

UDC 621.311.2:621.039:621.039.57

At present, nuclear stations containing pressurized-water reactors PWR such as the VVÉR have become most common in nuclear engineering in the USSR and elsewhere. In all, there are 27 stations containing VVÉR operating with unit electrical power levels from 70 to 1000 MW and total installed power of 12.14 GW (Tables 1 and 2) [1].

ATTAINMENT OF DESIGN PARAMETERS, OPERATION, AND REPAIR

Table 3 shows that stations containing VVÉR reactors work reliably and consistently. The power utilization factor (PUF) in these VVÉR units, on the whole, is higher than in foreign ones (Table 4) and in some cases attains 90-96%. In the main units, the PUF increase steadily as the working time increases at first and attain stable values in the third year, while in later units they stabilize in the second year. There have been substantial reductions in PUF in individual years for certain units because of long downtimes due to accident situations or control constraints. There are also differences in internal electricity consumption at units of the same type because of differences in output, load level, and local working conditions. When a station is operating stably, the internal use varies around a certain level, but all the parameters deteriorate when there are prolonged downtimes. The efficiency is dependent mainly on local conditions, as well as on the state of the equipment. As a rule, the efficiency increases after maintenance, condenser cleaning, the replacement of worn equipment, and other such measures.

The Ministry of Energy of the USSR operates a system for planned prophylactic maintenance (PPM) at nuclear stations, which includes periodic major, medium, and current repairs, whose sequence and duration are determined by the planned maintenance cycle. Each year, each unit is shut down for major or medium overhaul. The fule is also changed during this period. Working results show that the times taken in planned maintenance correspond to the standards (Table 5). Information is not given on nuclear stations containing VVÉR-1000 because they have not been operating long.

One of the obvious factors resulting in improved economics at nuclear stations is the reduction in the equipment upgrading time in annual PPM. This is dependent primarily on the organization of the operations, the staff qualification, and the equipment of the station with the necessary servicing facilities. The main operations in PPM are devoted to the equipment in the first and second loops (Table 6).

About 280 items of equipment and apparatus are used in maintaining the nuclear steam-producing plant at a nuclear station containing two VVÉR-440, which means that it is important to upgrade the maintenance operations on the equipment in the first loop. The following are required for high-grade and rapid upgrading and servicing:

1) a set of standardization documents laying down the specifications for checking the metal in nuclear station equipment, including the corresponding methods of checking the metal;

2) a set of means of checking the metal for use with those units and components whose checking is laid down by the standardization documents;

3) criteria for accepting or rejecting defects found in the metal;

4) methods (technologies) for repairing defects in the equipment; and

5) repair equipment.

TABLE 1. Nuclear Units Containing VVÉR Reactors as of Jan. 1, 1984

Nuclear station	Number and type of turbines	Installed electric power, MW	Installed district heat-tapoff, Gcal/h	Connection to grid
Novyi Voronezh				
first unit	3 AK-70-11, 3 TVF-100-2	210		IX.1964
second	5 K-75-30, 5 TVF-100-2	365		XII.1969
third	2 K-220-44, 2 TVV-220-2	417	2×25	XII.1971
fourth	2 K-220-44, TVV-220-2, TVV-220-2A	417	2×25	XII.1972
fifth	2 K-500-60/1500	1000	2×30	V.1980
Kola				
first unit	2 K-220-44, 2 TVV-220-2A	440	2×25	VI.1973
second	The same	440	2×25	XII.1974
third	2 K-220-44-3, 2 TVV-220-2A	440	2×50	III.1981
Armenian				
first	2 K-220-44, 2 TVV-220-2A	407,5	2×25	XII.1976
second	The same	407,5	2×25	I.1980
Rovensk				
first	2 K-220-44-3, 2 TVV-220-2AUZ	392	2×50	XII.1980
second	The same	416	2×50	XII.1981
South Ukranian				
first unit	K-1000-60/1500, TVV-1000-4	1000	200	XII.1982
Reinsberg (GDR)	—	70	—	V.1966
Nord				
first unit	2K-220-44-3, 2 TVV-220-2AUZ	440	2×50	XII.1973
second	The same	440	2×50	XII.1974
third	» »	440	2×50	XI.1977
fourth	» »	440	2×50	VIII.1979
Kozlodui (Bulgaria)				
first unit	2 K-220-44-3, 2 TVV-220-2AUZ	440	2×50	VI.1974
second	The same	440	2×50	XIII.1975
third	» »	440	2×50	XII.1980
fourth	» »	440	2×50	IV.1982
Lovisa (Finland)				
first unit	2 K-220-44-3, 2 TVV-220-2AUZ	440	2×50	II.1977
second	The same	440	2×50	XI.1980
Bogunice (Czechoslovakia)				
first unit	2 K-220-44-3, 2 TVV-220-2AUZ	440	2×50	XII.1978
second	The same	440	2×50	III.1980
Paks (Hungary)				
first unit	2 K-220-44-3, 2 TVV-220-2AUZ	440	2×50	XII.1982

TABLE 2. Basic Technical Characteristics of Reactor Systems Containing VVÉR

Characteristic	VVÉR-70	VVÉR-210	VVÉR-365	VVÉR-440	VVÉR-1000
Reactor thermal power, MW	265	760	1320	1375	30,0
Number of circulation loops	3	6	8	6	4
Pressure, MPa;					
in reactor	9,8	9,8	10,3	12,3	15,7
in steam generators	3,1	3,1	3,2	4,6	6,3
Temp., °C					
at reactor inlet	250	245	248	268	288
at reactor outlet	266	266	274	296	317
Coolant flow through reactor, m³/h	16000	33000	50000 *	45000	88000
Internal diam. of reactor body, mm	2640	3560	3560	3560	4139
Core					
equiv. diam., mm	1900	2880	2880	2880	3110
height in working state, mm	2500	2500	2460	2460	3560
power density, kW/liter	38	47	83	86	111
Number of fuel assemblies in core	148	343	349	349	151
Number of fuel pins	90	90	126	126	317
Fuel pins:					
outside diameter, mm	10,2	10,2	9,1	9,1	9,1
thickness of Zr + 1% Nb sheath, mm	0,6	0,6	0,65	0,65	0,67
mean linear power, W/cm	80	99	122	127	176
Uranium:					
loaded into reactor	17,0	40,0	41,5	41,5	66,0
specific power, kW/kg U	15,5	19	32	33	45,5
enrichment in new pins on replacing 1/3 of assemblies, %	2,0	2,0	3,0	3,5	3,3/4,4
mean burnup, MW·day/kg	13	14	28		27/40
Number of CPS units	19	37	73	73/37	109
Unit efficiency, %	26,5	27,7	27,7	32,0	33,3

*With seven loops working (one loop reserve).

Up to now, the monitoring of metal at nuclear power stations has been undertaken on individual programs agreed annually with the corresponding organizations. From July 1983, unified instructions apply for the monitoring of the state of the main metal and welded joints in equipment and pipelines in the first and second loops in nuclear power stations containing VVÉR, which make the fullest use of experience with metal monitoring at existing nuclear sta-

362

TABLE 3. Unit Parameters in Nuclear Stations Containing VVÉR

Nuclear station	Power production, billion kW·h		Power use factor, %		Internal power consumption, %		Net unit eff., %	
	1982	1983	1982	1983	1982	1983	1982	1983
Novyi Voronezh:								
first unit	1,591	1,602	86,5	87,1	6,96	6,57	25,61	25,29
second	2,8	2,851	87,6	89,1	6,53	6,04	25,98	25,36
third	3,012	2,682	82,5	73,4	8,02	8,03	25,94	25,82
fourth	3,057	3,219	83,7	88,1	8,49	7,96	26,22	26,12
fifth	5,338	7,085	60,9	80,9	5,59	4,76	29,77	29,94
Kola:								
first unit	3,080	3,471	79,9	90,0	7,53	6,67	28,87	29,16
second	2,648	3,311	68,7	86,9	6,99	6,60	29,09	29,14
third	2,049	2,632	53,2	68,3	7,72	5,95	28,35	29,82
Armenian								
first unit	2,304	0,873	64,6	24,4	7,8	12,10	26,48	25,02
second	2,179	3,073	61,0	86,1	8,2	8,32	26,25	26,01
Rovensk								
first unit	1,895	2,233	55,2	65,0	8,93	8,92	25,89	25,53
second	2,266	2,018	62,2	55,4	8,96	8,40	24,44	25,81
South Ukrainian								
first unit	—	2,763	—	31,5	—	4,76	—	—

TABLE 4. PUF for Foreign Nuclear Stations Containing PWR, % [2]

Region	1980	1981	1982	1983 (first half year)
All countries apart from Comecon members	59,3	61,9	60,0	59,2

tions.* These instructions cover not only the volume of work and the periodicity in monitoring the individual units and components in the two loops but also enumerate the main standardization documents on metal monitoring, including methods of metal monitoring for various purposes (ultrasonic, visual, magnetic-powder, color, etc.), in addition to the monitoring facilities and the basic criteria or standards for evaluating metal state.

One mainly uses manual monitoring facilities at nuclear power stations, although this tends to lead to high staff doses. Future facilities should be highly specific, for example for monitoring the metal in the reactor body, the collectors and tube bundles in the steam generators, the volume compensators, etc. Here we may note developments in this country (at the All-Union Nuclear Power Station Research Institute) and in Czechoslovakia, including the use of the miniature Prognoz-11 TV system for monitoring inaccessible locations, the UNIKOP specialized remote-sensing systems for monitoring steam generators, the KONAP units for checking reactor piping, and the UKOZ for monitoring volume compensators.

The metal defects at our nuclear power stations have the following percent distribution by cause: constructional 20, technological 40, metallurgical 16; installation 14, and operation 10.

There are ongoing studies designed to improve the reliability and safety, particularly on the basis of studies of failures. Long-term experience with VVÉR-440 reactors is confirmed by data on PWR stations from other countries indicates that failures (defects) in equipment are distributed in the following percent proportions: first-circuit equipment

---

*In January 1984, the unified instructions on operational monitoring of the state of the main metal and welded joints in equipment and pipelines in nuclear power stations containing VVÉR-1000 reactors were confirmed and put into operation.

TABLE 5. Durations of Downtimes for One
Unit Containing VVER-440 for Fuel Chang-
ing and Equipment Upgrading

Maintenance	Nuclear station		
	Novyi Voronezh	Kola	Arme- nian
Average from standards:	30	30	30
actual average	34	40	39
actual minimal	18	24	30
Major from standards	55	55	55
actual average	66	66	52
actual minimal	53	45	45

TABLE 6. Structure of the Costs for PPM
in the Volume of Major Equipment Mainte-
nance in the Main Sections of Nuclear
Power Stations

Section	Proportion of costs in overall maintenance costs, %	Proportion of total labor cost, %
Reactor	40—46	45—55
Turbine	25—30	18—20
Electrical	6—8	8—10
Thermal automatics and measurement	7—10	10—15
Others	4—5	2—3

15-20, turbines 25-30, electrotechnical and conversion equipment 35-45, and auxiliary thermo-mechanical equipment and pipelines 15-20. In 15-20% of the cases, the faults are due to staff errors. One unit on average shows 20-25 faults a year leading to power loss. For example, in 1981 this power loss from these causes was about 2% at nuclear stations in this country.

The most characteristic faults are leaks in condenser pipes, sealing failures in the high-pressure and low-pressure heaters, unsatisfactory operation (overheating or sparking) in the brush apparatus in turbine generators, sealing failures in the pipelines and other equipment in the second loop, failures in steam generator pipes, and incorrect operation of protection and interlock equipment.

The All-Union Nuclear Power Stations Research Institute has set up a system for acquiring and processing information on these failures, and this has been accompanied by an analysis of the earlier stages of operation, with the result that the design of power stations and equipment for them has been improved in many ways, which have substantially improved the reliability, where we may particularly note the following: more defined welding in steam-generator collectors for the water-steam interface section to protect it from corrosion; a modified throttling control for K-220-44 turbines and changes in the design of the high-pressure heaters; design changes in the SPP-220; and anticorrosion coating in the volume compensator to reduce corrosion.

The radiation backgrounds at operating power stations have been maintained within the limits set down by the standards for staff safety in any operations. The overall specific activity of water in the first circuit due to fission products is not more than 10^{-4}-10^{-3} Ci/liter (1 Ci = 3.7×10^{10} Bq). The low activity level and the good sealing in the first circuit have meant that the activity levels in the air in the sealed spaces are low. The mean annual collective dose to staff in systems containing VVER-440 reactors has been 362 ber (1 ber = 0.01 Sv), the average number of staff being 380. The fluctuations in annual dose are due to differences in the volume of servicing operations. The annual collective dose in the normal operation of a VVER-440 unit together with planned preventive maintenance and fuel reloading is distributed as follows: 130, 217, and 35 ber, respectively.

The radioactive discharges from power stations containing VVÉR-440 to the atmosphere have been stabilized at the level of 2.1-3.3 Ci/MW(el)·yr, which is close to the average for power stations containing PWR. The activity of liquid discharges to open bodies of water has not exceeded 300 mCi/yr. The radiation backgrounds in areas around nuclear power stations in the main are determined by global fallout and the natural ionizing-radiation background. In normal operation, the power stations have virtually no effect on the environment.

At present, the staff numbers at nuclear power stations exceed the standard level by 15%, mainly due to maintenance staff, which account for about 53% of the total. The staff numbers at Soviet nuclear power stations are higher by factors of 2.5-3.5 than those at nuclear power stations in the developed capitalist countries, while the numbers of maintenance staff are larger by factors of 3-5, mainly because in capitalist countries the equipment is maintained usually by the maker, whose staff are not included amongst the operating staff. The approach used in this country in organizing nuclear power station servicing is due to the lower equipment reliability, the absence of spare power, and the consequent higher equipment use.

UPGRADING VVÉR DESIGN

Improvements in nuclear systems containing VVÉR reactors follow the lines of increasing of the following:

1) unit power: in the 20 years since the first init at the Novyi Voronezh power station was commissioned, the unit power of the VVÉR has increased from 210 to 1000 MW(ed.);

2) first-circuit pressures and steam parameters: during this time, the pressure in the reactor has been raised from 9.8 to 15.7 MPa, and the steam pressure in the steam generators from 3.1 to 6.3 MPa;

3) the power density in the core has been raised from 47 to 111 kW/liter by equalizing the power distribution over the radius and revising the neutron-physics and thermophysics characteristics of the core; and

4) increasing the burnup from 13 to 40 MW·day/kg U by improved fuel-pin design and the use of boron regulation.

Some initial designs have been retained:

1) railroad transportability of the reactor body;

2) the use of hexagonal fuel assemblies in the core containing rod pins filled with uranium dioxide sheathed in an alloy of zirconium with 1% niobium;

3) the use of high-tensile chromium-molybdenum steels for the body; and

4) the use of horizontal steam generators to produce saturated steam.

We now mention some changes that have been made in the basic designs as a result of experience with the VVÉR.

Reactor and Enclosed Equipment (EE). The displacement of the thermal shield at the first unit in Novyi Voronezh power station in 1969 led to reconsideration of the flow and mounting conditions for all the EE components. The thermal screen has been completely eliminated in the VVÉR-1000 and later models of the VVÉR-440.

Originally, the body was made from 15Kh2MFA steel without anticorrosion coating, where suitable water treatment ensured a satisfactory state of corrosion in the inner surface. However, anticorrosion coating was applied beginning with the first unit in the Lovisa power station, in accordance with world practice and to simplify the water-treatment requirements.

Core and CPS. To increase the core power, the outside diameter of the fuel pins has been reduced from 10.2 to 9.1 mm, while the number of pins in an assembly has been increased. The reactivity margin in the first reactors was compensated by mechanical CPS. Starting with the third unit at Novyi Voronezh station, the reactivity margin compensating for burnup was compensated along with slow reactivity changes by introducing boric acid into the coolant, which reduced the number of mechanical CPS units in the VVÉR-440 from 73 to 37.

MCP. Originally, the units were fitted with low-inertia sealed pumps working at 1500 rpm, which were supplied when the external line was disconnected from the turbine generator.

365

In the VVÉR-1000 and the later designs of power stations containing VVÉR-440, pumps are used in which surges are absorbed by a special flywheel.

Steam Generators. The main design changes have been related to providing access to first-circuit collectors for examination and maintenance of the tube-mounting points directly from the central bay, and there have also been improvements in the collector unit at the boundary between the water and steam in the second circuit.

Safety Systems. In the first VVÉR, the maximum design emergency was taken as the instantaneous failure of a pipeline of diameter about 100 mm bearing a unilateral flow. In the current VVÉR-440 and VVÉR-1000, the protection and localization devices provide safety in emergencies extending to instantaneous failure of the main circulation pipe coinciding with complete current failure. Systems are also envisaged for emergency core cooling (hydraulic vessels connected in pairs to the inlet and outlet pipelines, with groups of low-pressure and high-pressure pumps), which prevent the fuel-pin sheath temperatures from rising above 1200°C.

Fission products escaping from the main circulation loop are localized in new power stations containing VVÉR-440 units by a system of sealed boxes, in which the maximum pressure is 0.15 MPa. It is guaranteed that this pressure is not exceeded by condensing the steam during the first period of a maximal design emergency using a special bubble condenser.

In power stations containing the VVÉR-1000, there is a protective containment around all the sections of the main circulation circuit and the reactor hall, which is designed to withstand a total pressure such as would arise from the escape of all the coolant (0.4 MPa) with provision for reducing it with a sprinkler system. A high level of independence is also provided in the duplicated protective and localizing systems by locating them in different buildings with separate power supplies etc.

THE UNIFIED PROJECT

A unified project has been drawn up for nuclear power stations containing VVÉR-1000 reactors. This design provides for flow production of the units and should substantially reduce the installation time, which will greatly increase labor productivity because the same operations are reproduced and are executed by specialized teams. The main and auxiliary items of equipment have been standardized to provide power stations with similar designs no matter where the equipment is manufactured, which will also increase labor productivity by leading to longer runs. The start of flow production began at Zaporozhe power station, where four reactor units are being installed simultaneously. Single-block styles were used for the first time in Soviet power stations, which eliminates the gap between the reactor and machine sections, and this reduces the loss in steam parameters and increases the unit power by 6 MW. The turbines have been fitted with modified condensers, which has reduced the size of the machine bay by 3 m. These and other design modifications have reduced the volume required for the main housing by 20%, with the consumption of reinforced concrete reduced by 6%, building labor involved by 30%, equipment mass by 9%, and pipelines by 12%. The unified project differs from the fifth unit at the Novyi Voronezh station also in having better physical characteristics. The number of control and protection units has been reduced from 109 to 61, while the number of absorbing components in one unit has been increased from 12 to 18, while the number of fuel-pin assemblies has been increased from 151 to 163 because jackets have been abandoned.

The Atomic Heat and Electricity Design Institute has compared the unified project for power stations containing VVÉR-1000 with foreign power stations. This has shown as follows:

1. The specific working area of analogous foreign power stations (France and the Federal German Republic) is less by 34-35% than that in the unified project because the principles used in determining these areas differ particularly as regards the set of buildings and structures required for auxiliary and maintenance services (there is no nitrogen-oxygen system or acetylene station with stock of carbide, nor are there mechanical maintenance workshops and stores). Also, foreign nuclear power stations are often built without access to railroad transport, which also reduces the area required.

2. A comparison has been made of volume characteristics for the reactor sections in the unified project and for power stations in France, the USA, and the Federal German Republic, which has shown that stations such as Paluel and Belfonte are substantially better (specific volumes 14% less, consumption of reinforced concrete and metal 30-35% less). In

366

these stations, there is high unit power in the main equipment within dimensions enabling one to fit them into the same building volumes as the unified project for the VVÉR-1000. The reductions in reactor-section volume in power stations such as Bouget and Tricastin has been attained also be using reactors with three circulation circuits and vertical steam generators. At the Mulheim-Kerlich and Biblis stations (in the Federal German Republic), better parameters have been obtained in particular because more compact electrical engineering and ventilation systems have been employed. In all cases, foreign power stations use closer spacing in the reactor section, which adversely affects maintenance and servicing on site.

3. The unified project differs considerably from the Biblis power station regarding volume of the machine bay: respectively, 300 and 150,000 m^3. This very substantial difference occurs because the turbines at Biblis are much smaller, as at most foreign nuclear power stations, including as regards the diameter of the low-pressure cylinders, while the numbers and dimensions of the separators, steam superheaters, and regenerative heat exchangers have been reduced, while the low-pressure heaters are built into the condenser connecting pipes and do not occupy any additional volume.

A substantial difference also is that foreign power stations provide minimal maintenance areas in the machine bay, in particular because the equipment is installed without modification at the building site (on wheels).

4. The area of special facilities is estimated as 7800-8200 m^2 for foreign stations and 9500 m^2 for the unified project, the difference being due to foreign stations not having long-time stores for radioactive wastes and having much smaller volumes of domestic accommodation and also the absence of laundries.

The unified project is inferior on specific parameters to foreign power stations also on certain auxiliary equipments, which is due primarily to the numbers of operating and maintenance staff, whose accommodation requires additional buildings, medical services, etc.

On the whole, this comparison of the unified VVÉR-1000 project with foreign stations has shown that the design parameters are comparable with current levels. Nevertheless, the designs for Soviet power stations still leave some margins that should be utilized in the next generation of designs.

SCOPE OF IMPROVING UNIT POWER ECONOMIC PARAMETERS

At present, various research and development organizations in the country are examining three basic ways of providing essentially new designs capable of giving a new level of economic performance in power stations containing VVÉR: fuel-cycle improvement, reactors with supercritical coolant, and substantial increases in unit power.

We consider the last of these as it is most fully developed. As traditional VVÉR have attained a high level and nearly optimum values have been obtained for parameters such as coolant pressure, steam production, and power level, one of the ways for improving reactors of this type is to increase the unit power substantially. All previous power-engineering developments in this country and abroad have been accompanied by the enlargement of power stations.

The main factors responsible for this tendency are firstly the economic advantages of concentrating production deriving from increased labor productivity, as is characteristic of other branches of heavy engineering, and secondly the difficulties in providing the required rates of increase in installed power without increasing unit power levels. However, as in thermal power stations, increasing the unit power on nuclear systems not only reduces the specific capital costs per station but at the same time adversely affects the system reliability, and to maintain this at a fixed level there must be additional costs involved in increasing the emergency backup and maintenance facilities. Therefore, increasing the unit power, including in nuclear systems, is effective only if the reduction in the specific power-generation costs is at least not less than the costs for providing the additional backup. This problem will have to be dealt with in the designs presently being drawn up by the Atomic Thermal Electric Project Organization for a unit containing VVÉR-1500 reactors.

LITERATURE CITED

1. F. Ya. Ovchinnikov et al., At. Énerg., 54, No. 4, 249 (1983).
2. L. Howles, Nucl. Eng. Int., 28, No. 347, 36 (1983).

367

STATE-OF-THE ART AND DEVELOPMENT PROSPECTS FOR
NUCLEAR POWER STATIONS CONTAINING RBMK REACTORS

E. V. Kulikov   UDC 621.039.577

Over a comparatively short period, there has been a substantial increase in the generating capacity in the country on account of nuclear stations containing RBMK-1000 reactors, which have been rapidly run up to nominal power and which have provided stable and safe operation, so one can say that this reactor type is promising for nulcear engineering in the next few decades. The following advantages are responsible for the major plans for building nuclear stations containing RBMK [1]:

1) the RBMK units and equipment are made at existing plants in the country and have not required, apart from construction in Yugoslavia, the building of new industrial organizations with the unique equipment for making large components working at high pressures;

2) for these reactors there are virtually no limits to the unit power associated with the manufacture, transportation, and installation;

3) the branching in the circulation system increases the overall safety because it eliminates a complete coolant loss from the core and enables one to build reliable protection systems and devices for localizing leaks;

4) the good physical characteristics of the reactor and the continuous fuel recharging make it possible to provide efficient use of low-enriched fuel together with extensive burnup giving low contents of fissile uranium isotopes in the spent fuel, and in addition there is a fairly substantial increment in the burnup as a result of the incidentally produced plutonium; and

5) the high reliability in the heat-engineering units is supported by wide parameter control ranges with monitoring in each channel.

The basis of a nuclear station containing RBMK is provided by two units of electrical power 1000 MW each with a common machine hall. Each unit is a reactor with its circulation system and auxiliaries, steam and condensate-feed units, and two turbine generators of power 500 MW each. The essential scheme of a unit is shown in Fig. 1.

The reactor is located in a concrete pit on welded metal structures, some of which are used simultaneously for radiation protection, and which in conjunction with the jacket form a sealed space filled with helium-nitrogen mixture (the reactor space), in which the graphite stack is located. The stack contains the fuel channels (FC) and the CPS channels, which run through the upper and lower metal structures.

A fuel channel (Fig. 2) is a welded tube construction intended to take a fuel assembly (FA) and to organize the coolant flow. The upper and lower parts of the channel are made of stainless steel, while the central part within the core is made of zirconium-niobium alloy having good mechanical parameters and corrosion resistance together with a low neutron absorption cross section. The central part of the channel is coupled to the upper and lower ones by special couplers.

Twelve units containing RBMK-1000 are now operated: 4 at Leningrad Lenin nuclear power station, 4 at Chernobyl, 3 at Kursk, 1 at Smolensk, and 1 unit containing an RBMK-1500 at the Ignala nuclear station. The overall installed power of nuclear stations containing RBMK is over 60% of the total nuclear power in the Soviet Union. These nuclear stations have very good performance parameters, on which they are in no way inferior to the best nuclear power stations in the most developed countries in the World. As an example, Table 1 gives the economic parameters of the units at Leningrad and Kursk stations.
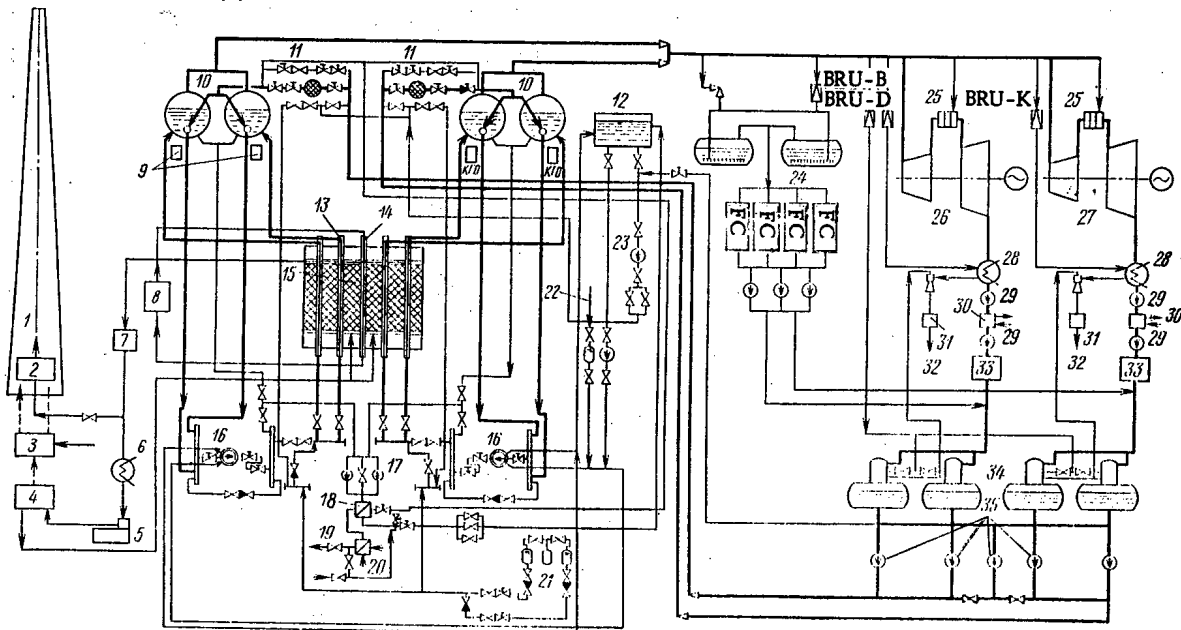
Fig. 1. Scheme for a nuclear station containing RBMK-1000: 1) stack; 2) wet gas holder; 3) delay gas holder; 4) helium purification system; 5) compressor; 6) gas loop condenser; 7) FC integrity monitoring system; 8) pumping and heat transfer system in CPS; 9) cladding sealing monitoring system; 10) separator; 11) control unit; 12) emergency feed pump tanks; 13) FC; 14) CPS channel; 15) reactor; 16) MCP; 17) cooling pumps; 18) regenerator; 19) pipe to purification system; 20) cooler; 21) emergency reactor cooling system; 22) compressed air; 23) emergency pump; 24) technological condensers; 25) superheaters and separators; 26 and 27) turbine generators 1 and 2; 28) condensers; 29) KN-1 condensate pumps; 30) condensate purification; 31) apparatus for burning explosion mixture; 32) pipeline to delay gas holder; 33) low-pressure heaters; 34) deaerators (0.7 MPa); 35) electric feed pumps.

The high reliability of the RBMK-1000 is confirmed by the operation of the units for 52-reactor-years and is indicated by numerous research studies, calculations, and design studies performed in the early stages of operating the units. Improved reliability in fuel recharging with the reactor working has been provided by modifying the sealing plugs in the FC, the ball flowmeters, and the control valves, while upgrading in the units within the containment has extended to the separator drums in the main steam pipes, which has provided more uniform loading on the separator drums and the required steam wetness under stationary and transient conditions.

Reliable core cooling is provided when there is emergency reduction in the feedwater flow rate, which can extend as far as complete stoppage, is provided by an automatic system for reducing the power involving constant automatic comparison of the thermal power with the feedwater flow rate [2]. Many experiments have been performed at the Leningrad station to determine the cooling parameters arising from the natural circulation directly with the unit working, which have shown that previous calculations and testbed results are reliable, and this has provided proposals for means of switching off the main circulation pumps MCP at an appropriate time and for accelerating the turbine unloading. The final stage in the research on the natural circulation conditions was carried out at the Kursk station in 1981.

Nuclear stations containing RBMK have safety systems that eliminate any hazardous escape of radioactive material even in the case of unlikely accidents, including failures in major pipelines [1]. From this viewpoint, the main hazard lies in failure in the pressurized MCP pipeline, since this halts the flow of coolant to the FC in the half of the reactor affected by the emergency. This hypothetical accident determines the characteristics of the emergency cooling system (ECS), including the response rate of this and the maximum capacity.

The water from the ECS is supplied to each distributing group collector (DGC), and to avoid water escaping through the failed section there are nonreturn valves at the inlet to

369
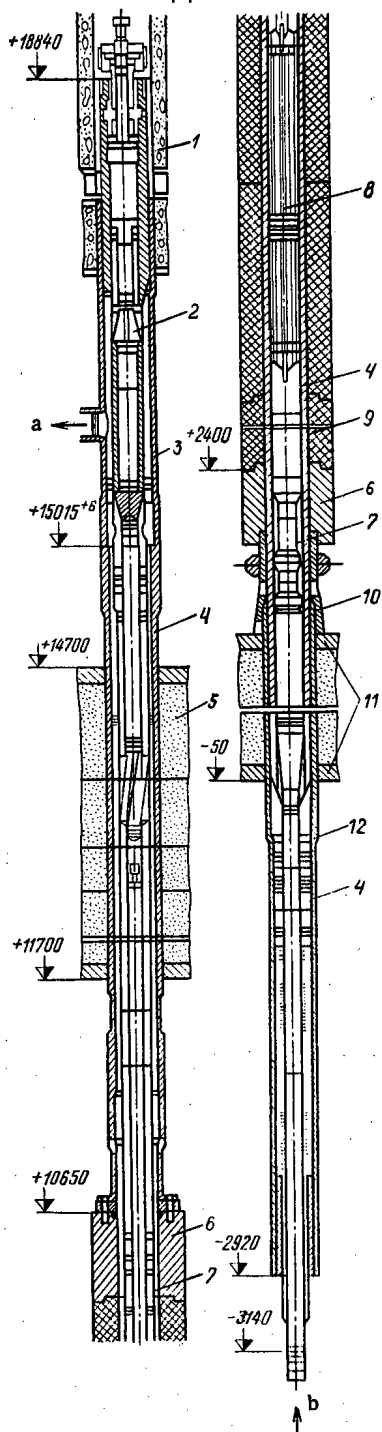
Fig. 2. A fuel channel: 1) protec-
tion unit; 2) FA suspension; 3) FC
head; 4) pressure tube; 5) upper
protection plate; 6) thermal shield;
7) steel—zirconium joint; 8) FA; 9)
stack block; 10) supporting vessel;
11) lower plate; 12) channel sec-
tion; a) steam—water mixture outlet;
b) water inlet.

TABLE 1. Economic Parameters in the Oper-
ation of Nuclear Units Containing RBMK-
1000

Nuclear station	Unit	1982		
		power pro-duction, million kW·h	PUF, %	eff., [*] net, %
Leningrad	1	6185,6	70,6	28,74
	2	7864,7	89,8	29,58
	3	7007,9	80,0	28,38
	4	7298,1	83,3	29,19
Kursk	1	7548,7	86,2	29,98
	2	6305,0	72,0	29,36

Nuclear station	Unit	1983		
		power pro-duction, million kW·h	PUF, %	eff., [*] net, %
Leningrad	1	7739,4	88,3	29,51
	2	7356,9	84,0	29,20
	3	6234,7	71,2	29,23
	4	7487,8	85,5	28,78
Kursk	1	7237,5	82,6	28,96
	2	6183,5	70,6	28,26

[*]Without allowance for heat use.

the DGC. The ECS consists (Fig. 3) of a major subsystem containing hydraulic accumulation
unit and a long-time cooling subsystem having special pumps and water stocks in tanks. The
cooling water is passed through pumps to the ECS collector in each half of the reactor and
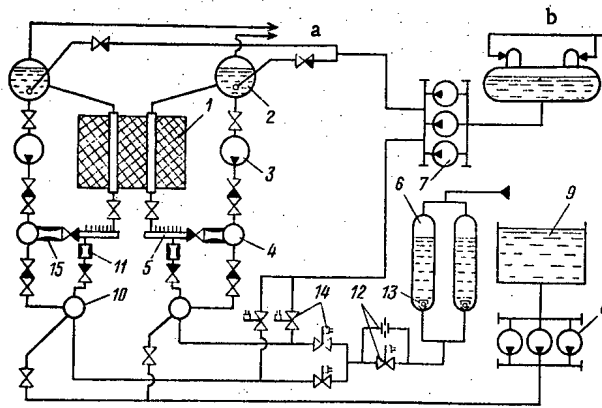
Fig. 3. Essential scheme for circulation loop and ECS:
1) reactor; 2) separator; 3) MCP; 4) pressurized collector; 5) DGC; 6) hydraulic accumulation unit in ECS; 7) feed pump; 8) ECS pumps; 9) water stock in condensation device; 10) ECS collector; 11) restriction nozzle; 12) intermediate throttling link; 13) cutoff float valve; 14) fast ECS valve; 15) DGC insert; a) steam to turbines; b) condensate return.

then along pipes to each DGC. Fast slide valves are mounted in the water feedlines and collectors, which open when the signal to actuate the ECS arrives. The algorithm for activating the main subsystem in the ECS provides for cooling the core when there is complete or partial failure in large pipes and eliminates incorrect operation in accidents not involving failure in the circulation loop.

The RBMK gives extensive burnup with low initial enrichment, which is provided by continuous fuel recharging with the reactor working. In all the nuclear stations containing RBMK, there is ongoing fuel recharging at power by means of an unloading and loading machine. The continuous-recharging mode enables one to roughly double to burnup by comparison with complete fuel change in one operation. The ^{235}U concentration is reduced from 18–20 to about 3.7 kg per ton of uranium, while the amount of fissile plutonium attains about 2.8 kg per ton uranium. This change in isotope composition results in substantial changes in the core neutron physics characteristics.

In the steady recharging state, only the local characteristics such as the power in the channels alter, while the characteristics of the reactor as a whole remain virtually unchanged, whereas during the first operation of the reactor loaded with fresh fuel and additional absorbers, there are fairly substantial changes in the physical characteristics, in particular in the reactivity coefficients (steam and temperature ones). The values of these coefficients are dependent not only on the fuel isotope composition but also on the number of absorbers in the core. Experience with the RBMK-1000 has confirmed the theoretical conclusions that the reactivity coefficients increase and that the stability in the power distribution decreases as the fuel burns up and the absorbers are extracted. The radial-azimuthal energy distribution is the least stable, where the form of the nonstationary deformation is determined by several of the lower harmonics. The distribution is stabilized in two ways:

1) improving the automation level by means of a branched reactor control system; and

2) increasing the fuel enrichment.

Under the first approach, essentially new systems have been introduced for local automatic control of the power distribution (LAC) and local emergency protection (LEP), which operate from transducers within the core [3]. The LAC system automatically stabilizes the lower harmonics in the radial-azimuthal distribution. This system maintains the overall set reactor power level, by using individual effectors to provide automatic power control in the individual core regions. The LEP system provides for emergency power reduction when there are impermissible local power rises, in spite of the action of the LAC. The LAC and LEP use groups of effector mechanisms (from 7 to 12 of them) uniformly distributed over the core and containing control rods each surrounded by two LAC transducers. The averaged and corrected
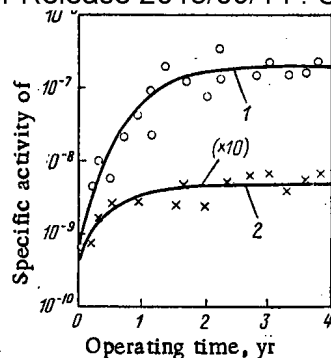
Fig. 4. Distributions of radioactive
products in deposits (Ci/cm^2) (1) and
in coolant (Ci/kg) (2).

signal from the LAC transducers is used to control the rods. The transducers in the LAC—LEP
system are triaxial chambers placed in central sealed sleeves in the FA.

Calculations on the performance expected from the second approach have shown that in-
creasing the initial ^{235}U content of the fuel improves not only the dynamic parameters but
also the economic characteristics by increasing the extent of burnup and reducing the specific
fuel consumption. It has been found that there is a substantial dependence of the time con-
stant for the first azimuthal harmonic on the steam reactivity coefficient. The less the
positive steam reactivity coefficient, the higher the power distribution stability and the
simpler the reactor control. The most rational way of reducing the steam coefficient is to
increase the ratio of the ^{235}U concentration to the moderator concentration in the core. The
reduction in the steam coefficient as a result of going to fuel with 2% enrichment is about
1.3 β.* These conclusions served as basis for increasing the RBMK enrichment.

We give below the basic characteristics of the RBMK-1000 fuel cycle for 1.8% and 2%
initial ^{235}U contents (first and second values correspondingly):

Uranium burnup, MW·day/kg	18.5	22.3
Final ^{235}U content in unloaded fuel, kg/ton	3.9	3.5
Reduction in steam reactivity coefficient, β	–	1.3
Annual input of enriched uranium, ton/GW (with PUF = 0.8)	50.5	42
Annual consumption of fuel pins to supply reactor (with PUF = 0.8), 10^3 per GW	16.0	13.3
Annual consumption of natural uranium, ton/GW*	169	158
Mean FA use, effective days	1100	1350

*With PUF = 0.8 and ^{235}U content in spent fuel of 2–3 kg/ton.

Since the first unit at Leningrad station began to operate, there has been continuous
monitoring of the radiation environment at the station and in the surroundings, which has
confirmed that the design is correct and has provided detailed data required in upgrading the
radiation safety systems in stations containing RBMK. These studies have shown that the ir-
radiation of the station staff on average is considerably below the permissible level: the
annual dose for over 35% of the operating staff does not exceed 0.2 ber, and only for 2% is it
between 4 and 5 ber. The collective dose to the staff in one unit after about 5 years of op-
eration was about 700 man-ber (1 ber = 10 mSv), which is virtually the same as the dose at
foreign nuclear stations of the same power. The largest contribution to the irradiation
(40–50%) comes from prophylactic maintenance operations and operations associated with mon-
itoring the metal; up to 60–65% of the dose to the station staff is due to operations dur-
ing prophylactic or major servicing, i.e., with the reactor shut down.

_____
*β is the effective proportion of delayed neutrons.

372

Fig. 5. Block construction of the control room at Ignala nuclear power station.

Fig. 6. Loading the RBMK-1500 with fuel at Ignala power station.

373

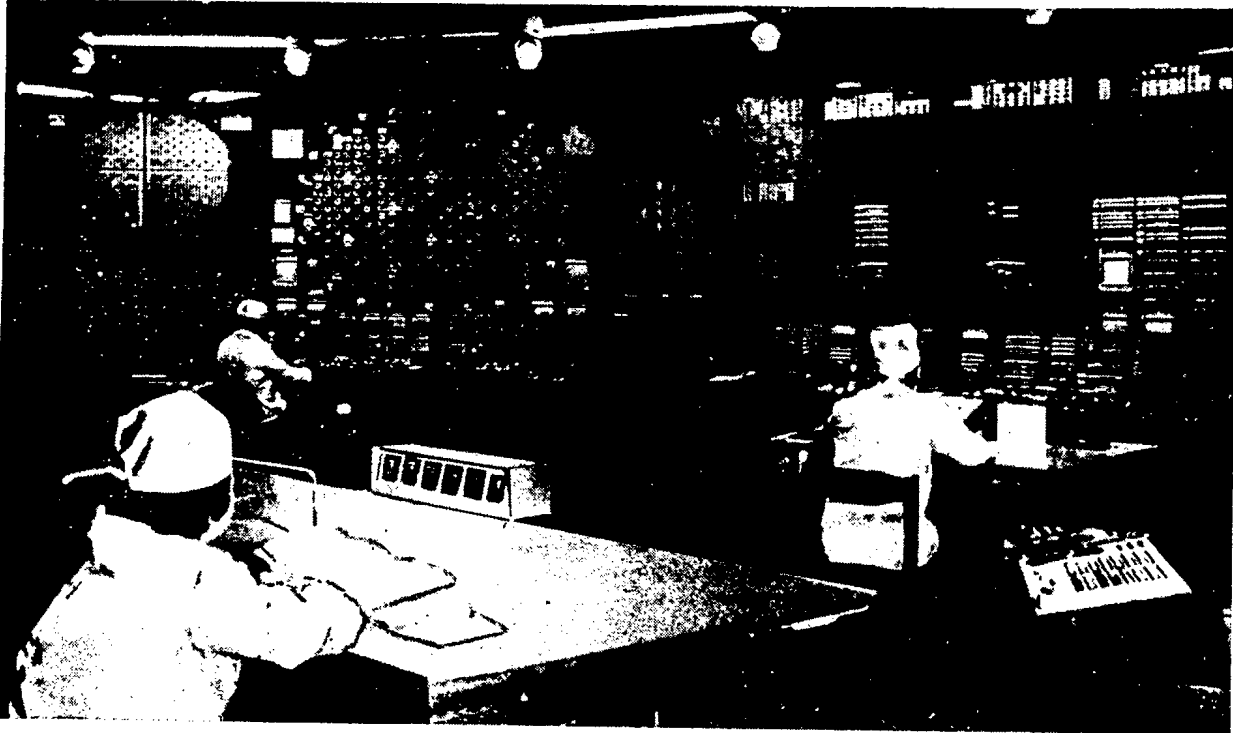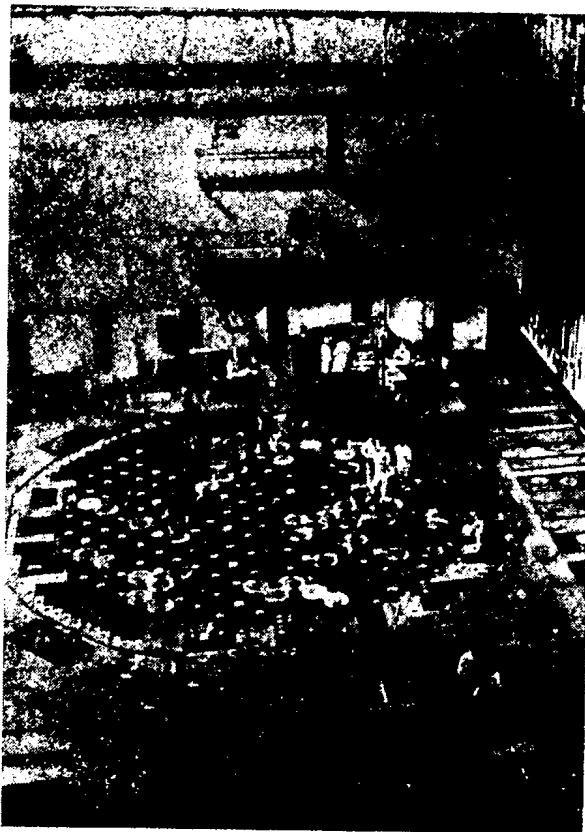During this period, the radiation environment around the first circuit is determined by the emission from radioactive corrosion products deposited on the inner surfaces (Fig. 4). The contributions from the γ rays from different nuclides to the dose rate vary during the operation, and after about 5 years the radiation environment is determined by the γ rays from ^{60}Co. The deposits on the equipment contain fission products, but their contribution to the γ-ray dose rate is not more than 10-15% on operating the station for 10 years.

During the entire period of operation for nuclear stations containing RBMK-1000, there have been no instances where the discharges of radioactive gases and aerosols have exceeded the permissible values laid down by SP AÉS-79 (or the earlier SP AÉS-68). As the permissible discharges have not been exceeded, the radiation background in the surroundings is satisfactory. Direct measurements on the γ-ray dose rate in the locality indicated no increase over the natural background throughout the area.

The definitive parameters restricting RBMK power are the fuel temperature, the temperature of the graphite and the metal construction, and the margin from the heat-transfer crisis. These parameters have not yet attained the limiting permissible values at existing RBMK-1000 reactors.

The margins of the temperature of fuel, graphite, and metal have led to the suggestion of building a more powerful reactor based on the RBMK-1000 without change in general design and dimensions. This requires a design that enables one to increase the critical channel power without changing the dimensions or number of the FA, i.e., to increase the margin up to the heat-transfer crisis. The solution is seen as FC with heat-transfer intensifiers. A design has been developed for a new FC for the RBMK-1500 with special devices enabling one to increase the heat loading, which is characterized by a high level of standardization in the units based on RBMK-1000 ones. This means that the production of FA of a single type will not only simplify the process by reducing the number of different types to be produced but will also give a considerable economic gain from using the new FA in existing RBMK-1000, which will increase the core reliability, improve the stability in the power distribution, and raise the fuel burnup. The FA with intensifiers enable one to increase the thermal power of these by 20-25% in the RBMK-1000 with separator drums of diameter 2600 mm. This broadens the scope for the wider use of the reactors in district heating.

The RBMK-1500 at the Ignala power station has been commissioned and is being run up to nominal power, the unit electric power being over 1500 MW. This unit has represented a start on a new generation of channel reactors, as more economical ones should ultimately replace the highly successful 1000 MW ones. Stations containing RBMK-1500 will reduce the specific capital investment by 20-30% relative to ones containing RBMK-1000 and will also reduce the fuel costs. Experience with designing, building, and operating the RBMK boiling-water reactors has shown that the correct decision was taken on building a large series of nuclear stations containing reactors of this type, and that there are good prospects for developing them further.

LITERATURE CITED

1. N. A. Dollezhal' and I. Ya. Emel'yanov, A Channel Nuclear Power Reactor [in Russian], Atomizdat, Moscow (1980).
2. I. Ya. Emel'yanov, S. P. Kuznetsov, and Yu. M. Cherkashov, At. Éner., 50, No. 4, 251 (1981).
3. I. Ya. Emel'yanov et al., ibid., 49, No. 6, 357 (1980).
4. A. P. Aleksandrov and N. A. Dollezhal', ibid., 43, No. 5, 337 (1977).

STATE-OF-THE ART AND DEVELOPMENT PROSPECTS FOR NUCLEAR
POWER STATIONS CONTAINING FAST REACTORS

O. D. Kazachkovskii

The scope for extending nuclear fuel breeding in fast reactors was predicted in the 1940s. In essence, this was a conceptual extrapolation from thermal reactors to fast ones on the basis of the scanty experimental data then available, i.e., the parameters of the interaction of fast neutrons with matter. Subsequently there were studies designed to confirm or reject this suggestion. It should be noted that these studies began before the first nuclear power station in the World had been commissioned, when it had not yet been shown that nuclear power stations were really feasible. However, the importance of the problem led to considerable effort being devoted to determine the scope for extended breeding. In essence, this corresponds to a requirement in the scientific revolution: the transition to operations in a new stage need not wait on the end of the previous one, since otherwise rates of progress would be inadequate. An unambiguous positive solution was obtained at the end of the 1950s, when it was established that the breeding factor in a fast reactor can be greater than one. This meant that fast reactors in principle allow one to use all of the mined uranium. The raw-material base for nuclear power was thereby increased by factors of tens or hundreds relative to the case where only thermal reactors are used.

The next stage involved determining the engineering feasibility of industrial fast reactors. This was concerned mainly not so much with construction of high-power fast reactors but instead the commercial fast reactors meeting certain requirements, particularly from the viewpoint of fuel-cycle economy: heat production density of 500-1000 kW/liter of core, and burnup of 10% of the heavy atoms in a run of more.

Right from the start, researches on fast reactors were directed to using sodium as the coolant. Water is unsuitable for fast reactors because of its nuclear-physics parameters. Sodium on the other hand has good thermophysical parameters and acceptable nuclear-physics characteristics. An important point also is the high boiling point (about 900°C), which means that a sodium-cooled reactor does not need to use high pressures, which is a considerable advantage from the engineering viewpoint. Also, simultaneously but mainly incidentally one attains a considerable advance in efficiency by comparison with a water-cooled reactor. For some time there was also a discussion on the use of sodium-potassium eutectic, although this is worse in thermophysical properties and was found to be less suitable than sodium. Therefore, one was involved in developing an entirely new industrial technology for using sodium as a coolant. The problem was solved in a short period. In any case, it was shown that there were no essential difficulties in setting up a large-scale industrial sodium technology.

At the start of the 1960s, when the BN-350 began to be developed as the first commercial fast reactor, an experimental fast reactor with sodium cooling, the BR-5, had already operated at Obninsk. The thermal power of this was only 5 MW, whereas the design thermal power of the BN-350 was 1000 MW. It must be emphasized that this was a very large step, which was not decided on at once, but it corresponded to the general requirements in the scientific revolution and the requirements for rapid devleopment. It is true that apart from the power level, the BN-350 parameters were moderate: the coolant temperature, the temperature of the working body (steam), and the pressure were low. This was deliberate, since one of the main purposes of the reactor was to determine the effects of the scale factor on the working characteristics of such systems while avoiding any additional difficulties. Almost simultaneously, work began on the BOR-60 research power reactor, which was designed to have operational determinations of the effects from high power levels, high temperatures, and other factors on the working characteristics of fast-reactor components and to define reasonable safety margins for the engineering parameters. The development of the BN-600 began

---

somewhat later. This was already a reactor with high and not excessively conservative thermal parameters. At the same time, the power was such as to approach the basic parameters of future standard fast reactors.

The BN-350 began to work at full power in June 1973, and the BN-600 in April 1980.

It is now possible to survey the operation of both reactors. Firstly, the design values were attained for physical parameters such as the critical mass, the distribution of heat production over the core, and the kinetic, thermophysical, and hydrodynamic characteristics. The basic engineering parameters also corresponded to the design values, apart from the power in the BN-350, whose nominal value was set somewhat below the initial design value on account of difficulties with the steam generators. At present, the BN-350 is operated at 720 MW (thermal) with the following parameters:

Electrical power, MW	up to 130
Distillate output, kg/sec;	1000
Sodium Temp., °C:	
at reactor inlet	283
at reactor outlet	425
Superheated steam pressure, MPa	4.5
Maximum burnup, MW·day/kg:	
in low-enrichment zone	54
in high-enrichment zone	60
Power use factor, %	∿ 88

The refined neutron-physics characteristics and other data obtained during the operation of the BN-350 provided a basis for modifying the core and screen reloading programs. Improvements in the CPS increased the working time between reloading cycles from 54 to 73.5 days. The burnup was thereby increased by about 15% relative to the design value.

The basic working parameters of the BN-600 are as follows:

Electrical power, MW	600
Sodium Temp., °C	
at reactor inlet	377
at reactor outlet	550
Superheated steam pressure at turbine inlet, MPa	12.7
Maximum burnup, MW·day/kg:	
in low-enrichment zone	41.0
in high-enrichment zone	61.0
Power-use Factor, %	∿71.8

The equipment in the sodium system (apart from the steam generators) worked almost entirely without faults in both of these reactors. In essence, the failures and unplanned shutdowns were due to the third loop (steam-water one).

The scale factor was substantial in relation to the steam generators. In the BN-350 and BN-600, there were water leaks into the sodium and corresponding failure in some steam generator sections. These failures were not due to any essential features of the steam generators, but they were due to the development of defects or rather to the nuclei of defects at welding points, which on account of their smallness could not be observed by monitoring during manufacture. An essential point was that the defect growth rates up to a certain critical size became large. This required the introduction of especial systems for early defect diagnosis. This also imposed certain requirements as regards promptness in action by the staff. Failure in the steam generators did not lead and could not lead to any catastrophic consequences. The instances of steam generator failure in either reactor occurred during the initial period of operation, essentially in the running-in period. The subsequent operation was free from faults. Nevertheless, there remains the problem of improving the reliability, or rather improving the degree of detection of defects during manufacture and also the scope for correcting errors and mistakes during operation. Here there is obvious scope for applying design improvement and for using more suitable materials for the pipes.

376

The scale factor also made itself felt to some extent in relation to the BN-600 fuel pins, which work under heavy stress. The working life of the pins and correspondingly the burnup are at present less than the planned values. Here there are some major factors characteristic of fuel-pin working conditions in fast reactors, including some that were not known in advance. Some constraints at present are imposed by the vacancy-swelling effect in constructional materials produced by intense fast-neutron fluxes.

Further improvements in fuel-pin life are based on advances in constructional materials. One can safely say that it is possible to improve the working life by a substantial factor, but the researches and the tests on the systems inevitably require long time, and in addition the studies after irradiation in hot laboratories are usually laborious and lengthy. This means that measures have to be taken to substantially expand the scale of the operations.

It can thus be said that clearly that the engineering feasibility of commercial fast power reactors has been demonstrated. After a certain initial startup period (which was very short for the BN-600), both reactors have been operated reliably with large power-use factors.

There are two major technical problems requiring research in order to improve the working characteristics of fast reactors further: improving fuel-pin life and increasing steam generator reliability.

The future fast-reactor development program must be based on the economic parameters. Economic aspects are ultimately always the last and final criteria for the desirability of the large-scale development in any area. Here the situation is as follows. Of course, we cannot determine the economic performance of future large standard commercial fast reactors by extrapolation from existing stations with any great accuracy. Inaccuracies always appear in extrapolation. However, at present we can say that the present fast reactors are foreseen as developing much the same thermal power per specific capital cost; an exact figure cannot be given but one can speak of a difference of 30-40%.

On the other hand, the fuel component for the fast reactor is less, since the fuel breeds at a higher rate than in a thermal reactor. Estimates in relation to the fuel component are even less reliable, since at present there is no experience with routine commercial fuel reprocessing. However, it seems that one can conclude that existing prices for natural uranium mean that the advantage over the fuel component (relative to thermal reactors) cannot compensate for the disadvantage over specific capital costs. In the future, as the cost of natural uranium rises, the cost relation will steadily improve in favor of fast reactors. At some time there will be an inversion, and fast reactors will be economically better than thermal ones. No date for this can be given. It should however be remembered that the working life of a nuclear power station is long at 30-50 years. As this life is long, it will be economically desirable to include fast reactors extensively in the nuclear power program before the time of economic inversion has been reached. On the other hand, it should be borne in mind that there are certain and by no means minor opportunities for reducing the specific capital costs. This scope is bettter for fast reactors than for thermal ones. Fast reactors have high efficiencies, which are almost 30% more than for thermal ones, which is already a great advantage. There is no particular point in raising the thermal parameters. Although the efficiency then increases somewhat, the specific capital costs will most probably not thereby be reduced but increased. However, the main point is that raising the temperature substantially reduces the fuel-pin life. Here one expects a sharply varying relationship, and this will certainly have a very adverse effect on the fuel component. On the other hand, it is desirable to increase the unit power, since the specific capital costs are thereby reduced. Fast reactors enable one to raise unit power, since they are compact and do have have pressures within the containment. One can say that it is already technologically possible to make fast reactors of power 2000 MW and more. Therefore, it is better to compare fast and thermal reactors not at identical power levels but at the power levels that are accessible with the existing manufacturing technology. Finally, there is scope for improving and simplying fast reactors, which extends to abandoning the intermediate circuit, heating the main pipelines, etc.

It should however be noted that although the unit power will increase, we at present cannot envisage and probably for a long time will not be able to envisage enlarging the steam generators in fast reactors. At present, the nuclear station containing the BN-600 employs a modular principle, with many sections (modules) of comparatively low power. When a module

fails, it is switched out without shutting down the reactor, as has been demonstrated with the BN-600. Then the module is replaced by a new one during the next planned preventative maintenance. The modular principle has been found to be fully justified and should be used in the future.

As regards the fuel cycle, a solvent-extraction technique has been developed for reprocessing the fuel rods. This will evidently be used in the first stage of large-scale fast-reactor development. It may be that a nonaqueous technique will subsequently be devised. Here there are no criticality constraints, and the wastes are obtained at once in solid form, which opens up good scope for shortening the external fuel cycle. It is possible that nonaqueous technology may not provide a sufficiently high degree of purification, but this is not necessary from the physics viewpoint, since the fast-neutron absorption cross sections in fission products are comparatively small. Instead, remote handling is required for the fuel. On the other hand, the inherent activity of the recirculated plutonium will be so high that remote handling will always be used. Also, the large scale of fuel-pin manufacture in the future will necessarily require automation, which naturally fits in well with remote handling.

We now consider the breeding rate. A breeding factor greater than one is already good, and this is the essential feature that distinguishes the scope for using all mined uranium completely from the partial use. However, higher values are desirable, because of the need for self-sufficiency in fuel in developing nuclear power. The required breeding rates at various stages may differ. Evidently, in the first stage the breeding rate should be high, in order that such reactors can rapidly take over a considerable part of the total nuclear power program. In the first stage, it is not essential to provide self-sufficiency in fuel, since the plutonium accumulated in thermal reactors can be used to fuel new fast ones. Plutonium is most valuable when it is used in fast reactors. It is clearly undesirable to burn it in thermal reactors. It is thus very necessary for the first stage, the stage where fast reactors take on an asymptotic mode of development. It is also possible that to fuel them, i.e., to provide the initial loading for new nuclear stations, one should use enriched uranium if the rate at which new capacity is introduced is high. Here one must remember that we have a certain enrichment capacity for thermal reactors, and this capacity can be used for fast reactors when these become the main line of development.

When the asymptotic growth mode has been attained for fast-reactor power, the rate will be determined by the required rate of power engineering development. Fast reactors could provide asymptotic development with self-sufficiency. It is also possible that they will be required to produce additional plutonium for other power systems such as thermal reactors not working in baseload mode. It is also possible that additional fuel will be required for commercial high-temperature reactors, etc. Fast reactors should be capable of providing this additional plutonium. It is true that in that case one cannot speak of the breeding rate, since this rate is the ratio of the excess plutonium produced to the total load in the cycle of a fast reactor. If the plutonium is diverted to other uses, there is no need to calculate the breeding factor, and it will be incorrect to refer the amount of excess plutonium is diverted to other uses. There is no need to calculate the breeding factor, and it will be incorrect to refer the amount of excess plutonium to the load in a cycle.

The breeding rate is determined primarily by the breeding factor and the specific heat production, i.e., the specific power per unit amount of fuel. The latter is controlled mainly by the scope for cooling the core and by the acceptable thermal stress on the fuel pins and does not exceed 1000 kW/kg of fuel. The breeding factor is also dependent to a substantial extent on the form of the fuel. When fast reactors began to be developed, they were oriented to a use of uranium-plutonium metal fuel. However, it soon became apparent that there were difficulties with metal fuel: swelling of the uranium and hazardous interaction between the metal fuel and the cladding. It was therefore necessary to abandon this temporarily and to use ceramic oxide fuel, which is less satisfactory from the viewpoint of the fuel breeding coefficient. There was a large reduction in the breeding factor because of the neutron moderation at the oxygen and the reduced fuel density. An important task is to increase the burnup, which is also important from the viewpoint of improving the breeding rate. The larger the burnup, the greater the fraction of plutonium formed in that run that is burned and correspondingly accelerates the breeding. The time spent in the external fuel cycle is also economized, and there are benefits over the chemical processing and fuel-pin manufacture. Table 1 gives some parameters characterizing the performance from extensive burnup.

378

At present, all these reactors here and abroad are designed to use ceramic oxide fuel, but studies on metallic uranium have not stopped, and it is currently evident that it should be possible to attain the necessary fuel-pin parameters with metallic fuel. In that case, one could provide a breeding factor up to 1.8-1.9, which would satisfy any concealable fuel requirement in the future. If all the same the transfer to metallic fuel is held up, and the demand for fuel increases, one could use the principle of a heterogeneous (hybrid) core, i.e., simultaneous use of fuel pins containing oxide or metal. From the physics viewpoint, this is equivalent to removing some of the oxygen from the core, with the corresponding partial increase in the breeding factor.

It is also desirable to use fast reactors to produce not only electricity but also heat for industrial purposes. Experience in that respect has been acquired with the BN-350, where part of the energy is used for desalinating sea water. Further research on this topic is favored by the fact that fast-reactor stations produce high-potential heat (over 500°C), which is very useful for some industrial technologies. Also, the industrial use of fast reactors at constant mode is equivalent to a baseload operation, which is most favorable from the economic viewpoint and which provides the largest amount of additional plutonium.

Many Comecon member-nations are interested in the fast-reactor researches. Those countries have collaborated in this area for 13 years via the Fast-Reactor Council. The collaboration has accelerated the resolution of problems in designing large and economically viable fast reactors. The program in he USSR envisages building the BN-800, which is essentially a modified and ungraded BN-600, with the work then extending to the next generation with the BN-1600. The basic reactor parameters are the following:

	BN-800	BN-1600
Power, MW:		
thermal	2100	4200
electrical	800	1600
No. of cooling loops	3	4
Coolant parameters in first circuit:		
flow rate, ton/h	31 000	62 000
Temp. at heat exchanger inlet, °C	547	547
Temp. at core inlet, °C	354	354
Coolant parameters in second circuit:		
flow through one steam generator, ton/h	10 000	15 000
inlet temp. for steam generator, °C	505	505
outlet temp. from steam generator, °C	309	309
Feedwater temp. at inlet to steam generator, °C	210	210
Steam temp. at outlet from steam generator, °C	490	490
Steam pressure at outlet from steam generator, MPa	13.7	13.7
Run time between reloads, days	120	150

Considerable attention is being given to the fast-reactor work in this country. There are statements on the need to accelerate the work and to make early use of fast reactors in the proceedings of the Twenty-sixth Congress of the CPSU and the plenary meeetings of the

TABLE 1. Effects of Burnup on High-Power Reactor Characteristics (type BN-1600 with oxide fuel) and Influence on the Fuel Cycle

Characteristics	Maximum burnup, % of heavy atoms			
	5	10	15	20
Reactor characteristics				
Breeding factor losses:				
from capture by fission products	0,033	0,067	0,101	0,135
due to chemical reprocessing (loss in cycle 2%)	0,047	0,025	0,016	0,012
Overall losses in breeding factor	0,080	0,092	0,117	0,147
Fuel cycle				
Breeding rate (external cycle 1 yr)	3,8	5,7	6,7	7,3
Specific volume of reprocessed fuel, kg/MW(el)·yr	20,9	10,4	7,0	5,2
Specific volume of reprocessed plutonium, kg/MW(el)·yr	3,5	1,9	1,4	1,12
Specific scale of fuel pin production, items/MW(el)·yr	90	45	30	22

Central Committee of the CPSU. Soviet scientists and engineers, and workers and technicians, and all who are involved with the problem will make efforts to carry out these resolutions.

CRITICAL ASSEMBLY OF THE WORLD'S FIRST NUCLEAR POWER STATION REACTOR

M. E. Minashin

UDC 621.039.524

Among the many questions and problems facing the developers of the world's first nuclear power station and particularly its reactor, one of the principal ones must be designated the determination and choice of physical characteristics of the reactor and also the study of its behavior during runup, operation, transitional regimes, cooling, and in emergency situations. All these characteristics can vary during a reactor run, as burnup of uranium and buildup of plutonium takes place. Fission products are accumulated, the ratios of the number of nuclei of fissile isotopes to the amount of structural materials and coolant vary and, consequently, the intensity of competing processes of the interaction between the neutrons and these materials varies. As a result of all these changes, as a rule, the effective neutron multiplication factor also varies, which determines the control ability of the reactor.

The determination of the nuclear-physics characteristics of reactors of selected design and power, as is well known, starts with the determination of the amount and enrichment of the uranium charge in order, in the final count, to ensure an acceptable duration of operation (or the amount of power produced from the reactor) and to have satisfactory characteristics with respect to controllability and the necessary economic indices.

When designing and constructing the world's first nuclear power station, the questions of economic operation of the station were not studied in detail, since the design did not pursue an economic goal, but the problem of the proof of the feasibility of construction of the nuclear power station and its operational capability was resolved. Only after startup and during further work on the creation of more powerful nuclear power stations were investigations on the economics and conditions for achieving economic competitiveness initiated. Just as for the first nuclear power station, so also for subsequent stations, the main attention was paid to questions of the operating reliability of each unit of the plant. The choice and development of designs, including such new elements of the reactor as the fuel channels (FC) and fuel elements, including the choice of the type of uranium fuel for it, were subordinate to a considerable degree to this problem. Prior to the contruction of the first nuclear power station, there was no design of fuel channel and fuel elements suitable for operation at the high temperature and high pressure of the coolant, nor even data published about this. The construction of the fuel channels and fuel elements was the most difficult problem in designing the first nuclear power station. In addition to the physicists' calculations of the reactor, experiments were also conducted on the assessment of the suitability of the alternatives being proposed by the designers and technologists for the designs of the fuel channels and fuel elements with different types of uranium fuel. When calculating the reactor alternatives, difficulties arose in the manufacture of graphite components of large dimensions for the reflector. However, these and many similar calculations associated with the choice of designs were only tasks of an incidental nature, whereas the search for designs of the fuel channels and particularly the fuel elements was conducted constantly right up to the end of 1953. Together with the use of tubular fuel elements, during planning the possibility of using rod-shaped fuel elements was considered. But from the point of view of reliability, the tubular fuel elements were assessed to be the most suitable, as they could be previously tested on a thermal test-rig under load. Other positive properties of these fuel elements also were noted. Because of the nonmastery in 1951 of zirconium production for the channel tubes, necessary for the use of rod-shaped fuel elements, the tubular type of fuel elements was assessed to be the main alternative. Towards the middle of 1953, test-rig trials of new samples of tubular fuel elements, which had been started in March 1953 by a group of specialists under the direction of B. A. Zenkevich, were mainly completed, and for which a uranium-molybdenum alloy dispersed in magnesium was used, developed by a group of specialists under the direction of V. A. Malykh. These samples were subjected to thermal tests with loads of more than 2.3 MW/m^2 ($2 \cdot 10^6$ kcal/m^2·h). In the quantity of materials — nonproduc-
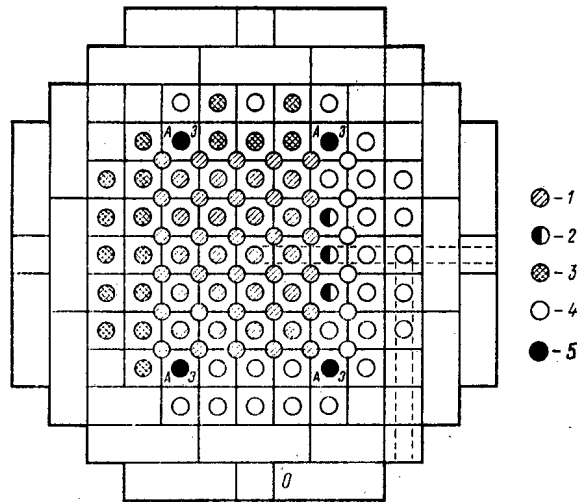
Fig. 1. AMF reactor (plan view): 1) loaded fuel channels; 2) fuel channels loaded to 2/7; 3) gaps filled with graphite samples; 4) unloaded gaps; 5) rod absorbers of scram system; 0) reflector.
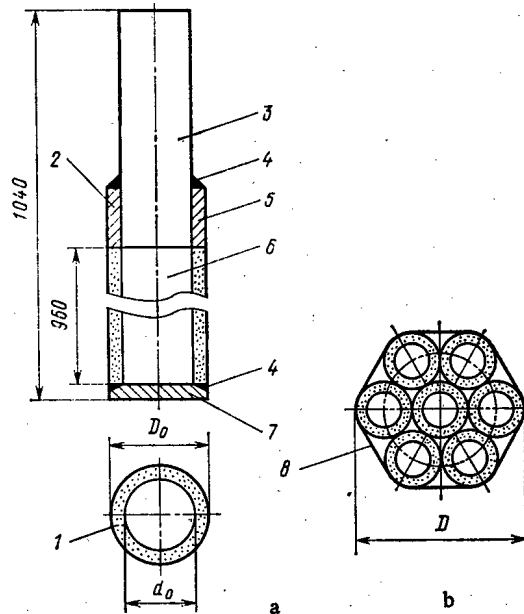
Fig. 2. Fuel element (a) and fuel channel (b) of the AMF reactor: 1) filling of U_3O_8 powder; 2, 3) 1Kh18NYaT steel tubes, with diameter 13.4 × 0.2 and 9 × 0.4 mm, respectively; 4) soldering; 5) steel sleeve; 6) water; 7) steel base with thickness 2 mm; 8) confining ring of tin plate.

tive absorbers of neutrons in the fuel elements and channels of this type (molybdenum, steel, water) — and in geometrical dimensions, this fuel element version differed little from that used in April 1952. For this fuel-element version, taking account of the availability at this time of new values of the constants (resonance integrals of absorption in ^{238}U, fission products, absorption cross-sections in molybdenum, etc.), new values were determined for the charge and enrichment of the uranium (570 kg and 5%, respectively, instead of 600 kg and 3% in the original design version). Although these values, just as the choice of the uranium compound for the fuel elements considered in April 1952, underwent almost no changes right up to the manufacture of a regular batch of channels, not one of the versions of fuel elements up to

TABLE 1. Volume of Materials and Gas Cavities per cm height of Cell, cm^3/cm

Materials and cavities	Lattice pitch a, cm	
	14	20
U	4,84	4,84
C	184,5	384,5
H_2O	3,7	3,7
1Kh18N9T steel	1,84	1,84
Gas cavities	9,12	13,12
Total in cell	204	408

TABLE 2. Values of Constants Used in the Calculations for Neutrons with $E_0 = 0.025$ eV, b

Material	ν_a	σ_f	σ_{a0}	σ_s	σ_{tr}	Σ_s, cm^{-1}	Σ_{tr}, cm^{-1}
C	—	—	0,0042	4,8	4,5	—	0,37
H_2O	—	—	$\Sigma_a = 0,021$	—	$\Sigma_{tr} = 2,33$	—	$\Sigma_{tot} = 2,35$
^{235}U	2,07	545	645	8,3	8,3	—	—
^{238}U	—	—	2,6	8,3	8,3	—	—
1Kh18N9T steel	—	—	$\Sigma_a = 0,247$	—	—	0,9	0,9

Note. For neutrons with $E > 0.025$ eV, $\sigma_{a0} \sqrt{E_0/E}$. Here ν_a is the number of secondary neutrons per absorption event; σ_f is the fission cross section; σ_a is the absorption cross section; $\Sigma_a = \rho\sigma_a$; $\Sigma_{tot} = \rho\sigma_{tot}$ is the total cross section; ρ is the density of the nuclei.

the end of 1953, however, could be considered as acceptable. This was explained by the fact that attempts to manufacture test samples of certain versions of fuel elements ended in failure (these samples were not even subjected to thermal tests: their surface was covered with pits, cracks, etc.) and the version placed as final still had not pressed reactor tests.

In view of the absence of a fuel-element version acceptable for the first nuclear power station project, it was not possible to order an experimental batch for the testing of a physics assembly. It was only in mid-1953, based on thermal tests (including also tests with thermocycling) of samples manufactured by a technology developed under the direction of V. A. Malykh, that confidence emerged that this type of fuel element was promising. Now the first nuclear power station reactor project became more substantiated. All developments could be refined. In June 1953, on the instructions of I. V. Kurchatov, the Commission of the Institute of Atomic Energy was formed at the Physicopower Institute (FEI) composed of V. S. Fursov, G. N. Kruzhilin, V. I. Merkin, and S. A. Skvortsov, which examined the design data of the first nuclear power station reactor. In particular, the Commission noted that the physics calculations of the reactor had no experimental verification and therefore could be erroneous.

Because of these comments by the Commission, verifying calculations were performed and a report was issued. It was shown in it that according to the concepts existing at that time about the constants, the margin of reactivity was sufficient for accomplishing the assumed running period. At the same time it was noted that, taking account of the entirely possible errors of the constants used in the calculations (and also the moderation length and diffusion length, existing for a reactor of small dimensions, resonance absorption of neutrons in ^{238}U, etc.), due to inaccuracy of the cross-sectional values, the relatively large amount of

water in the lattice of the reactor and the complex geometry of the fuel channels, there might not be a reactivity margin above the calculated value of the running time (100 days). On the other hand, it was not possible to increase, for example, the uranium enrichment, since the number of rod-absorbers necessary for compensation of the excess reactivity, calculated with consideration of the assumptions mentioned above about the accuracy of the constants (and the estimated value of $\Delta k_\infty \approx 28\%$), would be increased significantly and an excessively expanded grid of rod-absorbers would be used. This implied that it would be necessary to assign an additional number of cells for these rods and have coolant feed and outlet lines to them from both the main system of heat removal and from the heat-removal system from the control and safety rod channels, and to have feeder tubes for the cables of the rod actuators, etc. All this concerned the design of the reactor and the control and safety rod system as a whole. Therefore, it would be necessary to look for confirmation or discrepancy of the calculated and factual data on examples of critical assemblies of other reactors. Testing and verification of the procedures and constants used before and after this period were carried out by means of a calculation of the RFT reactor of the Institute of Atomic Energy and of other critical assemblies. The results obtained were quite good, and this checked the designers before a new change of design of the first nuclear power station reactor and its systems.

However, the results of the verification of the procedure and constants were obtained as applicable to reactors with significantly different fuel-element designs. Therefore, the question of accuracy of the calculations of the first nuclear power station reactor still remained open.

At the beginning of 1954 in the Physicopower Institute, an assembly of experimental fuel elements was received for physics models, which in their dimensions were similar to the fuel elements of the first nuclear power station reactor. The evalution calculations showed that this assembly of fuel elements (435 pieces) was sufficient for the construction of a uranium—graphite reactor of zero power and of small dimensions, with fuel channels similar in design to the channels of the first nuclear power station reactor. More detailed calculations, performed with the participation of Yu. A. Sergeev, V. Ya. Sviridenko, and G. Ya. Rumyantsev, confirmed this possibility. Z. M. Kurova, S. I. Shagalina, L. Yu. Dol'skaya, and V. M. Stroikova also participated in these calculations.

The spacing grid for the rod-absorbers was also chosen. The actuators for the rods of this test-rig were designed by G. N. Ushakov, and with the approval of D. I. Blokhintsev, the reactor was built in the Physicopower Institute with the vigorous participation of A. K. Krasin, B. G. Dubovskii, A. V. Kamaev, M. N. Lantsov, E. I. Inyutin, L. A. Matalin, etc. The schematic form of the reactor (designated AMF) is shown in Fig. 1, and a cross section of a fuel channel and fuel element in Fig. 2. Table 1 shows the quantity of materials occurring per cm of height of the cell, and in Table 2 the values of the constants assumed in the calculations are shown. The physics model was not an exact copy of the AM reactor, but in the design of the fuel channels, cell dimensions and quantity of materials in it, it was the closest to the reactor model by comparison with the one having been used earlier.

The distribution of thermal neutrons in the cell of fuel channels (Φ) and the thermal neutron utilization factor θ were computed on the basis of the solution of the diffusion equation for each zone of the cell:

$$\Delta \Phi_i - \frac{\Phi_i}{L_i^2} + \frac{q_i}{D_i} = 0, \tag{1}$$

where L_i and D_i are the length and coefficient of diffusion in the zone i, respectively, and q_i in the density of sources due to moderation.

At the boundaries of the zones, the fluxes Φ were "joined" and the resulting fluxes were $D_i \, d\Phi_i/dr$.

The coefficient of resonance absorption escape was determined by the formula of M. B. Egiazarov [M. B. Egiazarov, V. S. Dikarev, and V. G. Madeev, in: Session of the Academy of Sciences of the USSR on the Peaceful Utilization of Atomic Energy. Conference of the Division of Physicomathematical Science [in Russian], Academy of Sciences of the USSR, Moscow, (1955), p. 53] which, after its transformation for a cell of the first nuclear power station reactor, acquired the following form:

$$\varphi = \exp \left\{ - n \frac{5.4 \frac{F}{\pi} \sqrt{\varepsilon l} + 2.66 \frac{4V_U}{\pi} \varepsilon}{V_C + 22.8 \, (V\gamma)_{H_2O}} \right\}, \tag{2}$$

384

where F is the surface of the uranium turned towards the moderator (water or graphite); l is the mean free path of neutrons in the uranium; $l = 2d_r = 2(1.3-0.9) = 0.8$ cm; $\varepsilon = \rho_8/4.7 \cdot 10^{22}$ is the relative density of uranium nuclei; V_U, V_C, and V_{H_2O} is the volume of uranium, graphite, and water in the cell, cm^3/cm; n is the number of fuel elements in the fuel channel, and γ is the density of the water in the fuel channel.

The square of the neutron moderation length up to energy E in the lattice and in the reflectors was calculated for a homogenized medium on the basis of a computation only of elastic collisions (in view of the small concentration of heavy nuclei):

$$\tau(\ ) = \frac{V^2_{cell}}{3} \int_E^\infty f(E_0) \times \left\{ \int_E^{E_0} \frac{dE''/E''}{\left(\sum_k V_k \Sigma_{trk}\right)\left(\sum_k \Sigma_{trk}\xi\Sigma_{sh}V_k\right)} + \frac{\overline{r^2_s}(E_0)}{2V^2_{cell}} \right\} dE_0, \tag{3}$$

where $f(E_0)$ is the distribution of fission neutrons with respect to energy E_0;

$$f(E_0)\, dE_0 = \frac{e^{-E_0}\, \text{sh}\, \sqrt{2E_0}}{\int_0^\infty e^{-E_0}\, \text{sh}\, \sqrt{2E_0}\, dE_0}\, dE_0;$$

$\Sigma_{sk} = \rho_k\sigma_{sk}$ and $\Sigma_{trk} = \rho_k\sigma_{trk}$ are the cross sections of scattering and transport of neutrons by the nuclei of material of the kind k, occupying a volume V_k in a cell of the core or in the reflectors; $r^2_s(E_0)/6$ is the square of the mean free path of a fission neutron with energy E_0 before the first collision, as the average value of all mean free paths r;

$$\frac{\overline{r^2_s}(E_0)}{6} = \frac{\int_0^\infty \frac{r^2}{6} e^{-\Sigma_s(E_0)r} \Sigma_s(E_0)\, dr}{\int_0^\infty e^{-\Sigma_s(E_0)r} \Sigma_s(E_0)\, dr}. \tag{4}$$

The critical size for a given neutron multiplication factor K_∞ (or K_∞ with specified dimensions) is determined on the basis of the formula of age approximation

$$(1 + \varkappa^2 L^2_f) \exp(\varkappa^2\tau_f) = K_\infty, \tag{5}$$

where

$$\varkappa^2 = \left(\frac{\pi}{H+\delta_z}\right)^2 + \left(\frac{\xi_0}{R+\delta_R}\right)^2, \tag{6}$$

here H and R are the height and radius of the core, respectively, and $\xi_0 = 2.401$.

The values of the equivalent additions to the size of the core due to the end reflectors (δ_z) and the lateral reflector (δ_R) were estimated on the basis of the solutions of the two-group diffusion equations of age approximation, obtained on the assumption of an arbitrary separation of the spatial realtions of the fluxes $\Phi(r, z) = \Phi(r), \Phi(z)$. For this, in 1951-1952, a universal equation of critical sizes was developed and used for the first nuclear power station reactor, suitable for 10 different geometrical shapes of one-dimensional reactors, at first for $L^2_f = \tau_f$ (in the reflectors), and then also for $L^2 = \tau_f$.

The calculated data obtained by using these equations and formulas are given in Table 3, whence it follows that with the number of individual fuel elements available in our arrangement (435 pieces), a critical reactor with a lattice pitch of 20 cm could not be achieved, but with a lattice pitch of 14 cm criticality should be achieved with 49 channels. The physics model of the AMF reactor achieved criticality on March 3, 1954, when $51^2/7$ fuel channels were loaded with the presence of gaps in the lateral reflector. According to the experimental estimates, loading of the gaps with graphite reduced the critical mass to 50 fuel channels. The results of a comparison of the calculated and experimental data indicated the necessity for the use in the calculations of joining of the generation density of neutrons moderated in the core and in the reflectors, with weighting factors averaged over the square

TABLE 3. Calculated Values of the Physical Parameters for the AMF Reactor

Parameters	Core, channels with water		Reflectors	
	$a=14$cm	$a=20$cm	lateral	end
φ	0,923	0,956	—	—
θ	0,792	0,759	—	—
K_∞	1,511	1,503	—	—
Σ_a^{-1}, cm	124	259	3260	3260
Σ_{tot}^{-1}, cm	2,56	2,78	2,76	2,76
L^2, cm²	106	239,7	3000	3000
τ_T, cm²	300	360	370	370
$(\xi\Sigma_s)^{-1}$, cm	13,9	15,43	17,4	17,4
$(\xi\Sigma_s\Sigma_{tr})^{-1}$, cm²	60,5	69	67,4	67,4
g_0	1,08	0,984	—	—
g_1	1,25	1,128	—	—
g_2	1,11	0,976	—	—
δ { $a=14$ cm	—	—	32	28
$a=20$ cm	—	—	39	32
R_{cr}	55,8	132	—	—
n_{cr}	49	134	—	—

Note. R_{cr} is the critical radius of the core)
n_{cr} is the critical number of fuel channels.

$$q_0 = \left(\frac{\Sigma_{tr}}{\Sigma'_{tr}}\right) \text{thermal region}$$

$$q_1 = \frac{\frac{1}{\tau'_f}\int_0^{\tau'_f} d\tau/\xi\Sigma'_s}{\frac{1}{\tau_f}\int_0^{\tau_f} d\tau/\xi\Sigma_s}; \quad q_2 = \frac{\frac{1}{\tau'_f}\int_0^{\tau'_f} d\tau/\Sigma'_{tr}\xi\Sigma'_s}{\frac{1}{\tau_f}\int_0^{\tau_f} d\tau/\Sigma_{tr}\xi\Sigma_s}.$$

Symbols with primes refer to the reflectors.

of the moderation length, but not for 1 eV, as this was sometimes used in calculations prior to 1954.

The experiments conducted on the AMF showed that by using the procedure and constants assumed for the first nuclear power station reactor there were no large errors at least at the start of the reactor run. However, agreement with the experimental data on the AMF test-ring was obtained only for a cold reactor state. However, the first nuclear power station reactor was designed for operation at a high temperature, and there could be no such agreement.

At the start of the 1950s, experimental and theoretical investigations in the field of nuclear reactors, both in the Soviet Union and abroad, continued to expand. In this period reactor physics was rapidly enriched with new data about the values and behavior of the interaction cross sections of neutrons with the nuclei of different substances in different neutron energy ranges, and the values of the yield of secondary neutrons as a result of absorption were refined, etc. Under the influence of these new data, in May–June 1954, the procedure for reactor calculations of the first nuclear power station (mainly in the part of the calculation of the effects of absorption in the region of moderated neutrons) and the constants were refined. These refinements were caused by the necessity for detailing the neutron multiplication process, in order thereby to allow for the difference in the capture and fission cross sections in the thermal and epithermal energy regions, and to clarify the influence of other effects. From a comparison of the method of calculation of the first nuclear power station reactor [D. I. Blokhintsev, M. E. Minashin, and Yu. A. Sergeev, Atomnaya Énergiya, 1, 24 (1956)], carried out in the second half of 1954, with that used for the AMF test-rig and the first nuclear power station reactor in the first half of 1954, it follows that besides the calculation of the epithermal absorption, a method was recommended for determining the cutoff energy between the thermal and epithermal regions, partially used even at the present time. Present-day calculations differ first and foremost in that the thermal energy region is divided into several intervals. The calculations are performed on a computer, which allows many details of processes to be taken into consideration which previously were either unknown or

386

could not be considered. It must be mentioned that the fundamentals of knowledge concerning reactors, accumulated by many years of work by the scientists of the Soviet Union headed by I. V. Kurchatov, have remained unchanged since the time of planning of the first nuclear power station despite the complexity of the methods. Our debt and the debt of subsequent generations consists in simultaneously displaying those integral effects enumerated in Table 3, for all the complexities and refinements of the physical characteristics, which the physicists of previous generations obtained at the cost of an enormous expenditure of labor.

387

ARTICLES

HEAT ACCUMULATORS AT NUCLEAR POWER STATIONS

V. M. Chakhovskii   UDC 621.355

From the early days of nuclear power, the equipment and fuel for nuclear power stations have been designed for baseload operation, which is economically justified by the large capital investment in nuclear power stations and the requirement to maintain high rates of production for secondary nuclear fuel. However, the conditions in the unified power system (UPS) for the country have become such that the scope for increasing the control range in the output power from traditional plants are virtually exhausted. It has therefore become necessary to provide essentially new economic and technically accessible facilities. The traditional approach here is to devise load-following nuclear power stations based on specialized fuel pins and equipment stable under repeated thermal cycling, which is the method to be applied when other and more economical methods of covering load variations have been exhausted.

The engineering and technological problems in designing load-following nuclear power stations are so complicated that another approach has become necessary. This is to incorporate heat accumulators (HA). The main purpose of HA is to retain a high power use factor (PUF) in the nuclear power plant (NPP) when the station works under varying load. There are papers [1-4] on the working conditions in nuclear power stations containing HA, which give the essential schemes and designs. At present, the development of HA is taking various lines.

Table 1 gives the characteristics of HA for daily load graph control (HA of hot-water accumulator type (HWA), double steam-water accumulators (DSWA), phase-transition ones (PTA), ones containing chemicals (CA) or organic materials (OA)) and also for weekly load graph control (HWA, DSWA, PTA, and CA). Here we present results on research on nuclear power stations containing HA of HWA, DSWA, and PTA types.

Methodological Aspects of Efficient HA Use. The nonuniformity in the load graph for a power system makes it necessary to provide the optimum types of load-following system. When one combines load-following and baseload systems, one employs principles for equalizing the production of load-following and baseload power at the level of the station or system.

To make it possible to use nuclear power stations with HA in accordance with load-curve requirements, one has to consider various ways in which they can participate in the variable part of the load curve. When one determines the relation between the accumulated heat and output power from an HA, one has to know the load graphs for working and other days, together with the control characteristics of the system equipment. These data are used in establishing the load coefficients and the power increment in relation to the power of the reactor, which is taken as the nominal load of NPP with HA. To evaluate the participation of nuclear stations in power regulation and to choose the optimum equipment composition for the UPS, we use a modified form of model, whose basic concepts have been given in [5].

Two approaches can be used in determining the costs at nuclear stations with HA. Firstly, one identifies the components and systems in the HA loop (peak power) that provide for working the station with a variable load, and the costs for this system are referred to the additional energy production (peak) during the hours of maximum load (HA discharge), when the turbine power is above the nominal reactor power. On the other hand, the cost of the basic equipment is referred to the total power output less the peak output. In the second approach, the costs of a nuclear power station containing HA include those for the peak system and are referred to the total power production. In both approaches, the total costs are compared with those for alternative load-following and baseload systems. The forms may be compared separately on the production of load-following and baseload electricity. The alternatives may be nuclear power stations with load-following fuel pins, nuclear power stations with pumped-storage stations (PSS), nuclear power stations with gas-turbine systems (GTS), and other combinations.

0038-531X/84/5606-0388$08.50   © 1984 Plenum Publishing Corporation

TABLE 1. Basic HA Parameters

Parameter	HA type				
	HWA	DSWA	PTA	CA	OA
Working body	Water	Water	Salt	Reacting chemical matter	Organic matter
Working pressure, MPa	0,1—2,5	4,0—7,0	0,1	0,1—4,0	0,1—1,5
Thermal energy capacity, MJ/m³	170—690	670—800	300—3000	500—5000	100—300
Working temp., °C	До 200	До 280	До 1000	До 1500	До 400
Elect. energy capacity of HA, kW·h/m³	15—45	55—65	30—300	60—600	10—30
Cost of unit HA volume, rubles/m³	50—250	300—500	25—600	200—900	60—200
HA cost, rubles/kW	40—200	60—250	80—340	100—400	50—260
Cost of stored energy, kopecks/kW·h*	0,8—2,8	1,2—3,6	1,35—3,85	1,5—4,4	0,8—3,2

*The range in stored energy cost in HA is dependent on the mode of operation in the power system.

An important condition for the nuclear station is to provide the maximum PUF, and consequently high rates of secondary nuclear fuel production (under conditions of a closed fuel cycle). Figure 1a shows a possible integral daily load graph for nuclear power stations in the UPS in relative units, which is characterized by pronounced load peaks. With this graph, the load on the nuclear power stations should vary continuously, which involves ongoing changes in the technological process, which firstly are complicated to provide and which secondly reduce the station reliability. Therefore, in order to follow the graph for the real load (real graph) one is justified in organizing each nuclear station on the basis of a simple graph with the minimum number of load changes, for example as shown in parts b and c of Fig. 1 for nuclear stations without and with HA. The daily power outputs from the real and simple load graphs should be identical, as should be the conditions for running at the minimum and covering the maximum load, namely in other words the graphs should have equal areas, equal maximum heights, and equal minimum depths. Figure 1c shows a simple load graph for a station with HA in which the nominal load on the NPP corresponds to the mean daily nominal load in the real graph.

The following condition must be met for the station in the system when a set of simple load graphs is drawn up: the station must provide a given load P_{kv} and therefore produce power during time interval v, including the time of minimum load and the time of maximum:

$$\sum_{j=1}^{J} \varphi_{jkv} N_j = P_{kv}, \quad (k = \overline{1, n}; \ v = \overline{1, V}), \tag{1}$$

where φ_{jkv} is the relative load on nuclear power station j on day k during interval v, the number of these being V when a station works n days a year, while N_j is the nominal NPP power at nuclear station j, the total number of these in the power system being J.

The PUF for NPP with and without HA may be defined by the following for identical daily power outputs on the working and other days of the week with equal morning and evening peaks in the load with the nuclear stations operating on a simple load graph (subscript j is omitted):
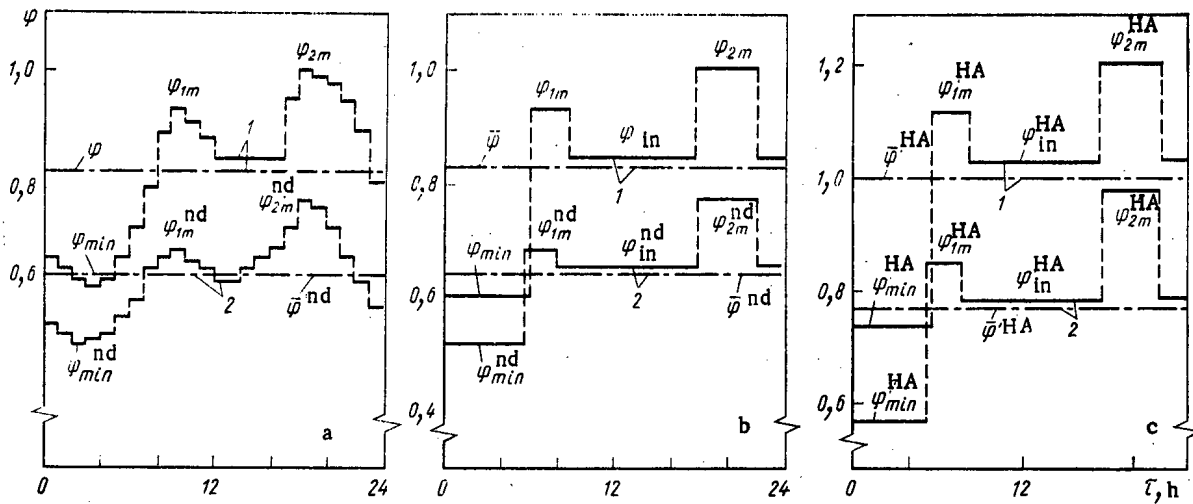
Fig. 1. Daily load graphs for nuclear stations on working days (1) and nonworking days (2): a) real daily load graph for nuclear stations in UPS; b) equivalent daily load graph for nuclear stations without HA; c) equivalent daily load graph for nulcear stations with HA.

$$\text{PUF}_{\text{NPP with HA}} = (\varphi_{\text{min}}^{\text{HA}}\bar{\tau}_{\text{min}} + \varphi_{\text{max}}^{\text{HA}}\bar{\tau}_{\text{max}} + \varphi_{\text{in}}^{\text{HA}}\tau_{\text{in}})\, n \cdot 8760^{-1}; \tag{2}$$

$$\text{PUF}_{\text{NPP without HA}} = (\varphi_{\text{min}}\tau_{\text{min}} + \varphi_{\text{max}}\bar{\tau}_{\text{max}} + \bar{\varphi}_{\text{in}}\,\tau_{\text{in}})\, n \cdot 8760^{-1} = \bar{\varphi}n \cdot 8760^{-1} \cdot 24, \tag{3}$$

where $\varphi_{\text{min}}^{\text{HA}} = 1 - \alpha$; $\varphi_{\text{max}}^{\text{HA}} = 1 + \rho$; $\varphi_{\text{in}}^{\text{HA}} = (1 + \alpha\bar{\tau}_{\text{min}}\, \eta_{\text{HA}} - \rho\bar{\tau}_{\text{max}})\, \tau_{\text{in}}^{-1}$ the coefficients for the minimal, maximal, and intermediate loads on the NPP with HA correspondingly, φ_{min}, φ_{max}, and $\varphi_{\text{in}} = (24\bar{\varphi} - \bar{\tau}_{\text{max}} - \varphi_{\text{min}}\,\bar{\tau}_{\text{min}})\, \tau_{\text{in}}^{-1}$ are the same for NPP without HA, $\bar{\varphi} = 24^{-1}\sum\limits_{i=1}^{24} \varphi_i$ is the mean daily (nominal) load, which is determined from the actual nuclear station load graph, $\alpha = \bar{\varphi}^{-1}\,(\bar{\varphi} - \varphi_{\text{min}})\, \eta_{\text{HA}}^{-1}$ is the nuclear station unloading coefficient under conditions of HA charging in relation to the reactor power, $\rho = \bar{\varphi}^{-1}\,(1 - \varphi_{\text{min}}) - \alpha$ is the coefficient for the increment in turbine power under discharging conditions in relation to the reactor power, $\tau_{\text{in}} = 24 - \bar{\tau}_{\text{max}} - \bar{\tau}_{\text{min}}$ is the time for which the nuclear station with HA works on intermediate load, τ_{max} is the total duration of the morning and evening load peaks on the basis of referring the duration of the morning peak to the largest value of the evening one, or $\bar{\tau}_{\text{max}} = (1 - \bar{\varphi})^{-1}\sum\limits_{i=1}^{\tau_{\text{max}}\text{ max}} (\varphi_i - \varphi)$ is the averaged time of maximum load, and n is the number of working days for the nuclear station in a year.

The durations of the cycles $\bar{\tau}_{\text{min}}$, $\bar{\tau}_{\text{max}}$, τ_{in} on the simple graph with minimal, maximal, and intermediate loads are calculated from the real graph on the basis that the energy $\bar{E}_{\text{min}}$ during the dip is set in relation to the load $\bar{\varphi}$ representing the energy $\bar{E}_{\text{max}}$ produced during the peak hours together with the intermediate load $\bar{E}_{\text{in}}$:

$$\bar{E}_{\text{min}} = \bar{E}_{\text{max}} + \bar{E}_{\text{in}}. \tag{4}$$

Expressions (2)-(4) apply if the nuclear station does not participate in reducing the baseload during weekend days. When allowance is made for the weekly nonuniformity in the base load on the nuclear stations, the PUF for the NPP with and without HA may be determined from (2) and (3) with identical characteristics for the load peaks on the working and weekend days at nuclear station j using the following relationships:

$$\text{PUF}_{\text{NPP with HA}}^{\text{p}} = \text{PUF}_{\text{NPP with HA}} (n_{\text{wd}} + \psi_{\text{w}}^j n_{\text{nd}})\, n^{-1}; \tag{5}$$

$$\text{PUF}_{\text{NPP without HA}}^{\text{n}} = \text{PUF}_{\text{NPP without HA}} \times (n_{\text{nd}} + \varphi_{\text{w}}^j n_{\text{nd}})\, n^{-1}, \tag{6}$$
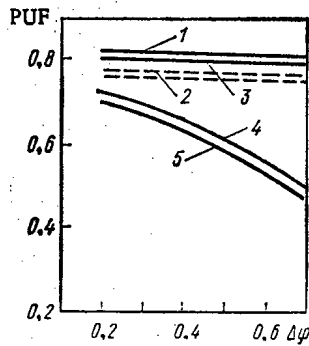
Fig. 2. Change in PUF of NPP in
relation to power control range:
1) with HA for efficiency of HA
0.9; 2) nominal PUF of NPP with
HA; 3) efficiency of HA 0.8; 4)
PUF of NPP without HA; 5) nominal
PUF of NPP without HA.

where n_{wd} and n_{nd} are the numbers of working and nonworking days when the nuclear station operates n days in a year, ψ_{jw} is the weekly nonuniformity coefficient in the baseload at nuclear station j, this being the ratio of the minimal loads (baseloads) on nonworking and working days.

Figure 2 shows the variation in PUF with and without allowance for the weekly nonuniformity in the baseload in relation to the nuclear station power control range. HA provide for high values of PUF relative to nuclear stations without HA. When there are HA, the turbine power exceeds the NPP power by a factor $1 + \rho$, which is equivalent to the capital investment in the NPP (the most costly part of a nuclear station) being reduced by comparison with the case without HA. The saving is partly consumed in the construction of the accumulating system, but most of it is released for other uses in power engineering. The results in Fig. 1b and c and in Fig. 2 have been obtained from (1)-(6), which enable one to incorporate the working conditions of nuclear stations with HA and which are necessary for determining the economic performance of nuclear stations in the UPS.

Calculating the Thermal Schemes for Nuclear Stations with HA. Particular attention has been given in devising methods of calculating these schemes to the modes of HA charging and discharging. There are the following specific features in devising the thermal scheme for a feed-water accumulator (FWA). In FWA charging and discharging, there are changes in the working conditions of the turbine system, steam superheater, separator, feed pump turbines, condensate pumps, condensers, and regeneration system on account of changes in the steam flow over the segments of the turbine and the flow of condensate in the feed water system. The flow directions may alter. For example, in discharging mode the condensate from the separator is run into the cold condensate tank or into the FWA, etc. In accordance with the working conditions, there are changes not only in the mass-flow balance for the components handling the hot water but also in the number of flows, which leads to changes in the heat balances in the components.

The turbine power is calculated for all modes of operation with the HA. A feature here is that the expansion of the steam is accompanied by change in the volume flow rate over the parts of the turbine. The efficiencies of the turbine stages alter during HA charging and discharging (particularly in the low-pressure cylinder LPC and in the last stage), on account of the changes in water content and the energy loss associated with the outgoing velocity of the steam flow. One uses universal characteristics for the efficiency changes in the parts of the turbine as functions of steam volume flow rate and pressure difference in order to determine the parameters and heat contents of the steam in the sections and after the last stage in the HA charging and discharging modes. These parameters are subsequently used in balance equations for the components.

The thermal scheme for the nuclear station with DSWA combines the basic principles realized in stations with FWA, and the method of calculation agrees with that for the latter. In
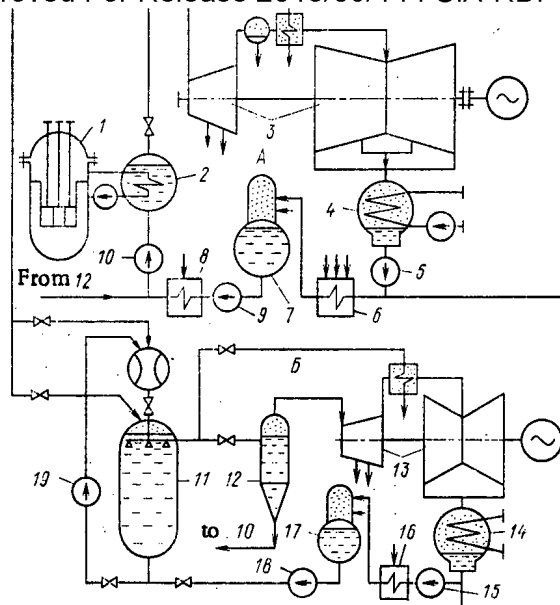
391

Fig. 3. Essential scheme for a load-following nu-
clear station with a steam-water accumulator and
peak turbine: A main system; B peak system; 1)
VVER; 2) steam generator; 3) main steam turbine;
4) condenser; 5) condensate pump; 6) low-pressure
regenerative heaters; 7) deaerator; 8) high-
pressure heaters; 9) feed pump; 10) circulation
pump in main and peak systems in feed water unit;
11) steam-water accumulator SWA; 12) expander; 13)
peak turbine PT; 14) PT condenser; 15) condensate
pump; 16) low-pressure water heaters in peak cir-
cuit; 17) PT deaerator; 18) PT feed pump; 19) SWA
circulation pump.

rdition, for nuclear stations with DSWA we have derived expressions relating the flow rate
of the hot water D_{hw} entering the feed water system for the main turbine together with the
flow rate for the generated secondary steam G_0'' supplied to the peak or main turbine. These
expressions include the unloading depth α, the durations τ_c and τ_d of the HA charging and
discharging cycles, and the parameters of the working medium under these conditions:

$$G_0'' = \alpha D_0 (i_0 - i_{hw}) (i_w - i_{hw}) (i_w' - i_c)^{-1} \times (i_0'' - i_{hw})^{-1} \tau_c \tau_d^{-1}; \tag{7}$$

$$\dot{D}_{hw} = \alpha D_0 (i_0 - i_{hw}) (i_0'' - i_w'') (i_w' - i_{hw})^{-1} \times (i_0'' - i_{hw})^{-1} \tau_c \tau_d^{-1}, \tag{8}$$

where i_0, i_0'' are the enthalpies of the main and secondary steam at the exit from the expander
correspondingly (Fig. 3), i_w, i_{hw}, and i_c are the enthalpies of saturated water at the corre-
sponding pressures in the DSWA, the hot water, and the condensate coming from the cold-conden-
sate tank in charging the DSWA.

To match the DSWA characteristics to the working-condition requirements for the nuclear
station, we have derived an expression defining the limiting discharging cycle time as a
function of the working-medium state parameters:

$$\tau_{li} \, 24 \, [1 + D_{hw} D_0^{-1} (i_w' - i_c) (i_0 - i_{hw})^{-1} \times (i_0'' - i_{hw}) (i_0'' - i_w')^{-1}]^{-1}. \tag{9}$$

The details of calculating the thermal scheme for a nuclear station with PTA are depen-
dent on the type of heat-accumulating substance HAS, the systems used to supply and remove
the heat from the PTA, and the point at which this is connected into the station system. If
the PTA is connected to the turbine system, the calculation principles differ little from
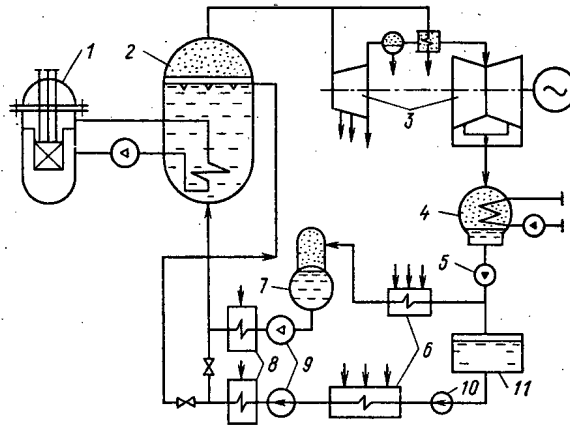
Fig. 4. Essential scheme of nuclear station
with accumulating steam generator: 1) reactor;
2) accumulating steam generator; 3) turbine; 4)
condenser; 5) condensate pump; 6) low-pressure
heaters in main system and steam-accumulator
charging system; 7) deaerator; 8) FWA; 9) feed
pump; 10) pumping accumulator-steam generator
charging system; 11) cold condensate tank.

those for the FWA case, if the PTA performs functions analogous to those of the FWA. There
will be a difference concerned with calculating the characteristics and working modes of the
PTA, which are extremely complicated and are not considered here. When the PTA is connected
to the coolant system, there are changes in the working conditions in the steam generator, so
one additionally introduces a condition for joint operation of the steam generator and the PTA.

Developing HA Schemes and Efficient Use of HA at Nuclear Stations. Existing methods of
accumulating heat have some major disadvantages as follows: storing heat as steam requires
large vessels, and the steam parameters alter during HA discharging, while the peak turbine
works with throttled steam or steam with varying parameters, which results in low efficiency;
it is impossible to use the volume of the HA, the accumulated heat, and the steam mass com-
pletely, which means that very large volumes are required for the vessels, which also have to
work at high pressures; and there are imperfections in the systems for organizing the heat
movements during HA charging and discharging, which complicate the design of the accumulating
system.

This has led to the design of thermal schemes for nuclear stations with HA to eliminate
these deficiencies. Some of these deficiencies. Some of these schemes have been published
in [1, 3, 4]. Technically speaking, the simplest schemes involve FWA and DSWA. Those with
DSWA provide higher efficiency than some power station schemes with forms of steam-water heat
accumulators [6], but they are inferior to stations with FWA. The efficiency of DSWA is
0.65-0.8, and the largest values are attained when one organizes the heating of cold con-
densate to the feed water temperature in charging mode using the classical regenerative heat-
ing scheme, while the heating to the saturation temperature of the water in the steam gener-
ator is performed with live steam in an additional heater after the feed water mains system.
The largest losses in thermal accumulation with DSWA occur in the expansion unit during dis-
charging. One can reduce the loss by increasing the power production by means of displacing
the regenerative steam flows (Fig. 3). In principle, one can realize a steam-power cycle
with high efficiency with DSWA, but then the latter becomes a double-acting hot-water accumu-
lator DHWA in which the water is fed from the DSWA directly to the steam generator. High ef-
ficiency (0.95 or more) in the DHWA (6.0 MPa) occurs because during charging the feed water
is heated in the additional heater (or in the accumulator itself) to the saturation tempera-
ture in a way analogous to that used in heating the feed water to the saturation temperature
in the steam generator. Consequently, the DHWA enables one to realize simultaneously effects
attained in the regenerative heating system and in a steam generator of drum type. The feed
water is heated to the saturation temperature in the steam generator using live steam in DHWA
charging, which reduces the turbine power by a value proportional to the flow rate of the live

393

TABLE 2. Economic Characteristics of Nuclear Power Stations with HA of the Water Class Fitted with VVÉR-1000 and Phase-Transition Stores

Characteristics	Heat accumulator type									
	DHWA		hp FWA		lp FWA		DSWA		PTA	
Working-body parameters in accumulator										
pressure, MPa	6,5		2,5		1,8		6,5		0,1	
temp., °C	275		220		189		275		560	
Accumulator eff., %	95		96		81		75		9.)	
HA charging time, h/day	7		7		7		7		7	
HA discharging time, h/d	5	10	5	10	5	10	5	10	5	10
Rel. power (load) on reactor during day, %	100		100		100		100		100	
Rel. turbine power, %:										
maximal*	141		123		115		139		169	
minimal	70	40	83	66	86,5	73	63	26	52	4
PUF of NPP with HA	0,825 / 0,733	0,82 / 0,781	0,821 / 0,782	0,82 / 0,781	0,818 / 0,78	0,815 / 0,777	0,805 / 0,768	0,78 / 0,743	0,815 / 0,777	0,8 / 0,76
PUF of NPP without HA	0,585 / 0,558	0,592 / 0,564	0,665 / 0,632	0,673 / 0,64	0,71 / 0,663	0,72 / 0,685	0,575 / 0,548	0,585 / 0,557	0,508 / 0,483	0,517 / 0,491
HA volume, 10^3 m^3	41	82	32	64	27,5	55	39	78	21	42
No. of HA vessels	3	6	2	4	2	4	3	6	2	4
Cost of accumulating system in relation to cost of power station block, %	13,3	22,1	7,6	11,9	6,1	8,8	14,4	22,2	21	34,6
for HA, %	8,2	16,4	4,25	8,5	2,75	5,5	7,75	16,5	14,2	28,4
Net eff. of HA system (elect.), %	31,4		31,6		27		24,5		37	
No. of hours of peak power use in year	1500	3000	1500	3000	1500	3000	1500	3000	1500	3000
Reduced cost of electricity produced by accumulating system, kopeck/kW · h	1,73	1,43	1,72	1,4	2,14	1,8	2,02	1,63	2,15†	1,85

*The maximum turbine power is determined by the HA type.
†The electrical energy costs for PTA have been calculated on the assumption that the heat-accumulating substance is completely renewed over 10 years.

steam passing to the accumulating system. In discharging mode, hot water is passed from the DHWA directly to the steam generator, and the output increases by the flow rate of the live steam passing in charging mode to the HWA (with allowance for the correction for the efficiency of the heater). Therefore, in DHWA discharging, the turbine power increases because of the increase in steam production from the steam generator and the disconnection of the regenerative tapoff of steam going to the water heater. Calculations have been performed for a new turbine based on the K-1000-60 design, which have shown that the overall power increment is 410 MW, of which 180 MW is due to the increased steam production by the steam generator and 230 MW due to disconnection of the regenerative steam tapoff.

Stations with DHWA provide the greatest increase in power relative to the nominal reactor power, although this involves increasing the output of a steam generator by 16-18% in DHWA discharging. In stations with DSWA, one can attain the same increment in power but with less economy with unchanged working conditions in the steam generator and with greater load relief on the unit if necessary (in part due to the efficiency being lower than with the DHWA).

A station with FWA provides reliable power control with an overall range of 60% by means of turbine power change relative to the nominal reactor power ranging from +20-10% to -40 to -50%. If necessary, one can provide a control up to 80-90% in relation to the nominal reactor power, for example over 2-3 h by reducing the turbine power by 70-80% while increasing the flow rate of the cold condensate in FWA charging. Here one has to provide a suitable margin in feed pump output or number of them. A station with DHWA can provide power regulation in the range up to 120% (excess turbine power in relation to reactor power of 40% and reduction by 80%), while the ranges up to 140% with DSWA. To realize stations containing DSWA and DHWA, it is necessary to develop reinforced-concrete heat-accumulator vessels designed for pressures of 6.0-7.0 MPa, which are higher by factors of 2-3 than for FWA. However, there are no essential technical constraints on making HA vessels of volume 10 thousand m^3 for such steam pressures [7].

TABLE 3. Economic Parameters of Load-Following Units

LFU type	No. of hours in year used	Rel. specific capital investment, %	Specific reduced electrical energy costs, kopeck / kW·h
GTU-100-95	1000	90	3,38
PSS charged	1000	160	2,72
from nuclear	1500	145	2,07
station	3000	140	1,6
Nuclear station	1000	100 *	2,19
with HA	1500	100	1,72
	3000	200	1,4
ABU	1000	80	2,25
	1500	80	1,77
SPU	1500	118	3,16
	3000	84	2,21
LFNPS†	3000	192	2,61

*As 100% we have taken the capital investments in accumulating systems for nuclear stations with HA for 1000, 1500, and 3000 h/yr.
†Operation of a nuclear station with load following is economically sound on operation for 3000 h a year or more.

Attention should also be given to the use of steam-generating accumulators, which may be made of prestressed reinforced concrete with the heat accumulator combined with the steam generator as shown in Fig. 4. The main advantage of a station with such an accumulator-generator is that it combines the functions of HWA and steam generator. This enables one to simplify the thermal scheme. However, this station design involves altering the structure of the main containment.

A new line is to use PTA at nuclear stations fitted with high-temperature gas-cooled and fast reactors. There are numerous HAS with acceptable thermophysical parameters and high latent heat of fusion, particularly above 400°C. Stations with PTA can provide power control from +70 to −90% relative to the nominal reactor power. The efficiency in energy accumulation in PTA is 0.80–0.95. However, before these accumulators can be realized, there is much research to be done on PTA heat input and output and control. The main advantage of PTA is the higher specific energy capacity relative to HA of water and organic types (Table 1).

An algorithm has been devised for calculating the thermal schemes for stations with HA of FWA, DSWA, DHWA, and PTA, and calculations have been performed on the economic performance (Table 2). The PUF of the NPP has been determined on the basis that a station works for 300 days a year and the HA is discharged for 5 h (peak) or 10 h (semipeak operation). With a given HA charging time, the load relief on the power station is the greater the longer the discharging time (Table 2).

The length of the charging and discharging cycle is determined by the working conditions in the unified system and is chosen on the basis of the control range required for a particular station. The models with different discharging times, in particular 5 and 10 h, indicate that in the one case the station works with a smaller control range and in the other with a larger one. The correspondence between these characteristics and the working conditions in the unified power system may be determined by considering the characteristics of all the system equipment.

Economic analysis shows that the thermal schemes for stations with DHWA, FWA, and PTA are thermodynamically effective, while as regards economic performance preference should be given to DHWA and FWA. Stations with DHWA and PTA deserve attention from the viewpoint of providing a large power control range.

In spite of the weekly load nonuniformity, the PUF for NPP with HA alter only slightly even when the reduction in baseload in the UPS during nonworking days is provided only by stations containing VVÉR-1000 reactors (Table 2, where the PUF for NPP with HA is given in

the denominator). If the load dips on nonworking days are covered only by the stations containing VVÉR-1000 reactors, the weekly base-load nonuniformity coefficient in the near future will be not less than 0.75 of the minimum load on working days. When nuclear stations participate in managing the Sunday load dips in conjunction with other systems, the weekly load coefficient can be made about 0.85-0.9, i.e., the reduction in baseload on nonworking days at stations containing VVÉR-1000 reactors will be not more than 10-15% relative to the minimum load on a working day.

In Table 2, the PUF for stations without HA are given in the bottom lines on the basis of the dips in baseload on nonworking days. Clearly, PUF is mainly determined by the daily nonuniformity of the load graph on working days. On this basis we have considered the economic desirability of nuclear stations participating in load graph following. If the nuclear stations with HA are to participate in covering the load dips on nonworking days, it is desirable to consider the accumulation of heat with high values for the parameters. For example, on working days of the week, one accumulates heat in the HA at pressures up to 2.5 MPa at 220°C, and on nonworking days at 6.5 MPa at 275°C. The increased energy capacity of the medium in the HA produces an additional reduction in the load on the VVÉR-1000 on nonworking days of about 10-15% (under otherwise equal conditions).

The performance of nuclear stations with HA in the UPS has been evaluated by comparison with the parameters of other types of load-following system, including load-following nuclear stations allowing the load to be reduced to a certain minimum, where the reactor power is designed to meet the maximum load (here the costs of load-following and baseload stations have been taken as identical); nuclear stations have also been compared with pumped-storage ones, where the nuclear plant has a constant 100% load and the load-curve following is provided by the pumped storage; also, a specialized semipeak unit (SPU) based on organic fuel or a gas-turbine unit GTU and an air-accumulating unit AAU in a nuclear station. The economic parameters of systems employing organic fuel have been determined at a fuel cost of 35 rubes/ton with specific consumptions for GTU of 0.4 kg/kW·h, 0.360 for SPU, and 0.140 for AAU. The efficiency for pumped storage was taken as 0.71. These parameters were taken from the data of [8, 9]. Table 3 gives the results.

The costs have been compared for various types of load-following unit (LFU) (Table 3), including load-following nuclear stations LFNS, which has shown that stations with HA, AAU, and PSS are effective. The largest economic effect in the UPS is attained when nuclear stations are operated with energy accumulators, where preference should be given to DHWA and FWA; nuclear stations with pumped storage and with DSWA are practically equivalent. AAU can compete with PSS and DSWA in the sharp-peak part of the load graph (if the parameters quoted for them can be attained and they operate for 1000 h a year). Similar calculations have been performed on using HA in CHPS. Estimates show that the economic effect from using HA in CHPS is 15-20% higher than that at condensation stations with low-pressure FWA.

Conclusions. It has been shown to be technically possible and economically desirable to introduce heat accumulators into nuclear power stations and CHPS, particularly FWA, DHWA, and DSWA. The largest power-control range is attained with HA of DHWA, PTA, and DSWA types and is 120-140% for stations with HA of the water class in relation to the nominal reactor power or up to 160% for stations with PTA.

The inclusion of HA in a nuclear station provides higher PUF and consequently maintains high rates of production for secondary nuclear fuel with nuclear stations working in variable-load mode. The introduction of HA at nuclear stations will enable one to fit turbines of power 1.2-1.4 times larger than the reactor power with HA of the water class or by more than a factor 1.5 for PTA, which provides a reliable means of covering peak loads by means of nuclear stations.

LITERATURE CITED

1. V. M. Boldyrev et al., At. Énerg., 51, No. 3, 153 (1981).
2. M. E. Voronkov et al., At. Tekh. Rubezhom, No. 9, 3 (1980).
3. A. P. Kirillov et al., Éng. Stroit., No. 2, 33 (1980).
4. A. P. Kirillov et al., Éng. Stroit., No. 1, 2 (1981).
5. V. M. Chakhovskii and V. V. Mattskov, At. Énerg., 38, No. 5, 287 (1975).
6. M. E. Voronkov et al., Inventor's Certificate No. 781378, Byul. Izobret., No. 43 (1980).
7. A. P. Kirillov et al., Éng. Stroit., No.6, 3 (1982).
8. V. A. Kirillov, Teploenergetika, No. 6, 2 (1982).
9. B. L. Baburin, Gidrotekh. Stroit., No. 10, 10 (1979).

A LOAD-FOLLOWING ATOMIC HEAT AND POWER PLANT

V. M. Boldyrev and V. P. Lozgachev

The capacity of condensation-type atomic power stations in the Unified Power Systems (UPS) in the European part of the USSR has been increasing, with a reduction in the proportion of installed power supplied by hydroelectric plants and an increase in the proportion supplied by load-following thermal power stations (TPS) using organic fuel, whose price has been rising and whose use in electric power generation has been more and more restricted because of ecological considerations; as a result, it has become necessary to use nuclear fuel to cover the variable portion of the UPS load curve. The establishment of a reactor installation whose thermal power varies in a daily-regulation regime requires the solution of serious technical problems, since the power plants already in existence or now under construction are not adapted to operating in such a regime [1]. It should be borne in mind that unlike load-following power stations that use organic fuel, the technological scheme of a load-following atomic power station of the same type as the basic one is more complicated. Consequently, there must be greater specific capital investments made for the construction of such a plant. Furthermore, the fuel component of the cost of generating electrical energy also increases owing to the greater specific consumption of nuclear fuel per unit of energy and the higher cost of the fuel itself for operation in a load-following regime. However, even if we disregard the increase in capital investment and in fuel costs, the use of atomic power stations in a load-following regime, as will be shown below, is economically unprofitable even today in comparison with organic-fuel plants. If we take into consideration the worsening economic indicators of load-following atomic power stations, we find that atomic power plants cannot be competitive with organic-fuel load-following plants even if we use very pessimistic estimates of future increases in the cost of organic fuel.

A preferable arrangement would be not to construct load-following condensation-type atomic power stations (APS) but to equip such stations with energy-accumulating systems. The first APS + HAPS (atomic power station + hydroaccumulator power station) energy complex is already being constructed in the USSR today, on the basis of the south Ukraine atomic power station. In such an energy plant the nuclear fuel can be used for covering the variable part of the load curve of the power system while the thermal power of the reactor is kept constant, which improves the reliability and safety of the APS.

The change from gravity accumulation of energy in HAPS to thermal accumulation in the hot-water accumulators of an APS makes it possible to reduce the specific volume of the accumulators by a factor of hundreds, with a possible increase in the efficiency of the accumulation [2]. In particular, the question of including line-water accumulators or feedwater accumulators (LWA or FWA) in the construction of AHPP (atomic heat and power plants) with condensation-type turbines of the TK-450/500-60 type is of great interest. In this case we do not necessarily have to develop new turbogenerators usable in AHPP or modify the existing ones. The reason is that the reduction in the rate of steam flow through the low-pressure cylinders into the condenser when the heat bypasses are connected enables us for the case of FWA to disconnect the regenerative bypasses and thereby increase the power of the unit above its nominal value in the heat-and-power regime. When FWA are used on an APS with condensation turbines and without heat bypasses, a new turbogenerator set must be designed.

The theoretical thermal scheme of an AHPP using a TK-450/500-60 turbine, LWA, and FWA is shown in Figs. 1a and 1b. For charging the LWA (Fig. 1a), we propose using a pair of unregulated bypasses after the third and sixth stages of the turbine. These bypasses are provided for by the turbine design and are intended for the peak line heaters H_{peak_1} and H_{peak_2}. However, for a specified value of the heat-power coefficient the use of these heaters in the peak regime is not necessary. Thus, from the lower part of the accumulator, cold line water at a temperature of about 60°C enters the heaters H_{peak_1} and H_{peak_2}. After being heated in
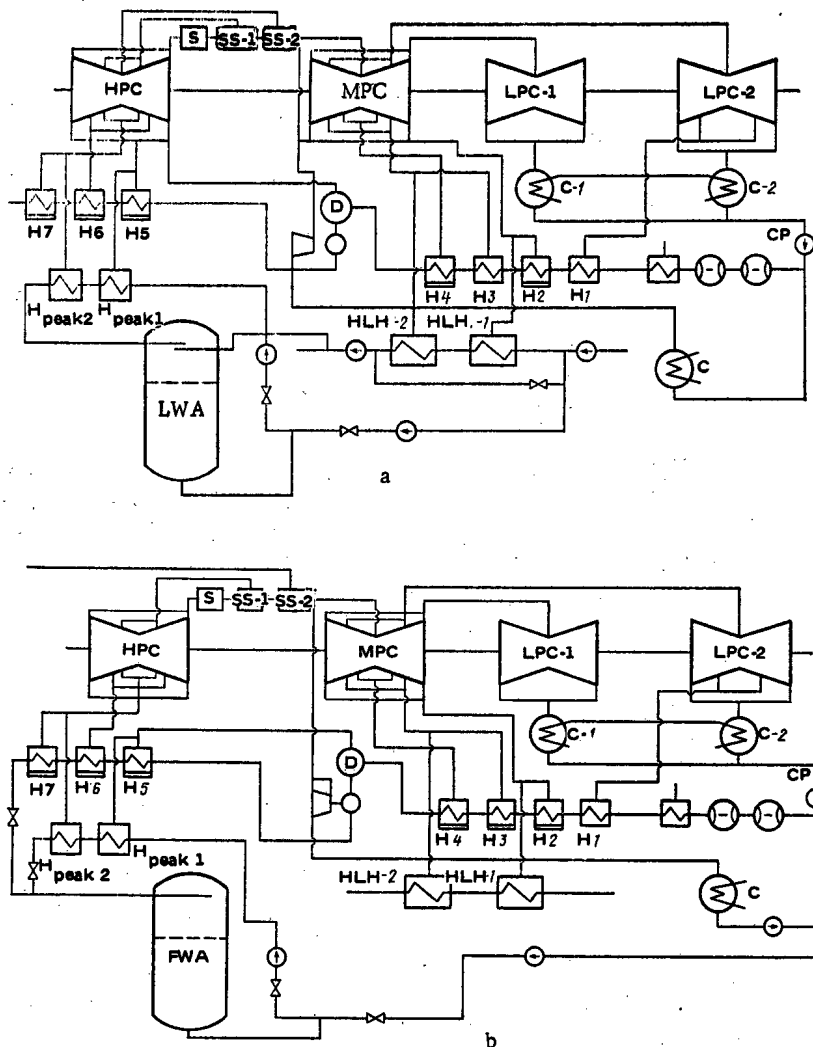

Fig. 1. Theoretical thermal scheme of an AHPP with LWA (a) and FWA (b): S) separator; SS-1, SS-2), steam superheaters; H1-H7) regenerative heaters; C-1, C-2, C) condensers; D) deaerator; CP) condensation pump; HLH) horizontal line heater; HPC, MPC, LPC) high-pressure, medium-pressure, and low-pressure cylinders.

the heaters to about 200°C, this water enters the upper part of the accumulator. The turbine power is reduced during this process because of the reduction in the steam flow rate through the flow-through part of the turbine. After the charging is completed, the accumulator will be full of hot line water.

When the accumulator is discharged, the hot line water from the upper part of the LWA is mixed with part of the returning line water and enters the thermal line at the nominal temperature of the direct line water. The other part of the returning line water is directed to the lower part of the accumulator; the bypasses that deliver steam to the line heaters of the accumulation loop are closed, and the turbine power increases to a value corresponding to the nominal amount of steam admitted to the condenser in a condensation regime. After the discharging is completed, the accumulator will be full of cold line water.

The scheme of an AHPP with FWA (Fig. 1b) differs from the preceding one (see Fig. 1a) in the fact that when the accumulator is charged, what is heated in the heaters H_{peak_1} and H_{peak_2} is not line water but feed water. When the accumulator is discharged, the feed water from the accumulator enters the steam generator, and the regenerative bypasses are disconnected. The steam flow rate into the condenser, because of the presence of heat-power bypasses, does not exceed the nominal flow rate in the condensation regime.
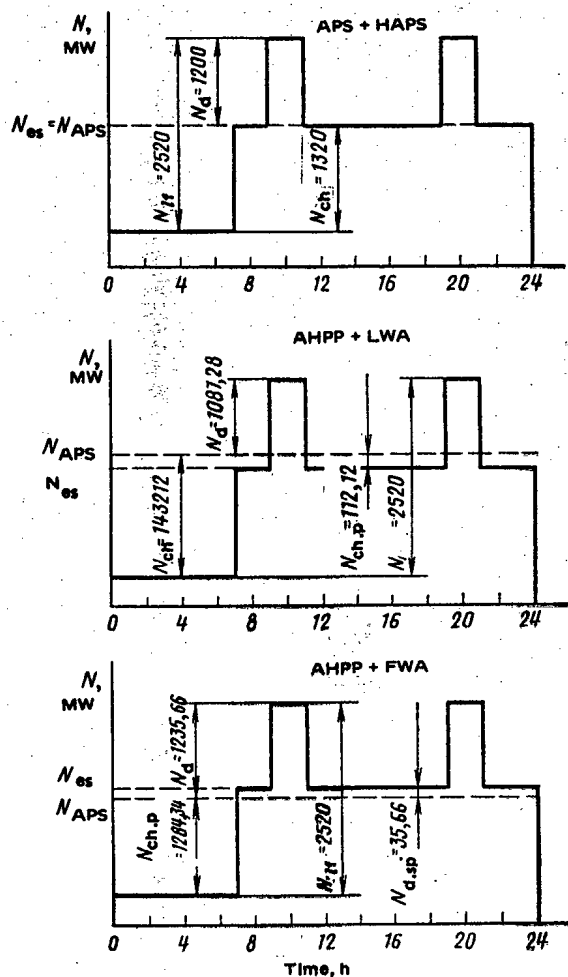
Fig. 2. Variants for covering the calculation load curves: N_{es}, power of the energy system; $N_{ch.p}$ and $N_{d.sp}$, peak power during charging and semipeak power during discharging.

Below are listed the limiting indicators of the complexes AHPP + LWA and AHPP + FWA (for one unit); during charging the maximum steam flow rate from the bypasses after the third stage is 200 tons/h, and from those after the sixth stage it is 300 tons/h; during discharging, line bypasses for LWA or regenerative bypasses for FWA are completely disconnected. The charging and discharging times are determined from the balance of accumulation and flow rate of the line or feed water in the accumulator over 1 day.

	AHPP + LWA	AHPP + FWA
Turbine power, MW:		
during charging (N_{ch})	700.8	700.8
nominal in heat-power regime (N_n)	891.2	891.2
during discharing (N_d)	1008.6	1100.6
peak ($N_p = N_d - N_n$)	117.4	209.4
compensating in UPS ($N_c = N_d - N_{ch}$)	190.4	190.4
load-following ($N_{lf} = N_d - N_{ch}$)	307.8	399.8
Time, h:		
charging	14.88	15.52
discharging	9.12	8.48
Water flow rate, tons/h:		
during charging	3672	3106
during discharging	5984	5680

399

TABLE 1. Technicoeconomic Indicators of Load-Following Power Plants

Indicator	$AHPP_{LWA}$ + $ACPS_c$	$AHPP_{FWA}$ + $ACPS_c$	$AHPP_{HAPS}$ + $ACPS_c$	AHPP + TPS	AHPP + APS_{lf}
Load in the energy system, MW:					
peak	1200	1200	1200	1200	1200
semipeak	1320	1320	1320	1320	1320
Duration of daytime peak load, h	4	4	4	4	4
Duration of nighttime dip in load, h	7	7	7	7	7
Reduction in the power of the APS when LWA is charged for the daytime dip in load, MW	112,72	—	—	—	—
Increase in the power of the APS when LWA is charged for semipeak load, MW	—	35,66	—.	—	—
Reduction in APS power when LWA or FWA is charged for nighttime dip, MW	1432,72	1284,34	1320,0	—	—
Increase in APS power when LWA or FWA is discharged for daytime peak load, MW	1087,28	1235,66	1200,0	—	—
Load-following power, MW	2520	2520	2520	2520	2520
Daily output of electrical energy, kWh:					
when LWA or FWA is discharged	$4,35 \cdot 10^6$	$5,406 \cdot 10^6$	$4,80 \cdot 10^6$	—	—
when LWA or FWA is charged	$22,89 \cdot 10^6$	$21,83 \cdot 10^6$	$22,44 \cdot 10^6$	—	—
Output of electrical energy for load-following power, kWh:					
daily	$27,24 \cdot 10^6$	$27,24 \cdot 10^6$	$27,24 \cdot 10^6$	$27,24 \cdot 10^6$	$27,24 \cdot 10^6$
annual	$68,1 \cdot 10^8$	$68,1 \cdot 10^8$	$68,1 \cdot 10^8$	$68,1 \cdot 10^8$	$68,1 \cdot 10^8$
Length of time the load-following power is used, days/yr	250	250	250	250	250
Total volume of accumulators, m³	$0,222 \cdot 10^6$	$0,447 \cdot 10^6$	$22 \cdot 10^6$	—	—
Specific capital investment in LWA or FWA, rubles/m³	236	354	—	—	—
Capital investment, millions of rubles:					
in LWA or FWA	52,31	51,91	—	—	—
in HAPS	—	—	188,4	—	—
in $ACPS_c$	401,16	359,61	369,60	—	—
total	466,55	424,5	558,0	—	705,6
Expenditures for nuclear fuel and deductions from the cost of the initial charge, millions of rubles/yr	30,20	27,08	27,82	—	27,36
Annual expenditures for organic fuel, millions of rubles/yr	—	—	—	99,15	—
Reduced calculated expenditures for the generation of load-following electrical energy, millions of rubles/yr	135,17	122,60	153,37	178,53	186,12
Specific reduced expenditures for the generation of load-following electrical energy, kopecks/kWh	1,984	1,800	2,252	2,620	2,733

Remarks.

1. Specific capital investment in load-following APS is taken to be 280 rubes/kW-(el.), i.e., disregarding the increase in investment needed to provide load-following operation.

2. For AHPP + TPS the capital investment in the TPS amounts to 352.8 million rubles per ton of nominal fuel for specific investment of 140 rubles/kW (el.). The annual rate of consumption of organic fuel is 2,478,840 tons of nominal fuel per year when the specific consumption is 364 g of nominal fuel per kWh. The cost of Kuznetsk coal is 40 rubles per ton of nominal fuel.

3. $AHPP_{LWA}$ means AHPP + LWA; $AHPP_{FWA}$ means AHPP + FWA; $AHPP_{HAPS}$ means AHPP + HAPS; APS_{lf} means load-following APS; $ACPS_c$ means condensation-type compensating APS.

For a comparison of the technicoeconomic indicators of AHPP + LWA and AHPP + FWA, as well as for a comparison of these data with the indicators of other alternative load-following energy sources, we must reduce them to identical energy and regime indicators. For this we have a condensation-type APS which compensates for the reduction in the basic power of the AHPP when it operates with accumulators.

As alternative load-following energy installations, we considered the following:

AHPP with a VVÉR-1000 + HAPS + compensating condensation-type APS with a VVÉR-1000;

AHPP with a VVÉR-1000 + TPS with semipeak K-500-130 units operating on Kuznetsk coal;

AHPP with a VVÉR-1000 + APS with a VVÉR-1000 operating in a load-following regime.

As the calculation curve, we used the UPS load curve which is shown in Fig. 2. The technical and economic indicators of the HAPS as part of the complex of APS + HAPS are:

Power, MW:	
in turbine operation	1200
in pump operation	1320
Head, m	100
Useful volume of upper reservoir, millions of m³	22
Operating time during one day, h:	
turbine operation	4
pump operation	7
Capital investment:	
total, millions of rubles	188.4
specific, rubles/kW	157

Since the number of energy-producing units per AHPP is the same for all the variants, we assume the same amount of heat release. In the case of AHPP + LWA, because of the need to work with the curve of Fig. 2, we have not fully utilized the potential of the power plants for depth of unloading, and in the case of AHPP + FWA for peak power output. Since in the variants with accumulator systems part of the basic power of the AHPP is used for generating electrical energy in the variable part of the load curve, in the technical and economic calculations we introduce a condensation-type APS which compensates for these losses. The costs for such APS are referred to the load-following electrical energy output, i.e., the electrical energy used in the variable part of the load curve. The costs for the equipment of the AHPP itself which are due to the heat release and the basic electrical energy output are the same in all the variants, and they were not considered in the comparison. The results of the comparative calculations of the technical and economic indicators of the alternative load-following power plants are shown in Table 1.

Analyzing the results obtained, we can draw the following conclusions:

1. Even if we disregard the necessary increase in capital expenditures and fuel expenditures for an APS in the production of electrical energy in a daily-regulation regime, the reduced calculated expenditures for the APS exceed the analogous expenditures for a TPS operating on Kuznetsk coal costing 40 rubles per ton of nominal fuel.

2. For the indicated cost of organic fuel, the production of electrical energy to cover the variable part of the load curve is economically more efficient in the case of an APS with accumulating systems (APS + HAPS, AHPP + LWA, AHPP + FWA) than the production of energy by a TPS.

3. If we use LWA and FWA on an AHPP, we obtain a considerable reduction in the calculated expenditures for the production of load-following electrical energy than in the case of an HAPS, with an investment saving of up to 50 rubles for each kilowatt of load-following electrical power, and the volume of the accumulators is reduced by a factor of hundreds.

4. An FWA installation on an AHPP is more efficient than an LWA, chiefly because of the lower volume of the feed-water accumulator tanks.

Taking into account the proposals made by VNIPIénergoprom [3] for setting up highly efficient load-following TPS using organic fuel, we carried out at VNIIAÉS a comparative analysis of the production of electrical energy in a load-following regime on such TPS and on load-following AHPP with FWA. The technical and economic indicators of the AHPP with FWA in the comparison were taken from Table 1. The saving in calculated expenditures in the variant with load-following AHPP was between 17 and 70 million rubles/yr (depending on the regime of operation of the AHPP during the summer), with a saving of up to 50% in annual expenditures for fuel. The results obtained confirmed once again the expected high economic efficiency of using accumulating systems on APS, especially AHPP + FWA.

LITERATURE CITED

1. B. B. Baturov et al., in: Proceedings of the International Conference on Nuclear Power Experience, Vienna (1983), IAEA-CN-42/353, p. 519.
2. V. M. Boldyrev et al., At. Énerg., 51, No. 3, 153 (1981).
3. L. A. Melent'ev et al., Teploénergetika, No. 8, 8 (1982).

COMPUTER-ASSISTED RADIATION TOMOGRAPHY OF SPHERICAL FUEL ELEMENTS

É. Yu. Vasil'eva, L. I. Kosarev,   UDC 620.179.15:621.039.546
N. R. Kuzelev, A. N. Maiorov,
and A. S. Shtan'

In recent years computer-assisted tomography has been used increasingly to investigate the internal structure of industrial products and, in particular, fuel elements [1-6]. The extensive capabilities of this method make it possible to obtain both layer images of the objects under examination and the quantitative characteristics of the volume distribution of the material.

Tomography is of particular interest for the investigation of the internal structure of spherical fuel elements since the traditional methods of inspection (x-ray radiography, fluoroscopy) give an integrated picture of the distribution of fuel microelements in a spherical fuel element, i.e., all the internal structures are superimposed upon each other, darken the image, and make interpretation of the results more complicated, while detection of zones in which microelements are accumulated above the prescribed limit can prevent them from overheating and fracturing locally.

Method of Tomographic Examination. The main principle of computer-assisted tomography consists in the following. If a radiation source and detector, collimated and arranged coaxially on opposite sides of the object under examination, are moved repeatedly in the plane of the desired cross section, the detector in this case records radiation that has traveled along a multitude of directions $L(r, \varphi)$:

$$-\ln \frac{I(r, \varphi)}{I_0} = \int_{L(r, \varphi)} \mu(x, y)\, dl \equiv P(r, \varphi), \tag{1}$$

where I_0 is the intensity of the radiation in the absence of the object, $I(r, \varphi)$ is the intensity of the radiation that passed through the object, $\mu(x, y)$ is the linear attenuation factor of the material of the object, r and φ are the parameters of the position of the beam along a straight line, and $P(r, \varphi)$ is the projection of the function. The solution of the integral equation (1) for $\mu(x, y)$ is the main task of tomography and the field $\mu(x, y)$ obtained as a result of the solution is the tomogram.

A variety of mathematical methods is used to reconstruct the cross section of the object from the results of x-raying it [6, 7] in accordance with Eq. (1). In recent years filtering out the inverse projections has become the most common method [8, 9], which is realized by the formula

$$\tilde{\mu}(x, y) = \frac{1}{2\pi^2} \int_0^\pi P^*(r, \varphi)\, d\varphi, \tag{2}$$

where $\tilde{\mu}(x, y)$ is the reconstructed value of $\mu(x, y)$ and $r = x\cos\varphi + y\sin\varphi$. The function $P^*(r, \varphi)$, corresponding to a particular angle φ, represents the filtered-out projection, which is calculated as the convolution of two functions: the projection $P(r, \varphi)$ and the filter function $A(r)$:

$$P^*(r, \varphi) = \int_{-R_0}^{R_0} P(r', \varphi)\, A(r' - r)\, dr', \tag{3}$$
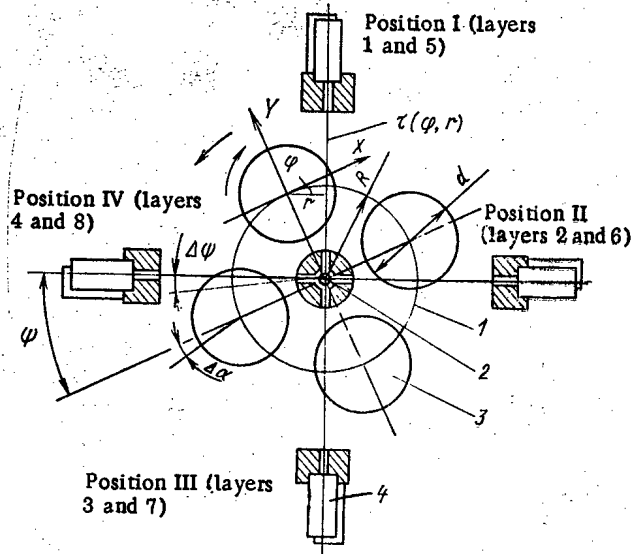

Fig. 1. Acquisition of information on tomograph: 1) turntable; 2) radiation source; 3) fuel element; 4) detectors; R is the turntable radius; d is the diameter of the fuel element or of the region of examination; φ and r are the parameters of the beam position $\tau(\varphi, r)$ in the XY coordinate system; ψ is the rotation angle of the turntable; and α is the angle of rotation of the fuel element about the axis of the holder.
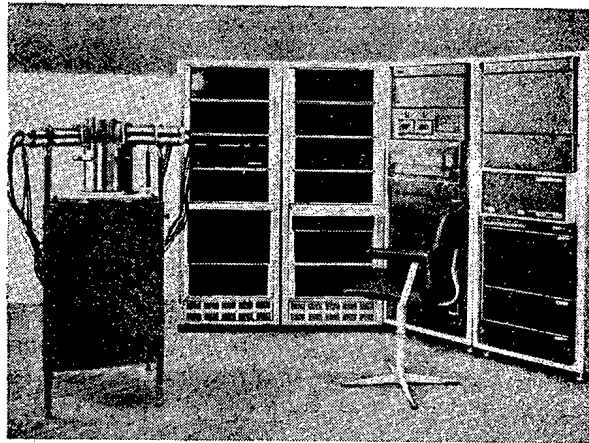

Fig. 2. General view of tomograph.

where R_0 is the radius of the region of reconstruction.

Different filter functions $A(r)$ were described in [9]. The application of different filters leads to some difference in the reconstructed image. With some filters a high resolution can be attained but the accuracy of reconstruction becomes worse, whereas other filters have good accuracy but do not ensure resolution of fine structures. Depending on the problem to be solved, provision must be made for the possible use of different filters or combinations of filters. This makes it possible to find the most successful relation between the reconstruction error and the resolution. Three different filters are used in the tomograph described below.

The data acquisition procedure illustrated in Fig. 1 was applied to the tomographic examination of spherical fuel elements. The objects to be examined are arranged in a circle, at the center of which is a stationary source of radiation. The radiation is recorded with a set of detectors located behind the control objects, two detectors per position.
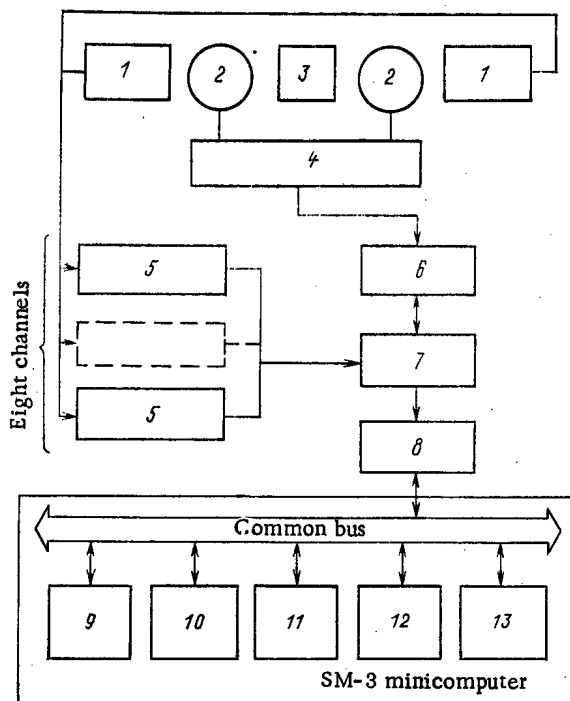
Fig. 3. Block diagram of tomograph: 1) detection block;
2) fuel element; 3) source; 4) automatic discrete scanner;
5) spectrometric channel; 6, 7) automatic control and con-
troller blocks; 8) computer interface; 9) processor of SM-3
computer; 10) memory; 11) alphanumerical printer; 12) dis-
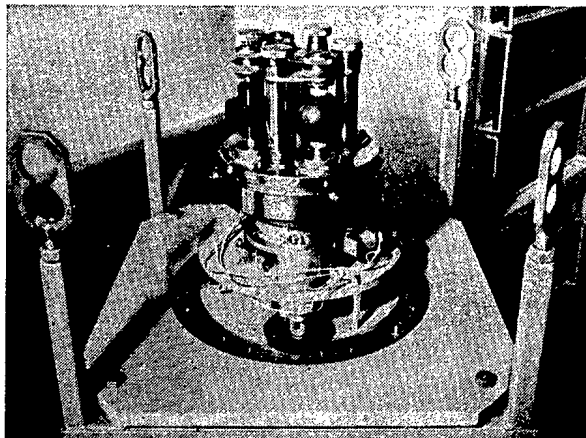play; 13) input/output unit.

Fig. 4. Automatic discrete scanner.

In the initial position the fuel elements are outside the beams of radiation and the de-
tectors record I_0. The process of acquisition of information consists of the following. The
control objects rotate discretely about the axes of the holders with an angular step $\Delta\alpha$. Dur-
ing the time when these objects stop in the position α_i, ψ_j the detectors record the intensity
$I(r, \varphi)$ of the radiation passing through the object. The objects rotate in steps of $\Delta\alpha$ until
they have described an angle of 2π, after which they are moved along the circle through an
angle $\Delta\psi$ so that

$$2r \sin \frac{n \, \Delta\psi}{2} \geqslant d,$$

where d is the diameter of the region of examination into which the object under study is
inscribed by its dimensions, R is the radius of the circle on which the objects are located,
and n is the number of displacements of the object within the limits of the control angle.
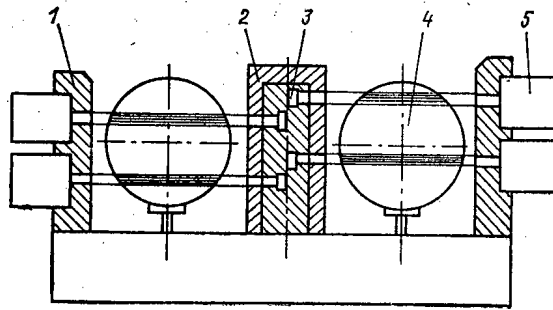
404

Fig. 5. Relative position of collimation systems and
inspected layers: 1) collimator of detection head; 2)
collimator of radiation head; 3) radiation source; 4)
fuel element; 5) detector.

The cycle is repeated until the object has been examined, i.e., until the product of the
number n of displacements of the object along the circle and the arc length $R\Delta\psi$ becomes equal
to d/2. The total number of measurements for one layer of the object is

$$N = \frac{2\pi}{\Delta\alpha} \frac{\psi}{\Delta\psi}.$$

During the movement of the objects about the axes of the holders the information undergoes
primary processing and is transmitted to a computer.

Radiation Tomograph for Examination of Spherical Fuel Elements. The computer-assisted
radiation tomograph for the inspection of spherical fuel elements is an automatic complex
of devices for moving fuel elements, measuring radiation passing through them, processing
signals obtained from the detectors, and computer-assisted reconstruction and display of
tomograms.

The tomograph (Fig. 2) consists of four main units: a discrete scanner, electronic re-
cording and automatic control equipment, a processing complex based on an SM-3 computer, and
a software complex. The block diagram of the tomograph is given in Fig. 3. The automatic
discrete scanner (Fig. 4) is designed to fix the spherical fuel elements and scan them with
collimated beams of radiation from [241]Am sources mounted in the radiation head.

The scanner is a turntable with four fuel-element holders on it. The holders are
fitted with clamps which allow fuel elements to be set up and fixed in place. Each fuel
element being examined is set into rotation about the axis of its holder and moves relative
to the radiation sources because of the turntable rotation. The electronic apparatus of the
tomograph consists of eight spectrometric channels and controller and automatic control blocks.
The controller block provides connections between all devices and an exchange of information
between the blocks of the spectrometric channels and the computer. The automatic control
block controls the automatic discrete scanner and allows the inspection regime to be selected.
The processing complex consists of an SM-3 computer and a set of programs for inputting and
processing the data and reconstructing and displaying tomograms.

Main Tomograph Parameters. The tomograph for the examination of spherical fuel elements
permits the simultaneous inspection of four objects. Two layers of each object are inspected
in one cycle. The collimation apertures of the radiation head form eight beams of radiation,
two for each inspection position. All the collimation apertures of the radiation head and the
detection blocks are shifted over the height, thus making it possible to examine eight layers
of each object as they are moved through an angle of 2π on the turntable. The relative posi-
tion of the collimation systems and the examined layers of objects in positions I and III (see
Fig. 1) is illustrated in Fig. 5. Altogether four cycles are carried out, as a result of
which information about 32 layers (i.e., eight layers for each object) is recorded on a mag-
netic disk.

The tomograph provides for three inspection regimes: a "mass" regime with $\Delta\alpha$ and $\Delta\varphi =$
6.0°; a "standard" regime with $\Delta\alpha$ and $\Delta\varphi = 3.0°$; and an "exact" regime with $\Delta\alpha$ and $\Delta = 1.5°$.
Below we give the main tomograph parameters:

405
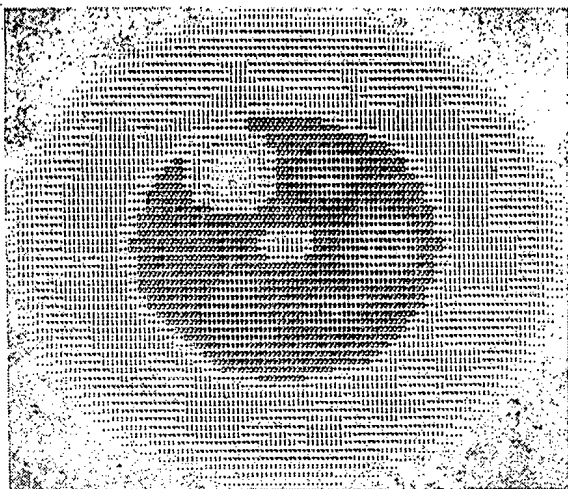
Fig. 6. Tomogram of a layer of a control specimen with seven inclusions.

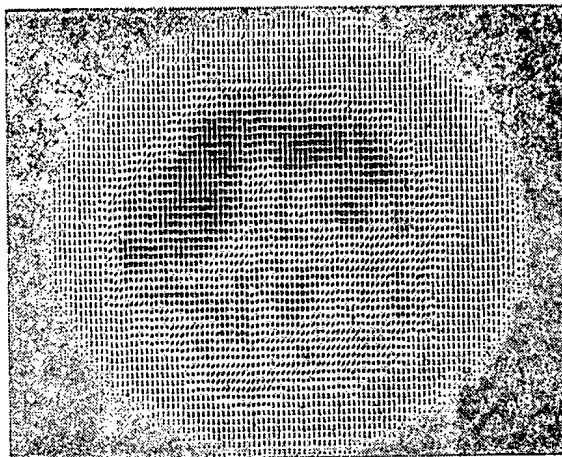Fig. 7. Tomogram of diametral layer of a spherical fuel element.

Maximum number of simultaneously inspected objects	4
Maximum number of inspected layers of object	8
Layer thickness, mm	2, 4, 8
Maximum overall size of object, mm	70
Recorded counting rate in open beam from ^{241}Am source, counts/sec	$2 \cdot 10^4$
Step of rotation of control objects in holder $\Delta\alpha$, deg	1.5, 3.0, 6.0
Step of rotation of control objects about sources $\Delta\varphi$, deg	1.5, 3.0, 6.0
Time of one count, sec	0.1–1, step 0.1 sec
Time of inspection of four objects (two layers in each) in different inspection regimes, min:	
mass regime	2.5
standard regime	7
exact regime	15
Size of reconstructed tomograms, pixels	From 20 × 20 to 62 × 62
Tomogram reconstruction time, min:	
at 30 × 30 pixels	4
at 62 × 62 pixels	14

Results of Experimental Investigations. The values $\tilde{\mu}(x, y)$ obtained during an experiment differ from the true values $\mu(x, y)$ owing to systematic and random components of the error.

The systematic component of the error arises because of the reconstruction algorithm and the regime for the inspection of the object. In order to estimate it we considered the results of mathematical simulation carried out on a conventional imitator, representing the circular cross section of a homogeneous object. Upon processing the results of the mathematic experiment it was established that the systematic component of the error varies depending on the regime of inspection, i.e., on the number N of measuring points. In this case as N increases the relative error of reconstruction decreases but the value $\tilde{\mu}(x, y)$ obtained does not reach $\mu(x, y)$, the difference being the value of the error due to the algorithm. In our apparatus the average attenuation factor is established with a relative error described by $\delta\mu = [(\tilde{\mu}-\mu)/\mu] \cdot 100\%$ (equal to 1.4% in the mass regime, 1.0% in the standard regime, and 0.6% in the exact regime). The fraction accounted for by the systematic component due to the functioning of the algorithm during reconstruction of a homogeneous structure does not exceed 0.1–0.2%.

The random component of the error is due to both the statistical nature of the radiation source and the errors in the operation of the apparatus. To estimate the random component we considered the results of experimental investigations carried out on the tomograph, using
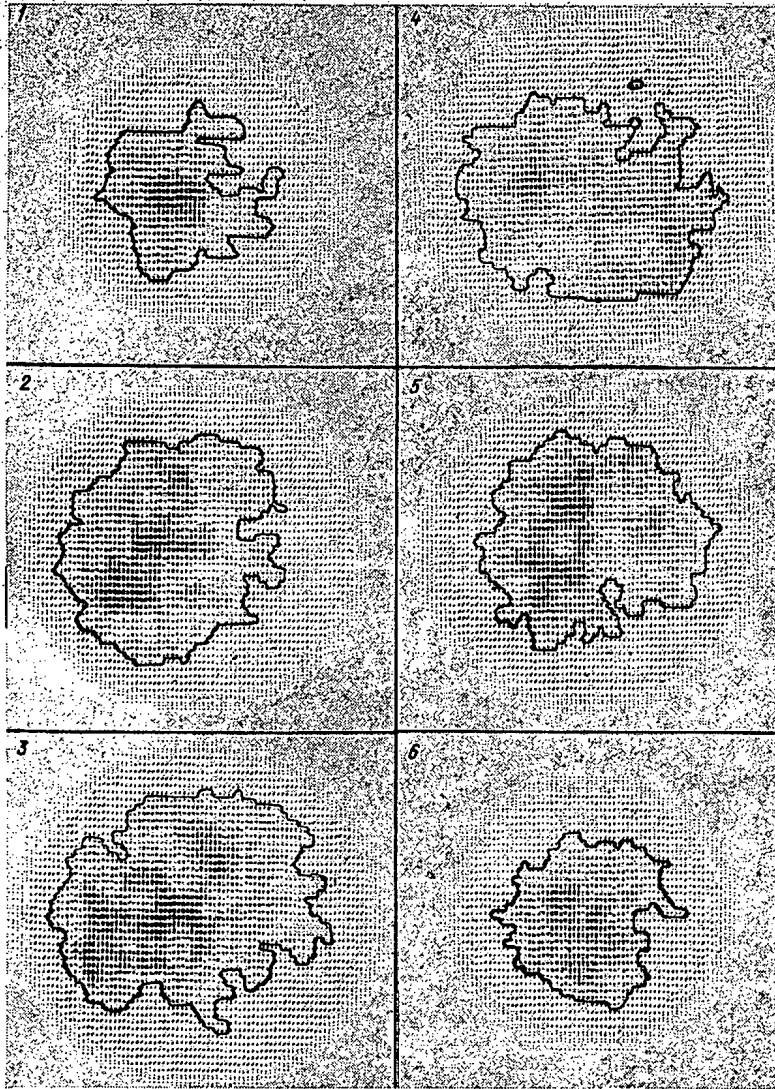
Fig. 8.   Tomograms of six layers (1-6) of spherical fuel
element (layer thickness 8 mm, core diameter 47 mm).

TABLE 1.   Mass Distribution of Metal in
Quarters of Fuel Element, g

No. of sphere quarter	Metal mass according to results of	
	tomography	chemistry
1	0,31	0,30
2	0,52	0,52
3	0,68	0,70
4	0,52	0,53
Total	2,03	2,05

imitators.   The imitators were a homogeneous aluminum cylinder of diameter 50 mm and a control
specimen, a cylinder of diameter 60 mm with a core of diameter 35 mm consisting of eight layers
with different inclusions.

On the basis of the results of the experiment we determined the random component of the
error which, according to the homogeneous structures of the imitators, is ±0.5%. The effect
of the systematic component on the determination of the average attenuation factor, depending
on the inspection regimes, is also traced in experiments on homogeneous imitators. This ef-

fect does not exceed the values obtained with mathematical simulation. Analysis of the experiments shows that the mass regime of inspection can be recommended as providing an estimate. When the standard and exact regimes are used the value of the attentuation factor of the homogeneous material is established with an error of no more than ±1.5%, with a confidence coefficient of 0.95.

One of the principal purposes of the tomograph is to detect zones of accumulation or rarefaction of fuel microelements in the core of the fuel elements. The detection of structures by the tomographic method depends substantially on their size and contrast. Different inclusions of different size and contrast were thus put into the layers of the control specimen. Since for a spherical fuel element accumulation or rarefaction of fuel microelements by ±5% or more occurs in zones no less than 0.1 cm³ in volume, inclusions were put into the control specimen on the basis of these premises.

The differences in the attenuation factors of the inclusions in the control specimen from the attenuation factor of the core material ranged from ±5 to ±20% while the differences in the volume ranged from 0.1 to 0.4 cm³. The prescribed attenuation factor μ_i of the inclusions was obtained by forming in the region of the inclusion a partial volume

$$\mu_i = \ln\left(\frac{H-h}{H}\right)\mu_1 + \ln\frac{h}{H}\mu_2, \tag{4}$$

where μ_1 and μ_2 are the attenuation factors of the core material and the insert and h and H are the heights of the insert and the inclusion.

Aluminum was used as the material for the insert. Two to seven inclusions were formed in a layer of the control system. The inclusions were deemed to have been detected on the tomogram if the difference between the value established for the attenuation factor of the inclusion and the surrounding material of the imitator was more than three times the rms deviation in the determination of the attenuation factor of the imitator material. For all the inclusions used this condition was observed in the standard and exact regimes of inspection. In the mass regime individual inclusions are not detected. This once again confirms the conclusion that the mass regime of inspection can be used only to get an estimate.

Figure 6 shows the tomogram of a layer with seven inclusions formed in accordance with formula (4). The reconstructed value of the attenuation factor of the formed inclusions in the range $\mu_i \pm 2\sigma$ coincides with that calculated from formula (4). The high reliability of detection of inclusions and the low error in the determination of the values of the reconstructed attenuation factors, obtained in experiments with a control specimen, indicate the legitimacy of using this method and apparatus for the inspection of real fuel elements. Figure 7 gives a tomogram of a real fuel element, showing that the core is not filled evenly with fuel microelements. A method of determining the fuel content in given volumes of the core was developed for a quantitative estimate of such unevenness.

Determination of the Fuel Content in Given Volumes of the Core of a Fuel Element. The linear attenuation factors obtained as a result of tomographic inspection are a function of the density of the material and, therefore, of its mass. It seems possible, therefore, to obtain an estimate of the unevenness of the mass distribution of the material over the cross section and, as a result of the joint processing of several tomograms, in the entire spherical fuel element, i.e., during tomogram processing the absolute fuel content in the spherical fuel element as a whole or in any part of it can be calculated. For any part of a layer identified by K elements of the tomogram, the mass of the fuel will be determined as

$$\sum_{i=1}^{K} m = \sum_{i=1}^{K} \frac{\mu_e V_e}{\mu/\rho} - \sum_{i=1}^{K} \frac{\mu_{gr} 0.8 V_e}{\mu/\rho}, \tag{5}$$

where m is the mass of the fuel (metal) [in g], V_e is the volume of the layer element represented by a pixel of the tomogram, μ/ρ is the mass attenuation factor of the metal, μ_e is the linear attenuation factor of the layer element, μ_{gr} is the linear attenuation factor of graphite, and 0.8 is the factor indicating the filling of the core matrix with graphite.

Passing from an estimate of the fuel over the entire layer and bearing in mind that graphite is present in the can and in the core in different weight fractions, we get

408

$$M = \mu_k \frac{V_k - \mu_{gr} (V - 0.2V_c)}{\mu/\rho},$$ (6)

where M is the mass of metal in the layer [in g], μ_k is the average attenuation factor over the tomogram, V_k is the volume of the layer corresponding to K × K elements of the tomogram, V is the volume of the entire layer under study or part of it, V_c is the volume of the entire core or part of it, and 0.2 is the porosity coefficient of the core. The result of mathematical simulation showed that, using formula (6), one can determine the metal content in half cross sections of a sphere to within ±0.2%.

In experimental investigation with a homogeneous aluminum imitator we established that in the determination of the mass of metal in a half-layer the error of the results also depends on the regime of the inspection: it is ±1.16% for the mass regime, ±0.82% for the standard regime, and ±0.69% for the exact regime.

Experimental inspections of a real fuel element were conducted in the standard regime. Six layers of the fuel element were examined and the results were processed in accordance with formula (6). The mass of metal in the sphere was determined as the sum of the masses calculated over all the layers or, similarly, for each quarter of the sphere. After the tomographic inspection the fuel element was cut into four pieces and the metal was isolated by chemical means (see Table 1 and Fig. 8).

Conclusions. Computer-assisted tomography can be one of the important tools necessary in the development of a technology of fuel-element fabrication or for sampling inspection. This method makes it possible to study the internal structure of a fuel element without destroying it and also to make a physical weighing of the fuel and to determine its content in the entire fuel element or parts of it. The metrological processing of the data obtained on this tomograph showed a high accuracy and reliability of the results.

LITERATURE CITED

1. R. Kruger and T. Cannon, Mater. Eval., 36, No. 5, 75 (1978).
2. É. Yu. Vasil'eva and A. N. Maiorov, At. Énerg., 46, No. 6, 403 (1979).
3. A. De Vuono et al., IEEE Trans. Nucl. Sci., NS-27, No. 1, 814 (1980).
4. F. Hopkins et al., IEEE Trans. Nucl. Sci., NS-28, No. 2, 1717 (1981).
5. E. Yu. Vasil'eva et al., in: Proceedings Tenth World Conference on Nondestructive Testing, Moscow (1982), Vol. 6, p. 153.
6. R. Brooks, Phys. Med. Biol., 21, No. 5, 689 (1976).
7. H. Barret and W. Swindell, TIIER, 65, No. 1, 107 (1977).
8. G. Scudder, TIIER, 66, No. 6, 5 (1978).
9. B. Horn, TIIER, 66, No. 5, 27 (1978).

PHYSICOCHEMICAL APPROACH TO THE DESCRIPTION OF THE DISTRIBUTION OF
MACROQUANTITIES OF Pu(IV) IN EXTRACTION BY TRIBUTYLPHOSPHATE
FROM NITRATE SOLUTIONS IN THE PRESENCE OF COMPLEX FORMERS
APPLICABLE TO THE REGENERATION OF SPENT NUCLEAR FUEL
FROM FAST REACTORS

A. S. Solovkin and V. N. Rubisov   UDC 66.061.5

In the regeneration of spent nuclear fuel from fast reactors, aqueous nitrate solutions with a metal — Pu(III), Pu(IV), or a mixture of both — content of not less than 20-30 g/liter appear in the operation of extractive refining of plutonium. To develop an adequate model of the state of macroconcentrations of Pu(IV) in aqueous nitrate solutions and the distribution of this element in two-phase extraction systems (with the aim of computer prediction of steady conditions of the extractional technology of regenerating spent nuclear fuel from fast reactors), it is necessary to have a thermodynamic approach to the interpretation of equilibrium in homogeneous and heterogeneous systems, which takes objective account of the state of the multicomponent extractive system.

Current theory is not in a state to predict the thermodynamic properties of the systems $H_2O-HNO_3-Pu(NO_3)_4$, $H_2O-HNO_3-Pu(NO_3)_4$-complex former nor the distribution of Pu(IV) between aqueous solutions of the given composition and solutions of tributylphosphate (TBP) in organic solvents [1, 2]. As a result of the inadequacy of the theory of solutions, there has recently been a trend in the literature away from the development of theoretically well-founded models (even for the classical pureks process), with the proliferation of purely empirical methods of describing the extractive equilibrium, on the basis of an analysis of enormous quantities of statistical material [3, 4].

Progress in terms of the quantitative description of extractive equilibrium in two-phase liquid systems of any complex composition (regardless of the number of components, their nature, and concentration) may only be attained on the basis of a thermodynamic approach to the interpretation of equilibrium; as shown in [5], the description must employ the activity coefficients of the individual ions involved in the reactions of complex formation or the distribution between two immiscible phases; see also [1, 2]. Such an approach has already been realized in the computer prediction of steady conditions of the extractive technology for regenerating spent nuclear fuel [6], and is extended in the present work to fast-reactor fuel.

State of Pu(IV) in Aqueous Nitrate Solutions. Thermodynamics.

Complex Formation. Extraction

In its chemical properties, Pu(IV) is closest to Zr(IV) [7], and therefore it may be considered that there is a qualitative analogy between the states of Zr(IV) [8, 9] and Pu(IV) [10] in aqueous nitrate solutions. It is known that, on account of the high electrostatic potential f in aqueous solutions of inorganic acids, the Zr^{4+} ion is easily hydrolyzed according to the equation

$$M^{4+} + iOH^- \overset{\beta_c^0}{\rightleftarrows} M(OH)_i^{4-i}. \tag{1}$$
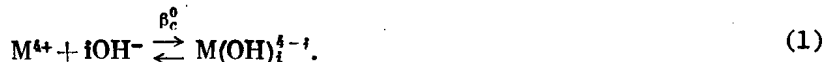
Since $fPu^{4+} < fZr^{4+}$, Pu^{4+} is considerably less hydrolyzed than the Zr^{4+} ion in aqueous solutions with high (<1 g-ion/liter) values of $[H^+]$. Nevertheless, when $[H^+] \lessgtr 1$ g-ion/liter, the chemistry of aqueous solutions of Pu(IV) is basically the chemistry of its hydrolyzed forms. The hydrolyzed forms of Zr(IV) and Pu(IV) readily form hydrolytic polymers. However,

TABLE 1. Thermodynamic Equilibrium Constants of the Reaction in Eq. (1) at $\sim 25°C$

M(IV)	$\beta_1^0 \cdot 10^{-14}$	$\beta_2^0 \cdot 10^{-28}$	$\beta_3^0 \cdot 10^{-42}$	$\beta_4^0 \cdot 10^{-56}$	Literature data
Zr	3,8	23,9	52,4	70	[10]
Pu	0,17	0,60	3,2	3,5	[10, 15]
Np	0,11	0,28	1,0	1,5	Present work
U	0,06	—	—	—	[10]

Note. $\gamma_{M(OH)_4} \approx 1.0$.

TABLE 2. Equilibrium Constants of the Complex-Forming Reactions of Pu(IV) and Zr(IV) with Some Inorganic and Organic Ligands at $\sim 25°C$

Reaction	Constant	Ref. data
$Pu^{4+} + HSO_4^- \rightleftharpoons PuSO_4^{2+} + H^+$	$3 \cdot 10^3$	[16]
$Pu(OH)^{3+} + HSO_4^- \rightleftharpoons Pu(OH)SO_4^+ + H^+$	$5 \cdot 10^4$	[16]
$Pu(OH)_2^{2+} + HSO_4^- \rightleftharpoons Pu(OH)_2SO_4 + H^+$	$6 \cdot 10^4$	[16]
$Pu(OH)_2^{2+} + (CH_3COOH)_2 \rightleftharpoons Pu(OH)_2(CH_3COO)_2 + 2H^+$	93	[15]
$Pu(OH)_3^+ + HCOOH \rightleftharpoons Pu(OH)_3(HCOO) + H^+$	20	Calc. from the data of [17]
$Pu(OH)^{3+} + H_2C_2O_4 \rightleftharpoons Pu(OH)C_2O_4^+ + 2H^+$	$2,4 \cdot 10^7$	[10]
$Zr(OH)_2^{2+} + H_2C_2O_4 \rightleftharpoons Zr(OH)_2C_2O_4 + 2H^+$	$4 \cdot 10^6$	[10]

Note. The ratios of activity coefficients $\gamma_{PuSO_4^{2+}}/\gamma_{HSO_4^-}$, $\gamma_{Pu(OH)SO_4^+}/\gamma_{HSO_4^-}$, $\gamma_{Pu(OH)_2SO_4}/\gamma_{HSO_4^-}$, $\gamma_{Pu(OH)_2(CH_3COO)_2}/\gamma_{(CH_3COOH)_2}$, $\gamma_{Pu(OH)_3(HCOO)}/\gamma_{HCOOH}$, $\gamma_{Pu(OH)C_2O_4}/\gamma_{H_2C_2O_4}$ and $\gamma_{Zr(OH)_2C_2O_4}/\gamma_{H_2C_2O_4}$ are approximately equal to unity or a constant. Taking account of the assumptions made, the values of K_{ij}^0 are constant (for ionic strengths in the range $I \le 5$). When $I > 5$, the ions $M^{4+} = Pu^{4+}$, U^{4+} (and possibly others) are involved in cascade reactions with NO_3^- ions, with the formation of $M(NO_3)_6^{2-}$ anions [10].

whereas polymers of Zr are observed when $[HNO_3] \lesssim 5$ M in the case of macroconcentrations of metal, the polymerization of Pu(IV) only occurs when $[HNO_3] \lesssim 0.15-0.2$ M. By analogy with Zr, it may be expected that the basic structural unit of Pu(IV) in dilute ($\lesssim 0.15-0.2$ M) aqueous solutions of HNO_3 is a tetramer. Since the literature has no quantitative characteristics of the polymerization of Pu(IV) and Zr(IV) [11, 12], a quantitative estimate of the state of Pu(IV) in aqueous nitrate solutions at macroconcentrations is made in the present work for $[HNO_3] > 0.15-0.2$ M, i.e, up to compositions of the aqueous system in which Pu(IV) exists in monomeric form.

As already noted, in describing chemical equilibrium, it is necessary to use the activity coefficients of individual ions (but not the stoichiometric activity coefficients). On the basis of an analysis of published data on the activity coefficients, the transfer numbers, the electrical conductivity, and the density of the aqueous solutions of electrolytes, phenomenological equations were proposed in [1, 2], allowing the activity coefficients of individual ions in aqueous solutions of 1,1-, 1,2-, 1,3-, and 1,4-electrolytes and their mixtures

411

TABLE 3. Equilibrium Constants of the Reaction in Eq. (2) at 25°C

M(IV)	K°_{0} $j=0$	K°_{1} $j=1$	K°_{2} $j=2$	K°_{3} $j=3$	Diluent	Range of application of Eq. (2)	
						HNO_3, M	TBF, vol.%
Zr	0,6	14	5	—	Kerosene	⩽ 6	⩽ 60
Zr	0,8	24	7	—	o-Xylol	⩽ 6	⩽ 60
Pu	190	41750	1195	9,4	n-Alkanes	⩽ 5	10—40
U	300	22000	—	—	Kerosene	⩽ 3,5	20—30
Th	150	—	—	—	Kerosene	⩽ 3,5	20—30

to be calculated sufficiently correctly over a broad range of concentration of components of the salt background. The equations of [1, 2] are based on a qualitatively new approach to the phenomenon of ionic hydration, developed in [13]. The values of the parameters of ionic hydration ρ_+ are given in [2]; from the experimental data of [4], values ρ_+ = 0.047 and 0.039 are obtained for the ions Pu^{3+} and $N_2H_5^+$, respectively. In using the equations of [1, 2] for the identification of the processes occurring in aqueous solutions of Pu(IV), and determining the thermodynamic equilibrium constants of the reactions of hydrolysis and complex formation and the distribution, the limited number of assumptions given in the notes to Tables 1 and 2 is employed.

On the basis of thermodynamic analysis of the present data, and those in the literature, on the relations between composition and properties, for the nitrates M = Zr(IV), U(IV), Np(IV), Pu(IV) it was concluded in [10] that the ions $M(OH)_i^{4-1}$ (i = 0-3) do not react with NO_3^- ions in the first coordination sphere, and the nonideality of aqueous nitrate solutions of M(IV) is due to the change in structure and extent of their hydrate shells with change in composition of the solutions. This conclusion, important for both theory and practice, was later confirmed in many works [9, 14].

Using the method developed in [1, 2], the thermodynamic constants of hydrolysis of M^{4+} ions shown in Tables 1 and 2 have been calculated, together with the constants of complex formation of $M(OH)_i^{4-1}$ with certain organic and inorganic adducts in aqueous nitrate solutions. It follows from Table 2 that, in complex-forming reactions, the ions which react with the organic ligands are not M^{4+}_{ad} but $M(OH)^{4-1}_{iad}$, which have a considerably weaker hydrate shell because of the reduction in charge and increase in radius of the hydrolyzed ions in comparison with M^{4+}_{ad} [10, 15].

In [16], the thermodynamic characteristics of the system Pu(IV)—HNO_3—H_2O were given. It was established that, with increase in [HNO_3] and [Pu(IV)], there is a significant change in the activity coefficients of the particles $Pu(OH)_i^{4-1}$ (i = 0-3), H^+, NO_3^- in the system, the yield and distribution of hydrolyzed forms of Pu(IV), the concentration of H^+ ions (especially when [HNO_3] < 1 M), and the degree of dissociation of HNO_3; the method of calculating the degree of dissociation, taking account of the activity coefficients of nondissociated HNO_3 molecules, was outlined in detail in [1]. It follows from the data of [16] that the description of chemical equilibrium with variation in the Pu(IV) concentration in the solutions from 1-2 g/liter (fuel elements of water-cooled—water-moderated reactors) to 20-30 g/ liter and more (fast-reactor fuel elements) both when [HNO_3] ≠ const and when [HNO_3] = const is impossible without taking account of the change in the given parameters as a function of the state of the solution. It is more significant that the use of the method of [1, 2] allows the chemical reactions occurring in complex multicomponent — and heterogeneous — systems to be identified.

On the basis of the method of [1, 2], using the results of the present work and literature data [7], it may be shown [10, 18] that the extraction of M(IV) by tributylphosphate (TBF) solutions occurs according to the equation*
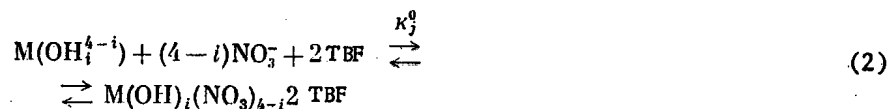
---

*Experimental proofs are given in [10].

TABLE 4. Comparison of Experimental [20, 21] and Calculated Data on the Extraction of Pu(IV) at 25°C

	Expt.		Calc.
$[HNO_3]_{aq}$, M	$[Pu]_{aq}$, g/liter	$[Pu]_0$, g/liter	$[Pu]_0$, g/liter
0,52	1,41	1,58	1,73
0,53	4,28	4,79	4,79
0,52	13,6	17,1	15,9
0,51	19,6	21,2	21,2
0,51	33,5	37,7	36,7
0,99	0,63	1,72	1,83
0,99	2,27	5,8	5,55
1,00	5,73	14,7	13,3
1,01	8,3	19,2	19,2
1,20	13,8	30,0	33,4
3,89	0,014	0,34	0,29
3,98	0,129	2,27	2,6
3,94	0,145	8,6	8,4
3,93	0,98	16,7	16,8
4,01	1,77	25,0	29,3

TABLE 5. Comparison of the Calculated and Experimental [19] Values of the Distribution Coefficients of Pu(IV) in the System HNO_3–Pu(IV)–HCOOH–H_2O–30% TBF Solution

$[HNO_3]_{aq}$, M	$[HCOOH]_{aq}$, M	D_{Pu}		D_{HCOOH}	
		data of [19]	calc.	data of [19]	calc.
0,246	0,49	0,17	0,15	0,49	0,46
0,246	1,01	0,084	0,088	0,37	0,37
0,246	2,02	0,043	0,042	0,27	0,27
0,246	3,02	0,024	0,024	0,23	0,22
0,56	2,05	0,17	0,18	0,27	0,26
0,56	3,1	0,12	0,105	0,22	0,21
0,8	1,0	0,74	0,88	—	0,35
0,8	2,0	0,48	0,44	—	0,26
0,8	3,0	0,3	0,27	—	0,21
1,05	0,56	1,7	1,81	0,36	0,38
1,05	1,09	1,24	1,25	0,30	0,32

$$M(OH_i^{4-i}) + (4-i)NO_3^- + 2\,TBF \underset{\longleftarrow}{\overset{K_j^0}{\longrightarrow}}$$
$$\underset{\longleftarrow}{\overset{}{\rightleftarrows}} M(OH)_i(NO_3)_{4-i}2\,TBF \tag{2}$$

where $i = 0$–3. The values of K_j^0 for the corresponding reactions (Table 3) are not strictly thermodynamic, since they are calculated by an empirical method, using the parameter E_a^q from Eq. (3) to take account of the nonideality of the organic phase [1, 2, 10, 18]. Nevertheless, the approach to the interpretation of extractive equilibrium developed in [1, 2, 10, 18] gives a sufficiently rigorous quantitative description of the distribution of M(IV) (and other metals) in multicomponent heterogeneous systems, since the empirical Eq. (2), taking account of nonideality of the organic phase, is obtained on the basis of statistical analysis of numerous literature data [17] on the distribution of uranyl nitrate and M(IV) in the systems H_2O–extractive agent–HNO_3–salting-out agent–TBF–diluent, taking account (this is most important) of nonideality of the aqueous phase [1, 2]. The validity of Eq. (2) has been proven for many examples [2, 6, 10, 15, 18].

The given approach to the interpretation of equilibrium in homogeneous and heterogeneous systems has been used to develop a mathematical model of the distribution of Pu(IV) and HNO_3 in reflux processes of the purification of plutonium in the regeneration of spent fast-reactor fuel.
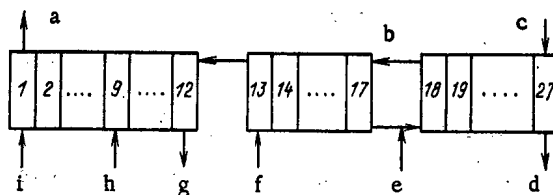
Fig. 1. Diagram of the extractional purification
of plutonium in nominal conditions: a) spent ex-
traction agent <2.0 mg/liter; b) plutonium extract;
c) the extraction agent, a 30% solution of TBF in
n-paraffins (organic-phase flow rate is 1.3 arb.
units); d) the refined material, <2.0 mg/liter Pu;
e) initial solution, 2.0 M HNO_3, 20 g/liter Pu(IV),
$L_{18} = 1.0$ (L is the aqueous-phase flow rate, arb.
units); f) washed solution, 1.0 M HNO_3, $L_{13} = 0.2$;
g) reextract (~50 g/liter Pu); h) 0.3 M HNO_3, 10 M
HCOOH, $L_9 = 0.15$; i) 0.3 M HNO_3, $L_1 = 0.25$; 1-27)
extractional stages.

Formalization of the Extractional Equilibrium in the System HNO_3–Pu(IV)–

Complex Former–H_2O–TBF Solution

According to Eq. (2), the distribution coefficient of Pu(IV) in the extractional system
is

$$D_{Pu} = E_a^q \sum_i K_i^0 \gamma_i M_i' a_{NO_3^-}^{i-i},$$

(3)

where the index i identifies the ion $Pu(OH)_i^{(4-i)+}$ (i = 0-4); K_i^0 are thermodynamic equilibrium
constants of the complex-formation reaction with TBF (Table 3); E_a^q is the active concentration
of the extraction agent, a factor that takes account of the nonideality of the organic phase
[1, 2, 10, 18]; γ_i and M_i are the activity coefficients and mole fractions of the correspond-
ing ions in the aqueous phase; $a_{NO_3^-}$ is the activity of NO_3^- ions in the aqueous phase.

Formulas for calculating the activity coefficients and M' of $Pu(OH)_i^{(4-i)+}$ in the sys-
em HNO_3–Pu(IV)–H_2O are given in [16]. For the system HNO_3–Pu(IV)–H_2O–complex former, the
formation of plutonium compounds with the complex former must be taken into account. There-
fore, in contrast to [16]

$$M_0' = 1 / \left\{ 1 + \gamma_0 \left[\sum_{i=1}^3 \beta_i^0 \left(\frac{K_{aq}}{a_{H^+}} \right)^i / \gamma_i \right] + R_K^{(j)} \right\};$$

(4)

$$M_i' = \beta_i^0 \left(\frac{\gamma_0}{\gamma_i} \right) \left(\frac{K_{aq}}{a_{H^+}} \right)^i / \{\text{idem}\}, \quad i = 1 - 4,$$

(5)

where idem is the denominator of Eq. (4); a_{H^+} is the activity of the H^+ ions; β_i^0 are the
constants of hydrolysis of Pu(IV) (Table 1); K_{aq} is the ionic product of water.

In Eqs. (4) and (5), $R_K^{(j)}$ reflects the formation of a compound of Pu(IV) with the j-th
complex former. According to the data of Table 2

$$R_K^{(S)} = \gamma_0 \frac{[HSO_4^-]}{a_{H^+}} \sum_{i=0}^2 K_i^{(S)} \beta_i^0 \left(\frac{K_{aq}}{a_{H^+}} \right)^i; \quad \beta_0^0 = 0;$$

$$R_K^{(E)} = \gamma_0 \frac{[HCOOH]}{a_{H^+}} K_3^{(E)} \beta_3^0 \left(\frac{K_{aq}}{a_{H^+}} \right)^3;$$

$$R_K^{(A)} = \gamma_0 \frac{[(CH_3COOH)_2]}{a_{H^+}^2} K_2^{(A)} \beta_2^0 \left(\frac{K_{aq}}{a_{H^+}} \right)^2,$$

where the superscripts S, E, and A correspond to H_2SO_4, HCOOH, CH_3COOH.

The concentration of free (not bound with plutonium) complex former is determined from
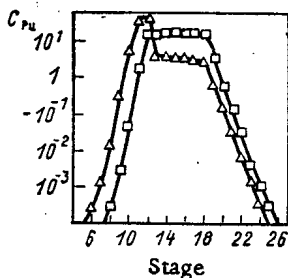the following expression

414

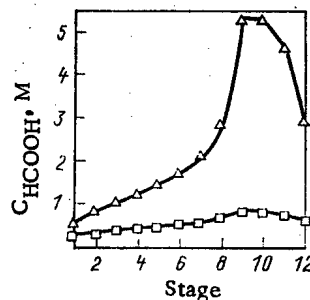Fig. 2. Distribution of plutonium over the stages of the process: ☐) organic phase; Δ) aqueous phase.

Fig. 3. Distribution of HCOOH over the stages of the reextraction apparatus: ☐) organic phase; Δ) aqueous phase.

$$[HSO^-] = [H_2SO_4]_{aq} \Big/ \Big\{ 1 + \frac{[Pu^{4+}]\gamma_0}{a_{H^+}} \sum_{i=0}^{2} K_i^{(S)}\beta_i^0 \Big(\frac{K_{aq}}{a_{H^+}}\Big)^i \Big\};$$

$$[HCOOH] = [HCOOH]_{aq}/\{1 + [Pu(OH)_3^+]\gamma_3 K_3^{(E)}/a_{H^+}\};$$

$$[(CH_3COOH)_2] = [(CH_3COOH)_2]_{aq}/\{1 + [Pu(OH)_2^{2+}]\gamma_2 K_2^{(A)}/a_{H^+}^2\};$$

$$[Pu(OH)_i^{(4-i)+} = [Pu]_{aq} M_i',$$

where $[H_2SO_4]_{aq}$, $[HCOOH]_{aq}$, $[(CH_3COOH)_2]_{aq}$, $[Pu]_{aq}$ are the analytical concentrations of the complex formers and plutonium in the aqueous phase. It is assumed here that CH_3COOH is present in aqueous solutions primarily in the dimer form.

To calculate the extractional systems discussed here, quantitative data are necessary on the extraction of tri-n-butylphosphate by nitric acid and complex former. The extraction constants of HNO_3 [1, 2], HCOOH [19], and CH_3COOH [18] appear in the expression for determining the concentration of free extractive agent

$$E_0 = \frac{E_{in} - 2[Pu]_0}{1 + K_{1H}[\overline{HNO_3}] + K_2H[\overline{HNO_3}]^2 + S_k^{(j)}},\tag{6}$$

Here $[Pu]_0$ is the Pu(IV) concentration in the organic phase; $[\overline{HNO_3}]$ is the concentration of undissociated nitric acid in the aqueous phase; E_{in} is the initial TBF concentration; $S_k^{(E)} = K_3^{(E)}[HCOOH]$; $S_k^{(A)} = K_2^{(A)}[(CH_3COOH)_2]$; K_1H, K_2H, $K_3^{(E)}$, $K_2^{(A)}$ are the equilibrium constants of the extraction reactions $HNO_3 + TBF \rightleftarrows HNO_3 \cdot TBF$, $\overline{2HNO_3} + TBF \rightleftarrows (HNO_3)_2 \cdot TBF$, $HCOOH + TBF \rightleftarrows HCOOH \cdot TBF$, and $(CH_3COOH)_2 + TBF \rightleftarrows (CH_3COOH)_2 \cdot TBF$; for the system TBF—n-alkanes, the values of the constants are 8.1, 0.8, 0.54, and 0.41, respectively.

Comparison of Experimental Data with the Results of Calculation

To evaluate the mathematical model of the equilibrium distribution based on the foregoing data, the experimental values of D [20, 21] obtained in the extraction of Pu(IV) by a TBF solution (30 vol.%) in n-alkanes from aqueous nitrate media are employed. A comparison of the experimental and calculated equilibrium concentrations of plutonium in the organic phase is shown in Table 4. In considering the data of Table 4, it must be remembered that extraction constants obtained from experimental results with microconcentrations of plutonium are used to calculate the distribution of microconcentrations of the metal. This is a reliable indication of the superiority of the thermodynamic model of extraction.

There are no published data on the extraction of macroquantities of plutonium from nitrate aqueous solutions in the presence of complex formers (H_2SO_4, CH_3COOH, HCOOH).* As a result, the possibility of using the mathematical model with macroconcentrations of plutonium for systems with complex formers must be regarded as hypothetical. However, the given results of modeling the extractional system HNO_3—Pu(IV)—H_2O—TBF allow an optimistic view to be taken of this hypothesis. This is confirmed by the data given in the next section on modeling the process of reextraction of macroconcentrations of plutonium by HCOOH solutions from a TBF solution (30 vol.%) in n-paraffins [22] for the purification of PU in the reprocessing of fast-reactor fuel elements.

*Results of modeling these extractional systems with microconcentrations of Pu(IV) are outlined in [15, 18] and shown in Table 5.

415

Calculation of the Reflux Process of the Pu(IV) Distribution

Calculation programs developed for the purposes of design, research, and optimization of the process must give information on the distribution of components over the extractional stages of the apparatus. The material-balance equations of the extractional process form a system as follows

$$X_{ij} + n_i Y_{ij} = \tilde{X}_{ij} + n_i \tilde{Y}_{ij};$$
$$i = 1, 2, \ldots, N; \tag{7}$$
$$\tilde{j} = 1, 2, \ldots, m,$$

where X_{ij}, Y_{ij} are equilibrium concentrations of the j-th component at the i-th stage in the aqueous and organic phases; n_i is the ratio of flow rates of the organic and aqueous phases; $\tilde{X}_{ij}$ and $\tilde{Y}_{ij}$ are concentrations of the components at the input to the i-th stage; N is the total number of extractional stages; m is the number of components of the extractional system.

A very effective method of solving Eq. (7) is simple iteration

$$\tilde{X}_{ij} = \frac{\tilde{X}_{ij} + n_i \tilde{Y}_{ij}}{1 + n_i Y_{ij}/X_{ij}}.$$

For extractional processes with a near-unity stage efficiency, the ratio Y_{ij}/X_{ij} determines the equilibrium-distribution coefficients of the i-th component. The thermodynamic characteristics given in the preceding sections are used in the calculations.

In conditions of extractive refinement of plutonium, it is expedient to use complex formers in the operation of reextraction of the metal. Complex formers significantly reduce the distribution coefficient of Pu(IV). In consequence, even when the reflux process is being organized with just a few extractional stages, the use of complex formers allows Pu to be practically completely separated from the phase of the extraction agent. The mathematical modeling of the reextraction process here shows that H_2SO_4, CH_3COOH, and $HCOOH$ may be used for the extractional refining of plutonium. The choice of a particular complex former must be made in relation to the processes of further processing of the reextract of plutonium and waste solutions. Formic acid is the most suitable for this purpose. Thus, the introduction of complex formers (for example, HCOOH) in one of the intermediate stages of the reextraction apparatus reduces the accumulation of plutonium in the apparatus and its content in the spent extraction agent.

The results of preliminary investigations have been used to choose the structure and parameters of the conditions of extractional purification of plutonium. The process consists of the following extractional units: extraction of Pu(IV), washing of the plutonium extract to remove radionuclides of some fission products, reextraction of plutonium.

The initial conditions and constraints in modeling the process on an EC-1055 computer (calculation time of the cascade ∿3 min) are taken to be as follows: in the initial aqueous solution, the Pu and HNO_3 concentrations are ∿20 g/liter and ∿1.5 M, respectively; in the spent extraction agent and the refined material, the plutonium content is <2 mg/liter; plutonium accumulation in the organic phase at any stage is <20 g/liter (this rules out the possibility of third-phase formation); the HNO_3 concentration in the reextracting solution is >0.2 M, which allows the formation of insoluble hydroxyl complexes of Pu(IV) with disruption of the reextraction process to be ruled out. A necessary condition on the topology and conditions of the process is the invariance of the indices of the process under deviations of the parameters of the operating conditions. The deviations are determined with an error of ±10% for the flow rates and ±20% for the reagent concentrations.

The results of mathematical modeling of the extractional purification of plutonium are shown in Figs. 1-3. In the range of assumed deflections from the nominal conditions, computer calculations are performed. The levels of the process parameters are determined using tables of random numbers. Altogether, 54 different operating conditions of the process are considered. The quality indices do not pass beyond the specified constraints in any of these conditions. Only in two cases does the calculated Pu concentration in the spent extraction agent approach the maximum permissible value. This is basically because of the decrease in reextraction-agent flow rate (L_1 = 0.227-0.229), complex-former flow rate (L_9 = 0.136-0.138),

416

and HCOOH concentration (6.5–6.7 M), and increase in extraction-agent flow rate (V = 1.398–1.422), in comparison with the nominal conditions. The probability estimate for these conditions is 0.00017–0.00023.

To sum up the overall results of modeling the process, it may be said that the indices of the process may only pass beyond the specified values (in practical conditions) when several parameters deviate simultaneously from the nominal conditions by a considerable (and hence improbable) amount.

LITERATURE CITED

1. A. S. Solovkin, Salting Out and Quantitative Description of Extractional Equilibrium [in Russian], Atomizdat, Moscow (1969).
2. A. S. Solovkin, "Salting out and quantitative description of extractional equilibrium," in: Results of Science and Technology, Inorganic-Chemistry Series [in Russian], Vol. 3, Izd. VINITI (1972).
3. Z. Kolarik and J. Petrich, Phys. Chem., 83, 1110, (1979).
4. H. Schmieder, J. Petrich, and A. Hollmann, J. Inorg. Nucl. Chem., 43, 3373 (1981).
5. V. V. Fomin, Radiokhim., 9, 652 (1967).
6. V. N. Rubisov and A. S. Solovkin, At. Energ., 52, No. 3, 404 (1982).
7. A. S. Solovkin, Radiokhim., 24, 56 (1982).
8. A. S. Solovkin and G. A. Yagodin, "Extractional chemistry of zirconium and hafnium. Part 1," in: Results of Science and Technology, Inorganic-Chemistry Series [in Russian], Vol. 1, VINITI (1969).
9. A. S. Solovkin and G. A. Yagodin, "Extractional chemistry of zirconium and hafnium. Part III," in: Results of Science and Technology, Inorganic-Chemistry Series [in Russian], Vol. 5, VINITI (1976).
10. A. S. Solovkin, J. Rad. Chem., 21, 15 (1974).
11. J. Bell, D. Costanzo, and R. Biggers, J. Inorg. Nucl. Chem., 35, 609, 623, 629 (1973).
12. Z. Toth, H. Friedman, and M. Osborne, J. Inorg. Nucl. Chem., 43, 2929 (1981).
13. O. Ya. Samoilov, A Structure of Aqueous Solutions of Electrolytes and Hydration of Ions [in Russian], Izd. Akad. Nauk SSSR, Moscow (1957).
14. A. S. Solovkin, "Association of aqueous solutions of electrolytes and hydration of ions," in: Results of Science and Technology. Solutions and Melts Series [in Russian], Vol. 1, Izd. VINITI (1975), p. 64.
15. A. S. Solovkin et al., At. Energ., 50, No. 4, 422 (1981).
16. M. Ya. Zel'venskii and A. S. Solovkin, Radiokhim., 22, 642 (1980).
17. Z. I. Nikolotova and N. A. Kartashova, Handbook on Extraction [in Russian], Vol. 1, Atomizdat, Moscow (1976).
18. A. S. Solovkin and Yu. N. Zakharov, Radiokhimiya, 22, 225 (1980).
19. V. I. Volk et al., Zh. Neorg. Khim., 27, 1773 (1982).
20. V. E. Vereshchagin and É. V. Renard, At. Energ., 44, No. 4, 422 (1978).
21. V. E. Vereshchagin and É. V. Renard, At. Energ., 45, No. 1, 45 (1978).
22. G. F. Egorov et al., At. Energ., 46, No. 2, 75 (1979).

CONTRIBUTION OF NUCLEAR INTERACTIONS TO THE DISTRIBUTION OF ABSORBED
ENERGY IN THIN PLATES BOMBARDED WITH FAST CHARGED PARTICLES

S. G. Andreev, I. M. Dmitrievskii,
and I. K. Khvostunov

In practical radiation physics it is necessary to take account of fluctuations of the energy absorbed in the bombardment of rather small volumes of material. A detailed interpretation of the experimental distributions of the number of ionizations produced by elementary particles in thin-layer proportional detectors [1], the calculation of microdosimetric functions and the biological effect of radiation on cells [2], the stability of operation of superconducting elements of accelerator complexes [3], are some of the questions whose answers require information on the distribution of absorbed energy (AE) in a specified microvolume. The expected effects in these problems were estimated by using the theory of fluctuations of ionization energy losses [4-6]. It was shown that the differences between the parameters of the energy lost [4, 5] and the energy absorbed distributions (moments, asymptotic behaviors) due to the escape of delta electrons from the volume may reach several tens and hundreds of per cent [7, 8]. The theories in [5, 8] take account of ionizing collisions of charged particles only. At higher energy nuclear interactions, in spite of the small cross-section ($\sigma_{nucl} \ll \sigma_{ion}$), begin to affect energy release processes. This is clear even in elastic interactions, which are nuclear reactions of the simplest type. The ratio λ of the average energy lost by a particle per unit path length in nuclear and ionizing collisions is

$$\lambda \equiv \frac{(dE/dx)_{nucl}}{(dE/dx)_{ion}} \cong \frac{\sigma_{nucl}T_0/2}{\sigma_{ion}\bar{I}\ln(\varepsilon_{max}/\bar{I})^2} \sim \frac{T_0^2}{\ln(\varepsilon_{max}/\bar{I})}, \tag{1}$$

where $\sigma_{ion} \cong \pi Z z^2 e^4/T_0\bar{I}$, Z is the atomic number of the atoms of the material, ze is the charge of the particle, $\bar{I}$ is the average ionization potential of an atom, ε_{max} is the maximum energy transferred to an electron in one collision, and T_0 is the initial energy of the particle. For a hydrogen target bombarded with protons with energies of 300 MeV or less, the threshold of inelastic processes [9], λ may be much smaller than or on the order of unity. For T_0 = 100 MeV, λ = 0.04; for T_0 = 300 MeV, λ = 0.3. The situation is more complicated for the AE, the actually measurable quantity in ionization detectors, since the average value is nontrivially dependent on the geometry of the volume. In addition, it is known that the number of secondary particles produced in a single interaction of a high-energy particle with a nucleus fluctuates [9]. Consequently, in investigating fluctuations of the AE this fact must be taken into account as an additional mechanism which is not present in ionizing collisions. In the present article we consider the problem of the distribution of AE, taking account of ionizing and nuclear interactions in the absorber.

When a particle of energy T_0 enters a layer of thickness x normal to its surface, we denote by $f(x, \Delta, T_0, \Omega_0 = 0)*$ dΔ the probability that the energy absorbed lies between Δ and $\Delta + d\Delta$. We consider the geometry of the "layer in a vacuum" (Fig. 1). For "thin" layers [4-6] the average ionization energy losses of a particle are small in comparison with the initial energy T_0, and the mean-square of the angle of multiple scattering is much smaller than unity. In these cases the corresponding equation can be solved for $f_{ion}(x, \Delta, T_0)$ [7], the required function for pure ionizing collisions ($\sigma_{nucl} = 0$). An estimate of the "nuclear"

---

*From now on everywhere $f(x, \Delta, T_0, \Omega = 0) = f(x, \Delta, T_0)$.
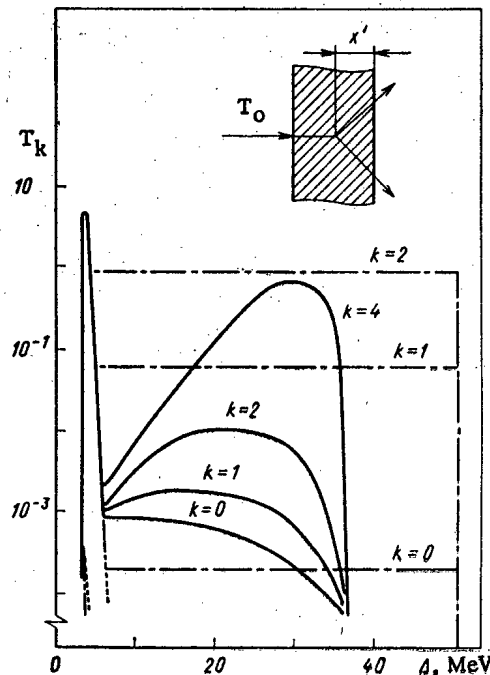

Fig. 1. $T_k(x, \Delta, T_0)$ (k = 0, 1, 2, 4) calculated by taking account (——) and not taking account (— — —) of elastic scattering of a bombarding particle by a nucleus; — · — ·) analogous distributions for energy lost in layer (k = 0) and moments of energy loss distribution (k = 1, 2), taking account of interaction with a nucleus. The abscissa Δ is the energy absorbed in a layer of hydrogen of thickness x = 0.27 g/cm^2 when bombarded with protons of initial energy T_0 = 100 MeV; the ordinate $T_k = \Delta^k(f, x, \Delta, T_0)/(\Delta)^{k-1}$; $T_0(x, \Delta, T_0) \sim f(x, \Delta, T_0)$ is the required distribution of absorbed energy calculated with Eqs. (3) and (4).

effects requires a new equation which takes account of the finite probability of nuclear interactions of the bombarding particles. We present it without derivation:†

$$\frac{\partial f}{\partial x}(x, \Delta, T_0) + n_0(\sigma_{nucl} + \sigma_{ion}) \, f(x, \Delta, T_0) = n_0 \sum_k \int \sigma_{ex}^k \, (T_0, \varepsilon) \, f \times$$

$$\times (x, \Delta - \varepsilon, T_0) \, d\varepsilon + n_0 \sum_i \int \int \int d^2\sigma_{ion}^i (T_0, T, \Omega) \, f(x, \Delta - \varepsilon - I_i, T_0) f^e(x, \varepsilon, T, \Omega) \, d\varepsilon + \qquad (2)$$

$$+ n_0 \sum_n \int \cdots \int d^{2n}\sigma_{nucl} (T_1, \ldots, T_n, \Omega_1, \ldots, \Omega_n, T_0) \, f(x, \varepsilon, T_1, \Omega_1) * \ldots * f(x, \varepsilon, T_n, \Omega_n),$$

where n_0 is the number of atoms per cm^3, $\sigma_{nucl} = \sigma_{in} + \sigma_{el}$ is the total nuclear interaction cross section, σ_{ion} is the total ionization cross section of an atom, $\sigma_{ex}^k (T_0, \varepsilon)$ is the cross section for the excitation of the k-th state of the atom by a particle of energy T_0, $d^2\sigma_{ion}(T_0, T, \Omega)$ is the cross section for the emission of a delta electron of energy T in the direction Ω during the ionization of the i-th shell of the atom by a particle of energy T_0, I_i is the ionization potential of the i-th shell of the atom, $f^e(x, \varepsilon, T, \Omega)$ is the probability density for a primary electron of initial energy T entering a layer x in the direction Ω to release ΔE ε, $d^{2n}\sigma_{nucl} (T_1, \ldots, T_n, \Omega_1, \ldots, \Omega_n, T_0)$ is the cross section for

†The derivation of the equation is completely analogous to the derivation of the equation of ionizing interactions [7, 8], and will be given in a more detailed publication.

419

the formation of n particles† with energies T_k and angles of emission Ω_k ($k = 1,...,n$) in the inelastic scattering of a bombarding particle of energy T_0 by a nucleus. The asterisk denotes convolution with respect to the variable ε. For $x = 0$ the condition $f = \delta(\Delta)$ must be satisfied, which indicates zero AE in a layer of thickness $x = 0$.

Equation (2), which is nonlinear in f, goes over into the equation for the ionization function f_{ion} [7] if we assume $\sigma_{nucl} = 0$. Equation (2) can be solved by perturbation theory, using $\gamma = \sigma_{nucl}/\sigma_{ion} \ll 1$ as a small parameter [9]. Substituting the required function in the form $f_{ion} + \gamma f'$ into Eq. (2) leads to an inhomogeneous linear integrodifferential equation for the function f', which we solve by taking the Laplace transform with respect to the energy Δ:

$$f(x, \Delta, T_0) = (1 - xn_0\sigma_{nucl})f_{ion}(x, \Delta, T_0) + n_0 \int dx' \int d\varepsilon f_{ion}(x+x', \Delta-\varepsilon, T_0) \times$$

$$\times \sum_n \int \cdots \int d^{2n}\sigma_{nucl}f_{ion}(x', \varepsilon, T_1, \Omega_1) * \cdots * f_{ion}(x', \varepsilon, T_n, \Omega_n). \tag{3}$$

The first term in Eq. (3) is the product of the probabilities that a primary particle traverses a layer x without interacting with a nucleus and releases an energy Δ in ionizing collisions in the layer. The second term describes the contribution of a primary particle to the distribution of AE in a layer $x - x'$ and secondary particles formed at a depth $x - x'$ in the layer x'. The application of (3) is restricted by the inequality $xn_0\sigma_{nucl} \ll 1$ (single nuclear interaction approximation). In this case $xn_0\sigma_{ion} \gg 1$, i.e. the bombarding particle may experience multiple ionizing collisions. These conditions are satisfied in most practically important cases.

In performing specific calculations with Eq. (3) it is convenient to investigate the simplest reaction in which two particles of the same kind are created (Fig. 1). This is valid, for example, for elastic nuclear scattering of a proton by hydrogen [9], which is one of the basic components of soft biological tissue. Then $d^{2n}\sigma_{nucl} = (d^2\sigma_{el}/dTd\Omega)\delta_{n,2} \cdot \delta(\cos\theta - \sqrt{T/T_0})$, and the second term in Eq. (3) takes the form

$$\int dx' \int d\varepsilon \int \int \frac{d^2\sigma_{el}}{dTd\theta} \delta(\cos 0 - \sqrt{T/T_0}) \sin 0 \, d\theta \times$$

$$\times f_{ion}(x - x', \Delta-\varepsilon, T_0)f_{ion}(x'/\sin\theta, \varepsilon, T_0-T) \times$$

$$\times f_{ion}(x'/\cos\theta, \varepsilon, T). \tag{4}$$

For protons of energy $T_0 = 100$ MeV and $x = 0.27$ g/cm^2, f_{ion} in the first term of Eq. (3) is well approximated by the Vavilov energy loss distribution function ($\varkappa = 1$) [5], since for $\varkappa \gtrsim 1$ the differences in the energy loss distribution and the AE in f_{ion} are small (the situation is different for $\varkappa \ll 1$ [7, 8]). The integrals for f_{ion} in Eq. (4) were obtained in analytical form by using the simple continuous slowing-down approximation [6]. The contribution of nuclear interactions, taking account of the second term in Eq. (3), for energies well above the average ($\Delta \gg \bar{\Delta} \sim \Delta_{ion}$) is controlling (Fig. 1). Appreciable fluctuations of the AE ($\Delta \gg \bar{\Delta}$) appear in the moments of the distribution. The first two moments calculated by taking account and not taking account of nuclear interactions differ appreciably in spite of the small value of $\gamma = 10^{-4}$ [9]: $(\bar{\Delta} = \bar{\Delta}_{ion})/\bar{\Delta}_{ion} = 0.01$; $(\bar{\Delta}^2 - \bar{\Delta}^2_{ion})/\bar{\Delta}^2_{ion} = 0.55$, where $\overline{\Delta^k} = \int \Delta^k f \, d\Delta, \overline{\Delta^k_{ion}} = \int \Delta^k f_{ion} d\Delta$, $k = 1, 2$. Figure 1 also shows that the distribution of AE differs greatly from the distribution of the energy lost by a fast particle in the layer, taking account of elastic nuclear scattering. This is a result of the high probability of the escape of scattered protons from the layer. The difference between the AE and the energy loss distributions, which results from the escape of secondary particles from the volume of material, indicates a substantial correlation of energy release processes in adjacent layers of the material. This fact probably must be taken into account in processing measurements in multilayer ionization detectors. It is natural to expect that analogous effects should occur also for inelastic nuclear reactions of high-energy particles, and also for more complicated bombarding geometry, for example a "layer in matter" [8].

---

†For simplicity we assume they are all of the same kind as the primary particle. The generalization for particles of different kinds leads to a more cumbersome notation for the last term in Eq. (2).

420

LITERATURE CITED

1. V. A. Lyubimov, in: Elementary Particles [in Russian], No. 2, Atomizdat, Moscow (1980), p. 91.
2. V. I. Ivanov and V. N. Lystsov, in: Problems of Microdosimetry [in Russian], Énergoatom-izdat, Moscow (1982), p. 3; I. M. Dmitrievskii, ibid., p. 88.
3. A. G. Alekseev et al., in: Third All-Union Conf. on Microdosimetry, Moscow Eng. Phys. Inst. (1979), p. 122; L. N. Zaĭtsev, Physics of Elementary Particles of the Atomic Nucleus [in Russian], Vol. 11, No. 3 (1980), p. 525.
4. L. D. Landau, Collected Works [in Russian], Vol. 1, Nauka, Moscow (1969), p. 482.
5. P. V. Vavilov, Zh. Eksp. Teor. Fiz., 32, No. 4, 920 (1957).
6. N. P. Kalashnikov, V. S. Remizovich, and M. I. Ryazanov, Collisions of Fast Charged Particles in Solids [in Russian], Atomizdat, Moscow (1980), p. 61.
7. S. G. Andreev, Author's Abstract of Candidate's Dissertation, Moscow Eng. Phys. Inst. (1981); S. G. Andreev and N. P. Kalashnikov, in: Third All-Union Conf. on Microdosimetry [in Russian], Moscow Eng. Phys. Inst. (1979), p. 12.
8. S. G. Andreev, in: Shielding Against Ionizing Radiations of Nuclear Industrial Plants. Proc. Third All-Union Scientific Conf. on Shielding Against Ionizing Radiations on Nuclear Industrial Plants [in Russian], Tbilisi State Univ., Vol. 3 (1983), p. 15.
9. V. S. Barashenkov, Interaction Cross Sections of Elementary Particles [in Russian], Nauka, Moscow (1966), p. 15.

STABILITY OF SCINTILLATION DETECTORS VIS-A-VIS RADIATION

V. V. Pomerantsev, I. B. Gagauz,   UDC 539.1.074.3
Yu. A. Tsirlin, and O. V. Levchina

Scintillation detectors which are used to monitor background radiation or radiation in geological prospecting or other research work are in a continuous flux of γ-radiation. We consider in the present work the influence of ^{137}Cs γ-radiation ($E_\gamma = 0.662$ MeV) of various flux densities (10^5, 10^6, and 10^7 quanta·cm^{-2}·sec^{-1}) upon the spectrometric characteristics of detectors of the most frequently employed type (diameter 40 × 40 mm) with various activator concentrations. The absorbed dose was constant and amounted to $\sim$0.1 Mrad (1 rad = 0.01 Gy). The detectors were supplemented by ^{241}Am α sources ($E_\alpha = 5.486$ MeV) with a flux of 400 particles·sec^{-1} to study the α/γ ratio which in the crystal develops from the light yield of the α line on the energy scale of the γ radiation (subsequently termed "γ equivalent").

We irradiated in our experiments 37 detectors in lots of 5-10 detectors; the detectors had the standard activator concentration of 10^{-2} mass %. The influence of the radiation was assessed from the relative changes of the light yield on the ^{137}Cs γ line (δC_γ) and the γ equivalent ($\delta C_\alpha/\lambda$) and on the basis of the changes in the intrinsic α and γ line broadening of the detectors (ΔR_α and ΔR_γ). The average changes and the greatest changes in the parameters at the probability level P = 0.95 are listed in Table 1.

Since the experiment lasted for a long time (3000 h at a flux density of 10^5 quanta·cm^{-2}·sec^{-1}), changes in the characteristics of three detectors which had not been irradiated were monitored. All detector characteristics remained constant within the error limits of the measurements; more specifically, the variation in light yield did not exceed ±1.5%. Figure 1 illustrates the changes in the light yield obtained via the γ line in three lots of detectors. It follows from Fig. 1 and Table 1 that the detector light yield decreased (by about 40%) in all γ radiation fluxes considered; the average change of the resolution of the γ line was significant when the flux density of the irradiation was 10^5 and 10^7 quanta·cm^{-2}·sec^{-1} and statistically probable at a flux of 10^6 quanta·cm^{-2}·sec^{-1}.

This means that γ radiation produces in the crystal volume damage which may change the spectrometric characteristics of the detectors on the γ line. The statistical evaluation of the data concerning the change of the γ equivalent in individual sets of detectors shows that changes of the γ equivalent are either probable or statistically significant. But only

TABLE 1. Influence (%) of γ Radiation Upon the Detector Parameters

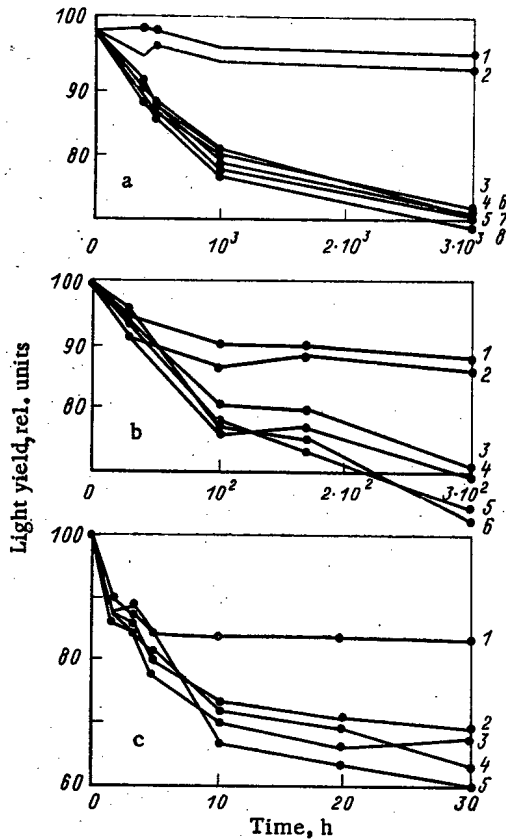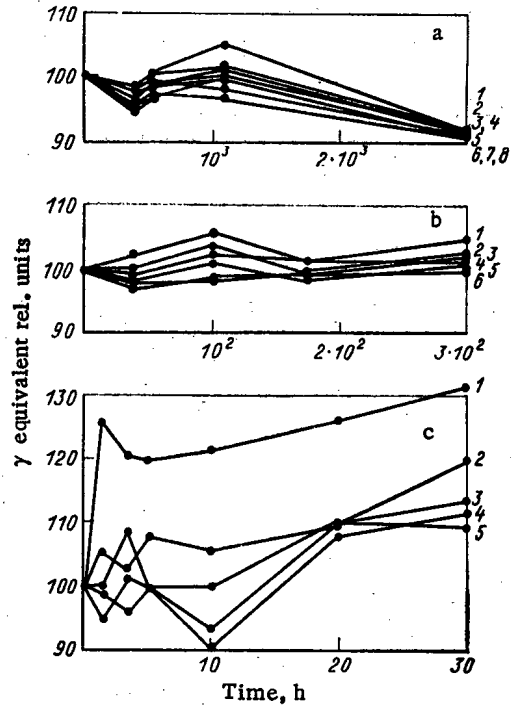| Flux density (quanta·cm^{-2}·sec^{-1}) of the γ radiation	No. of irradiated detectors	Relative change				Change in the intrinsic detector resolution			
		light yield σC_γ (meas. error ±5%)		γ equivalent $\sigma C_\alpha/\gamma$ (meas. error ±3%)		ΔR_γ (meas. error ±5%)		ΔR_α (meas. error ±0.5%)	
		av.	max.	av.	max.	av.	max.	av.	max.
10^5	26	—16,1	—28,0	—3,4	—6,0	1,2	1,7	0,0	0,3
10^6	6	—39,2	—47,1	3,5	5,2	0,3	0,8	0,2	1,0
10^7	5	—39,9	—43,6	5,9	6,5	1,1	1,7	0,4	1,0

Fig. 1

Fig. 2

Fig. 1. Dependence of the detector light yield of the ^{137}Cs γ line upon the time of irradiation at identical irradiation doses and flux densities of a) 10^5, b) 10^6, and c) 10^7 quanta·cm^{-2}·sec^{-1}. In this figure and in Fig. 2, the numbers at the curves denote the detector numbers in each lot.

Fig. 2. Dependence of the γ equivalent of the detectors upon the time of irradiation for a particular absorbed dose and flux densities of a) 10^5, b) 10^6, and c) 10^7 quanta·cm^{-2}·sec^{-1}.

at a flux density of 10^7 quanta·cm^{-2}·sec^{-1} is the measurement error exceeded by the greatest possible change of the γ equivalent at the probability P = 0.95 (see Table 1 and Fig. 2).

Thus, the α/γ ratio of the crystals is practically not affected by gamma radiation with a flux density below 10^7 quanta·cm^{-2}·sec^{-1}. Accordingly, when detectors are operated in continuous γ-radiation fluxes with a density not exceeding the above-indicated value, the γ lines under inspection must be identified with the aid of the γ equivalent.

A change in the resolution is at the α line statistically insignificant for all γ radiation fluxes employed. The greatest possible change at the probability P = 0.95 does not exceed the measurement error (±0.5%), i.e., this parameter is also stable. Accordingly, the α line can be used to stabilize the measuring channel of a scintillation γ spectrometer operated in a γ-radiation field.

The light yield of the detectors is restored after γ irradiation in individual form and takes place in more than 1 month but, in the majority of cases, takes one year and more, i.e., the restoring processes can compete with aging [A. A. Burshtein et al., Metrologiya, No. 2, 59 (1981)].

Similar results concerning the influence of weak γ radiation upon detector characteristics were obtained with activator concentrations of as high as $3 \cdot 10^{-1}$ mass % in a single crystal (18 samples). A further increase in concentration results in coloring of the crystals and a substantial change of all detector characteristics by radiation. A decrease of the concentration to $5 \cdot 10^{-3}$ mass % increases the stability of the detectors.

The authors thank E. A. Bugai, É. L. Vinograd, L. S. Zubenko, V. F. Lyubinskii, and A. P. Meshman for their collaboration and help in the present work.

RADIATION STABILITY OF SCINTILLATING POLYSTYRENE

I. B. Gagauz, A. P. Meshman,
V. F. Pererva, V. V. Pomerantsev,
and V. M. Solomonov

UDC 539.1.074.3

Scintillating polystyrene is widely employed in β radiometry. In some applications, for example in monitoring the contamination level of various objects, the behavior of the detectors must be checked while the dose absorbed during the detector operation increases cumulatively.

We consider in the present work industrial polystyrene samples of standard composition (2% PT and 0.1% POPOP) exposed to the radiation of a β particle source consisting of ^{90}Sr + ^{90}Y with an average energy $\bar{E}_{Sr} = 0.196$ MeV and $\bar{E}_Y = 0.936$ MeV [1] and the activity $A = 9.25 \cdot 10^7$ Bq.

The rate of the absorbed dose is

$$M = NE/V\rho, \tag{1}$$

where N denotes the flux of β particles with the energy E, which are absorbed in the scintillator; V denotes the volume of the irradiated scintillator mass; and ρ denotes the density of the scintillator material ($\rho = 1.06$ g·cm^{-3}).

The irradiated volume was given by the sum of the volumes of 1) a cylinder of diameter d = 3 cm (equal to the diameter of the active spot of the source) and a height equal to the range l of β particles of average energy $\bar{E}$, and 2) the body formed by rotation of a curve around the cylinder axis:

$$x = \frac{d}{2} + h \cot \alpha + l \cos \alpha; \quad y = l \sin \alpha,$$

where h denotes the distance between the source and the sample (h = 0.02 cm); and α denotes the angle under which a β particle from the edge of the source is incident on the sample.

The curve connects the ends of the trajectories of β particles which leave from the edge of the source surface under an angle α ($\alpha_{min} \leqslant \alpha \leqslant \pi/2$), where $\alpha_{min} \approx \arctan(2h/(d_{equiv} - d - 2l))$ denotes the angle under which the edge of a sample of diameter $d_{equiv} = 1.95$ cm is seen from the edge of the source. The volume of the irradiated mass is (when terms of an order greater than the zeroth order in α_{min} are disregarded):

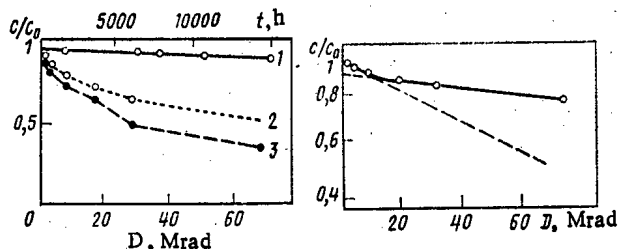---

423

Fig. 1   Fig. 2

Fig. 1. Relative light yield of samples of
scintillating polystyrene after aging during
the experiments (curve 1); the light yield in
dependence upon the absorbed β-radiation dose
(curve 2); and the relative light yield at the
maximum change (0.99 probability level) due
to absorption of the corresponding β-radiation
dose (curve 3): o denotes experimental points,
●) calculated results.

Fig. 2. Approximation of the exponential de-
pendence of the relative light yield upon the
absorbed dose for the initial irradiation per-
iod at D ≤ 6 Mrad (---); at a further interac-
tion of β radiation at D ≥ 10 Mrad (——).

$$V = \frac{\pi d^2 l}{4} + 2\pi l\left(\frac{lh}{2} + \frac{l^2}{3} + \pi\,\frac{dl}{8} - h^2\right) + \frac{2\pi lh^2}{\sin\alpha_{min}} - 2\pi l^2 h \ln\sin\alpha_{min} - \pi dlh \ln\operatorname{tg}\frac{\alpha\,min}{2}. \qquad (2)$$

The range of average-energy β particles from ^{90}Sr is $l_{Sr} \approx 0.042$ cm in polystyrene and
that from ^{90}Y is $l_Y \approx 0.390$ cm [1]; the volumes irradiated by the β particles are, accord-
ingly, $Y_{Sr} = 0.02$ cm^3 and $Y_Y = 0.58$ cm^3.

At these dimensions of the source and the target scintillator, we determined in accord-
ance with [2] the solid angle in which the β particles are incident on the detector and the
corresponding flux values: $N_{Sr} = 4.7 \cdot 10^6$ and $N_Y = 2.8 \cdot 10^7$ particles/sec. The dose rate
was 1.3 rad/sec (1 rad = 0.01 Gy).

The stability of the material was assessed from the change of the light yield of the
samples as the basic scintillation parameter of the detectors. The dependence of the light
yield upon the irradiation dose is shown in Fig. 1 (curve 2). Each point is the result of
averaging the data from two sets of samples (4 and 20 samples). Curve 1 of Fig. 1 illus-
trates the light-yield variation which resulted from the aging during the time of testing
and which was determined from a control-sample set (6 samples) which had not been irradiated.
The average change of the light yield due to aging during the time of the experiment (~15,000
h) amounts to 3.9%; the changes resulting from the β radiation with a dose of ~70 Mrad
amount to 22.6%.

The Student criterion was used to estimate the greatest possible changes in the light
yield at the 0.99 probability level for all absorbed doses with and without taking into
account aging. The changes in the light yield due to aging do not exceed 7.4% with the
above probability. Figure 1 (curve 3) depicts the smallest possible light-yield values at
the 0.99 probability level and at various absorbed β-radiation doses.

One usually assumes that detectors can be successfully used when their light-yield var-
iations do not exceed 15 or 20%. The detectors can be operated with 0.99 probability after
a dose of 18 or 24 Mrad, respectively. The dependence of the light yield upon the absorbed
dose is satisfactorily approximated by two exponential functions with exponents of the
change of the relative light yield per unit of acting dose amounting to $\varkappa = 0.01$ and 0.002
Mrad^{-1} (Fig. 2); the intersection of the straight lines on the corresponding scale is ob-
served at a dose of ~7.5 Mrad.

The fact that our results differ from the results of [3] is obviously associated with
the low absorbed doses considered by the authors. The change in the rate of the decreasing
light yield obviously has to do with competing processes of molecular destruction and molecular

424

recovery (taking place at different rates [3]) and gradual attainment of stationary detector operation in β irradiation.

The authors thank Yu. A. Tsirlin for his attention to, and help in the present work.

LITERATURE CITED

1. O. F. Nemets and Yu. V. Gofman, Handbook on Nuclear Physics [in Russian], Naukova Dumka, Kiev (1975).
2. V. I. Lozgachev, Zh. Tekh. Fiz., 30, No. 9, 1109 (1960).
3. V. M. Ékkerman et al., Radiokhimiya, 12, No. 6, 907 (1970).

YIELD OF ELECTRON BREMSSTRAHLUNG FROM THICK TARGETS

V. I. Isaev and V. P. Kovalev
UDC 539.163:539.124

In [1], a method of calculating the total yield of electron bremsstrahlung from thick targets without taking account of the electron transmission coefficient was considered. In the present work, this method is used to obtain a simple analytical expression for the bremsstrahlung yield, taking account of the transmission coefficient.

Suppose that at a target depth t there are $n(E_0, E, t)$ electrons of energy E, where E_0 is the initial energy of the electrons. The state of the electrons at depth t will be characterized by some mean energy $\overline{E}(t)$. For a high energy, its value will be given by the expression [2]

$$\overline{E}(t) = E_0 \exp(-\xi t),$$

where ξ is the ratio of the total electron energy loss to its initial energy.

When the electrons pass through a layer dt, they lose some part of their energy in the form of bremsstrahlung radiation, the numerical value of which is

$$dY = \frac{N_0}{A} \int_0^{\overline{E}} (E_0, \overline{E}, t) \sigma(\overline{E}, Z, k) k \, dk \, dt, \tag{1}$$

where Z is the atomic number of the target; A is the mass number of the target; $\sigma(\overline{E}, Z, k)$ is the cross section of bremsstrahlung formation with the energy k.

Suppose that the bremsstrahlung formed in layer dt is directed forwards, and attenuates exponentially in the subsequent part of the target; then

$$dY = \frac{N_0}{A} \int_0^{\overline{E}} n(E_0, \overline{E}, t) \sigma(\overline{E}, Z, k) k \, dk \, \exp[-\mu(k)(T-t)] \, dt. \tag{2}$$

Then, summing over the whole thickness of the target, the energy of the bremsstrahlung leaving the target is obtained

$$Y(t) = \frac{N_0}{A} \int_0^T \int_0^{\overline{E}} n(E_0, \overline{E}, t) \sigma(\overline{E}, Z, k) k \, dk \, \exp[-\mu(k)(T-t)] \, dt. \tag{3}$$

In calculations of the protection, it is approximately assumed that the attenuation of the dose rate of "shower" γ quanta occurs with near-minimal absorption coefficient in the chosen material; therefore, it is assumed that $\mu(k) = \mu_{min}$, which is denoted henceforward by μ.
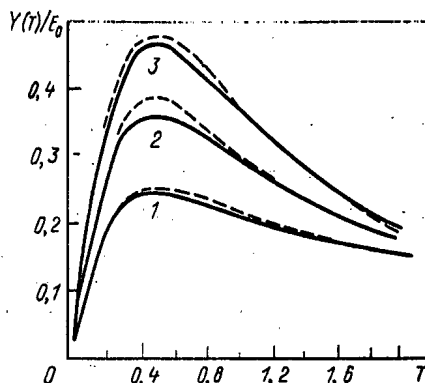
425

Fig. 1. Dependence of the electron-brem-
sstrahlung yield on the thickness T of a
tungsten target ($\mu = 0.04$ cm$^2 \cdot$g^{-1}) at an
energy of 15 (1), 30 (2), and 60 MeV (3):
the continuous curve corresponds to calcu-
lation by Eq. (7) and the dashed curve to
calculation by the Monte Carlo method [4];
the thickness is expressed in fractions
of the mean electron path.

TABLE 1. Values of $Y_{rad}(E_0)$ in Fractions
ε of the Initial Electron Energy

Element	E_0, MeV	
	30	60
Tungsten	0,576	0,735
	0,53	0,67
Lead	0,6	0,75
	0,55	0,682

Note. The first value for each element is
calculated from Eq. (10) and the second is
the result of calculations in [5]; the dis-
crepancy is no more than 10%.

The integral with respect to k is the mean radiational loss, and for high-energy electrons
may be written in the form

$$(dE/dx)_{rad} \approx cE.$$

Thus, determining the energy of the bremsstrahlung leaving the target reduces to calcu-
lating the single integral

$$Y(T) = \frac{N_0}{A} \int_0^T n(t) cE(t) \exp[-\mu(T-t)] dt. \tag{4}$$

The following expression was obtained for n(t) in [3]

$$n(t) = \exp[-a(t/R_E)^b, \tag{5}$$

where $b = [387 E_0/Z(1 + 7.5 \cdot 10^{-5} ZE_0^2)^{0.25}$; $a = (1 - 1/b)^{1-b}$; R_E is the extrapolated path.

Substitution of n(t) and E(t) into Eq. (4) gives

426

$$Y(T) = cE_0 \exp(-\mu T) \int_0^T \exp\left[-a(t/R_E)^b - (\xi-\mu)t\right] dt. \tag{6}$$

To calculate the integral in its final form, the integrand is replaced by an expression representing it with an error of 10% in the thickness range $0-R_E$

$$\exp\left[-a(t/R_E)^b - (\xi-\mu)t\right] \approx 1/(1+c_1^2 t^2),$$

where $c_1^2 = \{2\exp[(\xi-\mu)t_0] - 1\}/t_0^2$; t_0 is the thickness at which the transmission coefficient n(t) is equal to a half:

$$t_0 = R_E (\ln 2/\alpha)^{1/b}.$$

Calculation of Eq. (6) then gives

$$Y(T) = cE_0 \exp(-\mu T) \arctan(c_1 T)/c_1 \quad \text{(MeV)}, \tag{7}$$

where T is the target thickness.

The results of calculating the bremsstrahlung energy are shown in Fig. 1. Good agreement of the results of the calculation is seen, both in terms of absolute values and in terms of the form of the curves. The greatest discrepancy (7%) is observed for curve 2 at the maximum.

Taking $\mu = 0$ in Eq. (7), the electron energy converted to bremsstrahlung energy on deceleration in a target of thickness T is obtained:

$$Y_{rad}(T) = cE_0 \arctan(c_2 T)/c_2, \tag{8}$$

where $c_2^2 = [2\exp(\xi t_0) - 1]/t_0^2$.

The difference between Eqs. (8) and (7) is the energy of the bremsstrahlung absorbed in the target

$$Y_{abs} = cE_0 \{\arctan(c_2 T)/c_2 - \exp(-\mu T) \arctan(c_1 T)/c_1\}. \tag{9}$$

Taking $T = \infty$ in Eq. (8), the maximum possible electron energy converted into bremsstrahlung energy is obtained:

$$Y_{rad}(E_0) = cE_0 \pi/(2c_2). \tag{10}$$

Table 1 gives values of $Y_{rad}(E_0)$.

Note, in conclusion, that taking account of the electron transmission shifts the maximum of the distribution curve toward smaller thickness and reduces the bremsstrahlung yield.

LITERATURE CITED

1. V. I. Isaev et al., At. Energ., 36, No. 5, 400 (1974).
2. C. Emigh, LA-4097-MS, University of California (1970).
3. P. Ebert et al., Phys. Rev., 183, 422 (1969).
4. M. Berger and S. Seltzer, Phys. Rev., 2, 621 (1970).
5. M. Berger and S. Seltzer, Tables of Energy Losses and Ranges of Electrons and Positrons, NASA, Washington (1964), SP-3012.

How To Comply With The New Copyright Law

CHANGING YOUR ADDRESS?

In order to receive your journal without interruption, please complete this change of address notice and forward to the Publisher, 60 days in advance, if possible.

(Please Print)

Old Address:

name
_____

_____

address
_____

city
_____

state (or country)   zip code
_____

New Address

name
_____

_____

address
_____

city
_____

state (or country)   zip code
_____

date new address effective
_____

name of journal
_____

Plenum THE LANGUAGE OF SCIENCE
PUBLISHING CORPORATION   **233 Spring Street, New York, New York 10013**

MEASUREMENT TECHNIQUES *Izmeritel'naya Tekhnika* Vol. 27, 1984 (12 issues) $520	**SOVIET APPLIED MECHANICS** *Prikladnaya Mekhanika* Vol. 20, 1984 (12 issues) $520
MECHANICS OF COMPOSITE MATERIALS *Mekhanika Kompozitnykh Materialov* Vol. 20, 1984 (6 issues) $430	**SOVIET ATOMIC ENERGY** *Atomnaya Énergiya* Vols. 56-57, 1984 (12 issues).................... $560
METAL SCIENCE AND HEAT TREATMENT *Metallovedenie i Termicheskaya Obrabotka Metallov* Vol. 26, 1984 (12 issues) $540	**SOVIET JOURNAL OF GLASS PHYSICS AND CHEMISTRY** *Fizika i Khimiya Stekla* Vol. 10, 1984 (6 issues) $235
METALLURGIST *Metallurg* Vol. 28, 1984 (12 issues) $555	**SOVIET JOURNAL OF NONDESTRUCTIVE TESTING** *Defektoskopiya* Vol. 20, 1984 (12 issues) $615
PROBLEMS OF INFORMATION TRANSMISSION *Problemy Peredachi Informatsii* Vol. 20, 1984 (4 issues) $420	**SOVIET MATERIALS SCIENCE** *Fiziko-khimicheskaya Mekhanika Materialov* Vol. 20, 1984 (6 issues) $445
PROGRAMMING AND COMPUTER SOFTWARE *Programmirovanie* Vol. 10, 1984 (6 issues) $175	**SOVIET MICROELECTRONICS** *Mikroélektronika* Vol. 13, 1984 (6 issues) $255
PROTECTION OF METALS *Zashchita Metallov* Vol. 20, 1984 (6 issues) $480	**SOVIET MINING SCIENCE** *Fiziko-tekhnicheskie Problemy Razrabotki Poleznykh Iskopaemykh* Vol. 20, 1984 (6 issues) $540
RADIOPHYSICS AND QUANTUM ELECTRONICS *Izvestiya Vysshikh Uchebnykh Zavedenii, Radiofizika* Vol. 27, 1984 (12 issues) $520	**SOVIET PHYSICS JOURNAL** *Izvestiya Vysshikh Uchebnykh Zavedenii, Fizika* Vol. 27, 1984 (12 issues) $520
REFRACTORIES *Ogneupory* Vol. 25, 1984 (12 issues) $480	**SOVIET POWDER METALLURGY AND METAL CERAMICS** *Poroshkovaya Metallurgiya* Vol. 23, 1984 (12 issues) $555
SIBERIAN MATHEMATICAL JOURNAL *Sibirskii Matematicheskii Zhurnal* Vol. 25, 1984 (6 issues) $625	**STRENGTH OF MATERIALS** *Problemy Prochnosti* Vol. 16, 1984 (12 issues) $625
SOIL MECHANICS AND FOUNDATION ENGINEERING *Osnovaniya, Fundamenty i Mekhanika Gruntov* Vol. 21, 1984 (6 issues) $500	**THEORETICAL AND MATHEMATICAL PHYSICS** *Teoreticheskaya i Matematicheskaya Fizika* Vol. 58-61, 1984 (12 issues)..................... $500
SOLAR SYSTEM RESEARCH *Astronomicheskii Vestnik* Vol. 18, 1984 (6 issues) $365	**UKRAINIAN MATHEMATICAL JOURNAL** *Ukrainskii Matematicheskii Zhurnal* Vol. 36, 1984 (6 issues) $500

Send for Your Free Examination Copy

RUSSIAN JOURNALS IN THE PHYSICAL AND MATHEMATICAL SCIENCES

AVAILABLE IN ENGLISH TRANSLATION

ALGEBRA AND LOGIC
Algebra i Logika
Vol. 23, 1984 (6 issues) $360

ASTROPHYSICS
Astrofizika
Vol. 20, 1984 (4 issues) $420

AUTOMATION AND REMOTE CONTROL
Avtomatika i Telemekhanika
Vol. 45, 1984 (24 issues) $625

COMBUSTION, EXPLOSION, AND SHOCK WAVES
Fizika Goreniya i Vzryva
Vol. 20, 1984 (6 issues) $445

COSMIC RESEARCH
Kosmicheskie Issledovaniya
Vol. 22, 1984 (6 issues)......................... $545

CYBERNETICS
Kibernetika
Vol. 20, 1984 (6 issues)......................... $445

DIFFERENTIAL EQUATIONS
Differentsial'nye Uravneniya
Vol. 20, 1984 (12 issues) $505

DOKLADY BIOPHYSICS
Doklady Akademii Nauk SSSR
Vols. 274-279, 1984 (2 issues) $145

FLUID DYNAMICS
Izvestiya Akademii Nauk SSSR,
Mekhanika Zhidkosti i Gaza
Vol. 19, 1984 (6 issues) $500

FUNCTIONAL ANALYSIS AND ITS APPLICATIONS
Funktsional'nyi Analiz i Ego Prilozheniya
Vol. 18, 1984 (4 issues) $410

GLASS AND CERAMICS
Steklo i Keramika
Vol. 41, 1984 (6 issues) $590

HIGH TEMPERATURE
Teplofizika Vysokikh Temperatur
Vol. 22, 1984 (6 issues) $520

HYDROTECHNICAL CONSTRUCTION
Gidrotekhnicheskoe Stroitel'stvo
Vol. 18, 1984 (12 issues) $385

INDUSTRIAL LABORATORY
Zavodskaya Laboratoriya
Vol. 50, 1984 (12 issues) $520

INSTRUMENTS AND EXPERIMENTAL TECHNIQUES
Pribory i Tekhnika Éksperimenta
Vol. 27, 1984 (12 issues) $590

JOURNAL OF APPLIED MECHANICS AND TECHNICAL PHYSICS
Zhurnal Prikladnoi Mekhaniki i Tekhnicheskoi Fiziki
Vol. 25, 1984 (6 issues) $540

JOURNAL OF APPLIED SPECTROSCOPY
Zhurnal Prikladnoi Spektroskopii
Vols. 40-41, 1984 (12 issues) $540

JOURNAL OF ENGINEERING PHYSICS
Inzhenerno-fizicheskii Zhurnal
Vols. 46-47, 1984 (12 issues) $540

JOURNAL OF SOVIET LASER RESEARCH
A translation of articles based on the best Soviet research in the field of lasers
Vol. 5, 1984 (6 issues) $180

JOURNAL OF SOVIET MATHEMATICS
A translation of Itogi Nauki i Tekhniki and Zapiski Nauchnykh Seminarov Leningradskogo Otdeleniya Matematicheskogo Instituta im. V. A. Steklova AN SSSR
Vols. 24-27, 1984 (24 issues)......................... $1035

LITHOLOGY AND MINERAL RESOURCES
Litologiya i Poleznye Iskopaemye
Vol. 19, 1984 (6 issues) $540

LITHUANIAN MATHEMATICAL JOURNAL
Litovskii Matematicheskii Sbornik
Vol. 24, 1984 (4 issues) $255

MAGNETOHYDRODYNAMICS
Magnitnaya Gidrodinamika
Vol. 20, 1984 (4 issues) $415

MATHEMATICAL NOTES
Matematicheskie Zametki
Vols. 35-36, 1984 (12 issues)......................... $520